Beta-decay and transition probabilities near closed shell and deformed nuclei

Henryk Mach
Universidad Complutense de Madrid
Uppsala University, Sweden

Basic text books:

K.S. Krane: Introductory Nuclear Physics
John Wiley and Sons, 1988

Povh, Rith Scholz and Zetsche: Particles and Nuclei
3rd Eddition, Springer 2002

G.F. Knoll: Radiation Detectors and Measurements
3rd Eddition, John Wiley and Sons

Three "laboratories" to study neutron-proton neutron-neutron and proton-proton interactions

- Free particles

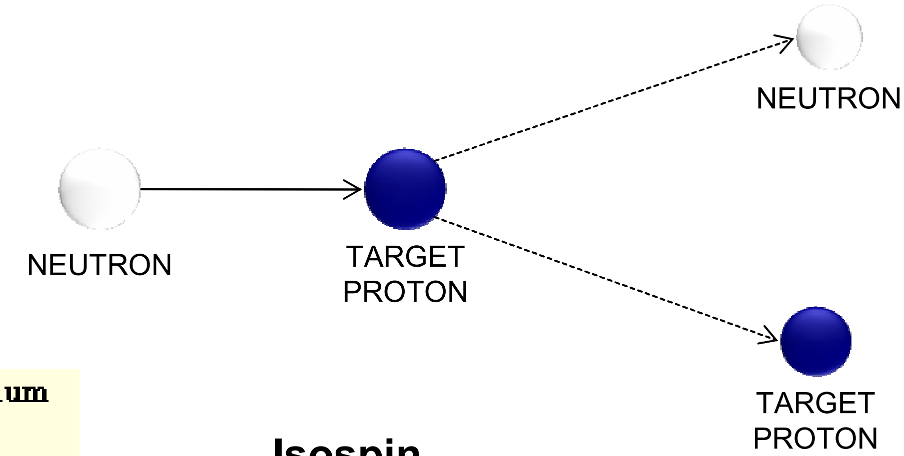

- Simple systems

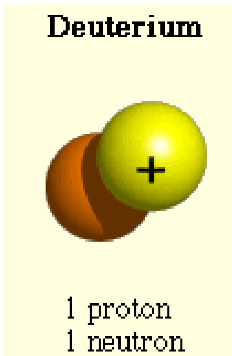

Isospin

singlet $\frac{1}{\sqrt{2}}\left(|\uparrow\downarrow\rangle - |\downarrow\uparrow\rangle\right)$

triplet $\begin{pmatrix} \uparrow\uparrow \\ \frac{1}{\sqrt{2}}(\uparrow\downarrow + \downarrow\uparrow) \\ \downarrow\downarrow \end{pmatrix}$

- Within complex nuclei

From E.White

Complex Nuclei

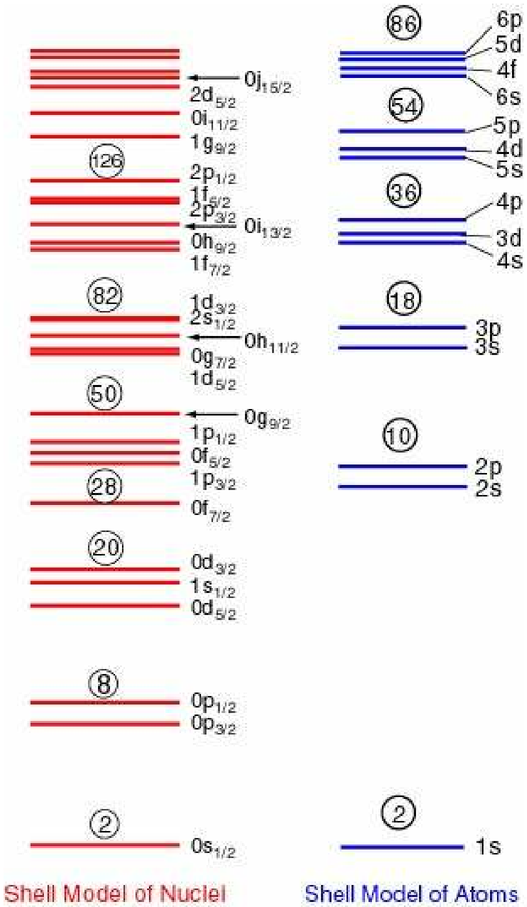

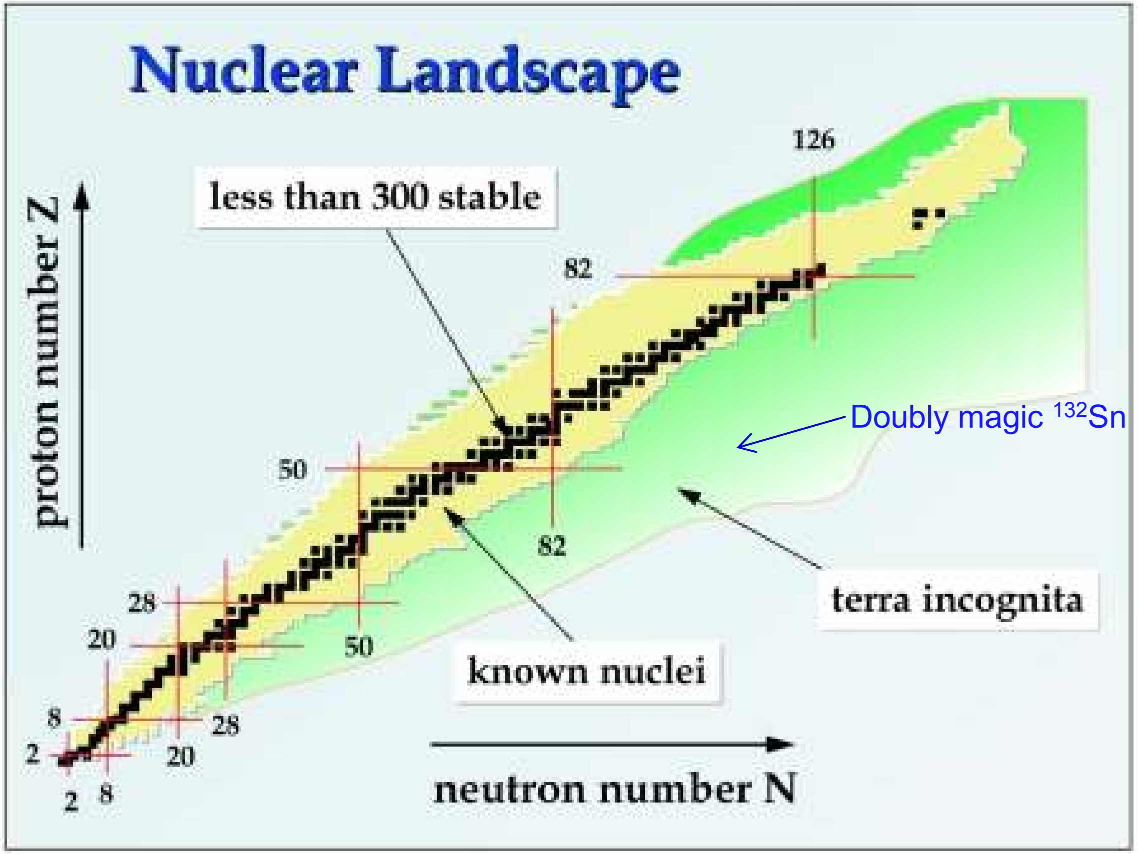

Nuclear Shell Model

Magic numbers: 2, 8, 20, 28, 50, 82, 126

From E.White

Core and valence particles

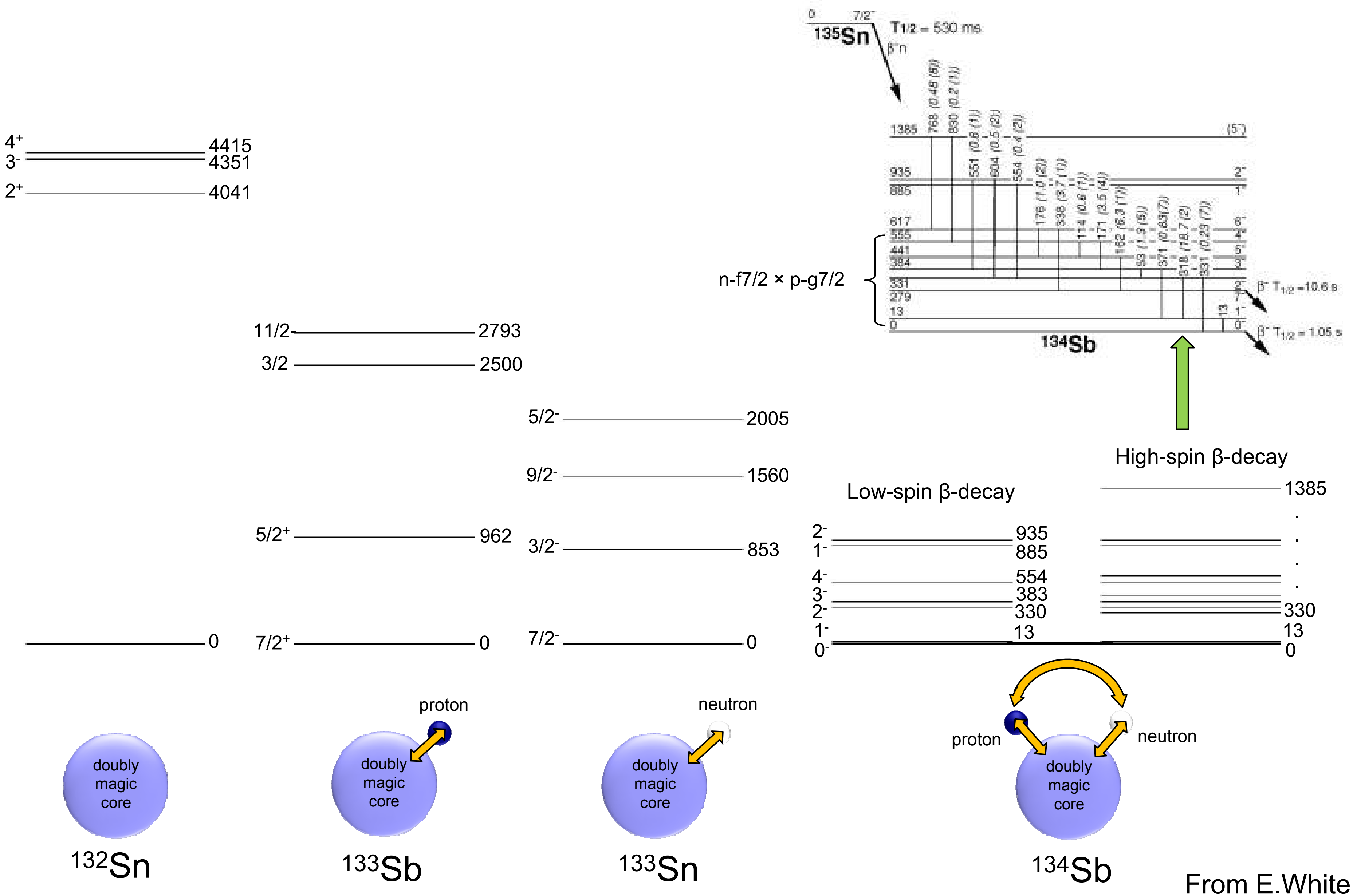

From E.White

What is a β-decay ?

Beta decay is a transformation of a neutron to a proton or a proton to a neutron. It has some peculiarities.

Neutron

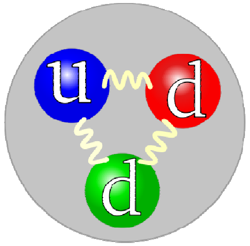

Baryon

1up 2down quarks

fermion

Spin ½

Isospin ½

parity +1

Mass 1.008664915(6) u

τ 885.7(8) s (free)

el. charge 0 e

Magn.m. -1.9130427(5) μ_N

Proton

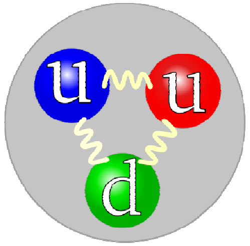

Baryon

2up 1down quarks

fermion

Spin ½

Isospin ½

parity +1

Mass 1.007276466(10) u

τ >2.1 x 10^{29} years (stable)

el. charge 1 e

Magn.m. 2.792847351(28) μ_N

Within a nucleus neutron can be stable and proton can beta decay!

Why ?

This is due to nuclear masses and binding energies.

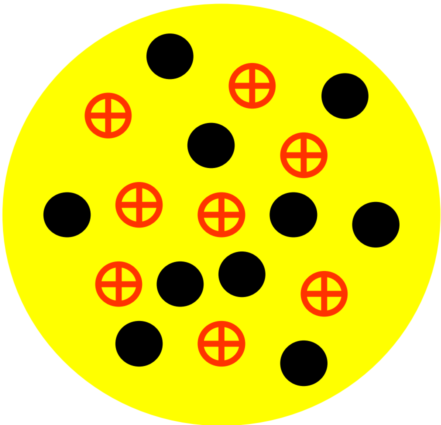

The binding energy BE of the nucleus is the difference between the mass of the nucleus and the mass of the Z protons and N neutrons.

$$BE = (Z \cdot m_p + N \cdot m_n - M) \cdot c^2$$

The mass is often expressed in terms of amu (atomic mass units) which is defined by

$$1 \text{ amu} = 1/12(M(^{12}C)) = 1.66 \cdot 10^{-24} g$$

EXAMPLE binding energy for ^{18}O (8 protons and 10 neutrons)

particle	mass (amu)	ΔA (keV)	BE (keV)
proton	1.007596	7299	0
neutron	1.008486	8021	0
^{18}O	17.99916	-782	$1.382 \cdot 10^5$

8 protons => 8x1.007596

10 neutrons => 10x1.08486 for a total of 18.14563 amu

BE= 0.14647 amu = 2.43×10^{-28} kg => 2.19×10^{-11} J = 1.37×10^{8} eV

= 137 MeV or 7.6 MeV/nucleon

Binding Energy of Nuclei

The breaking of heavy elements can produce energy

Binding Energy is negative.

Energy is released as nucleus is more bound.

Note Ni and Fe are special.

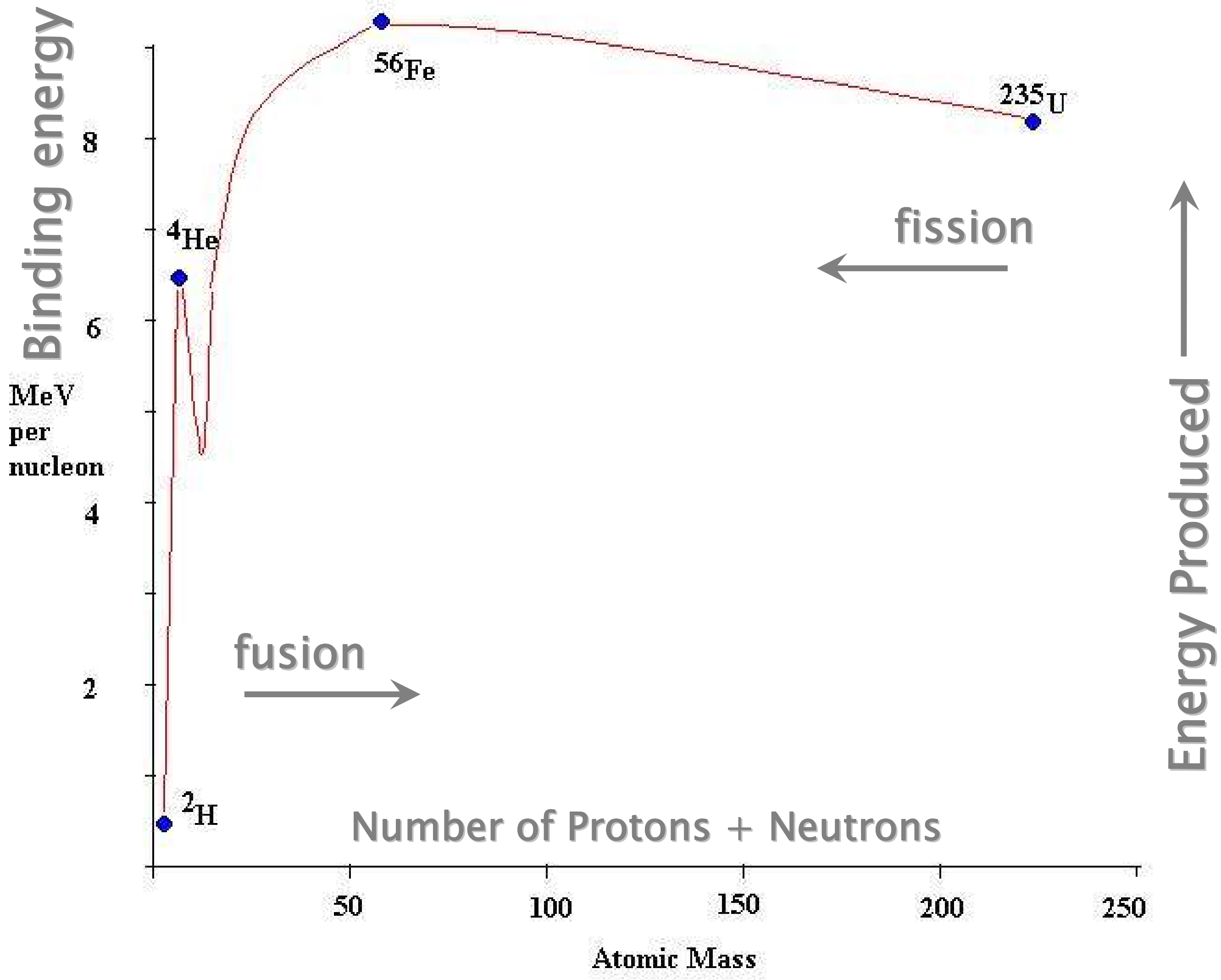

The nucleus is bound by the strong force. Stable nuclei will tend to have more neutrons than protons at large A due to Coulomb repulsion.

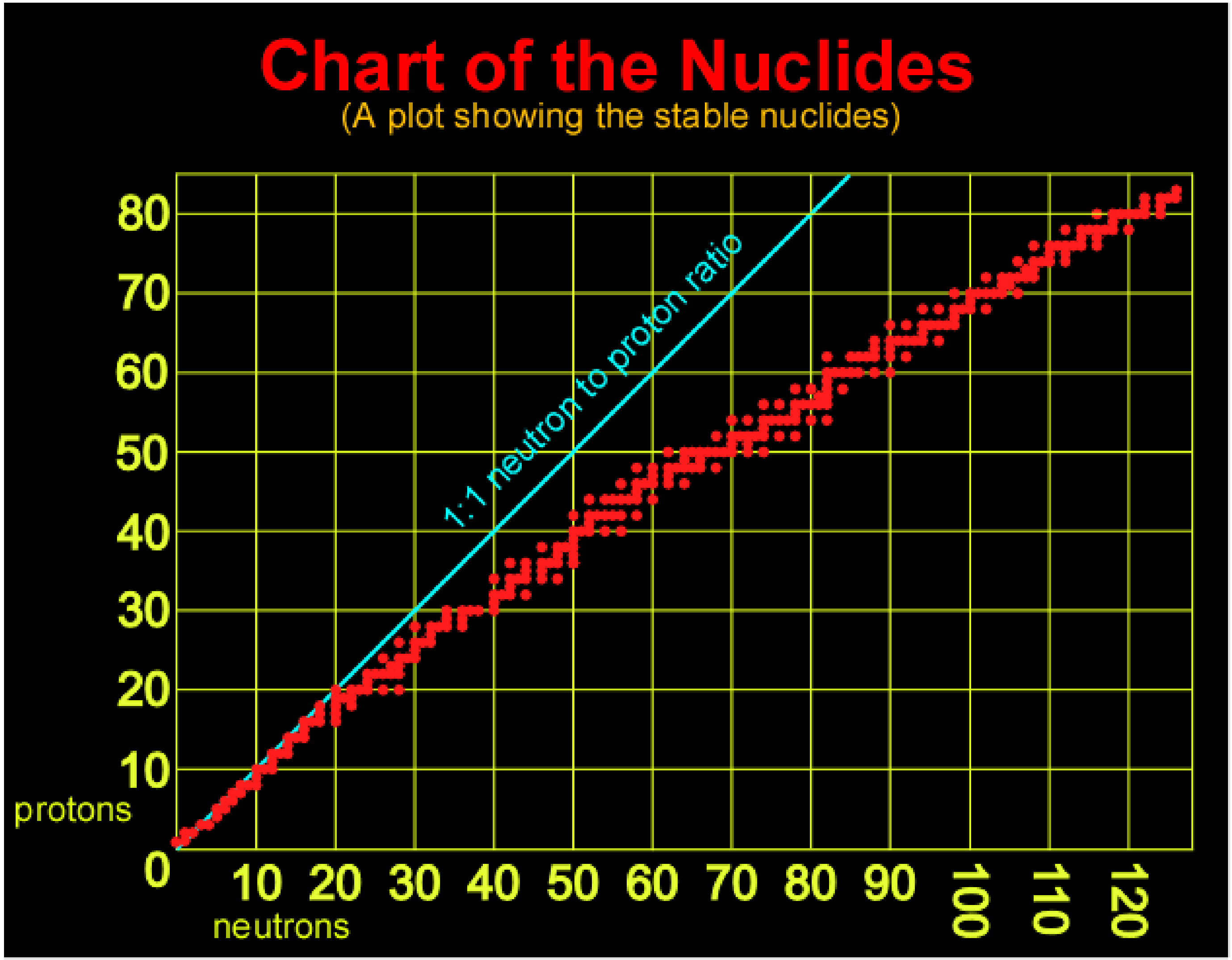

Fission and Neutron-rich nuclei

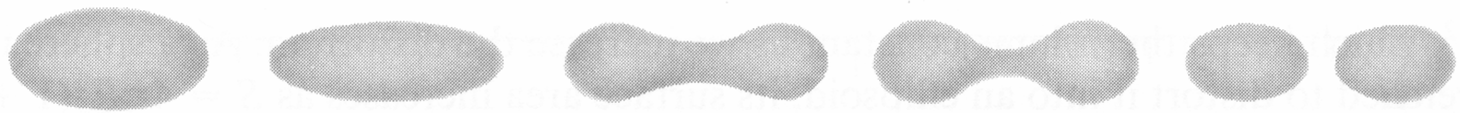

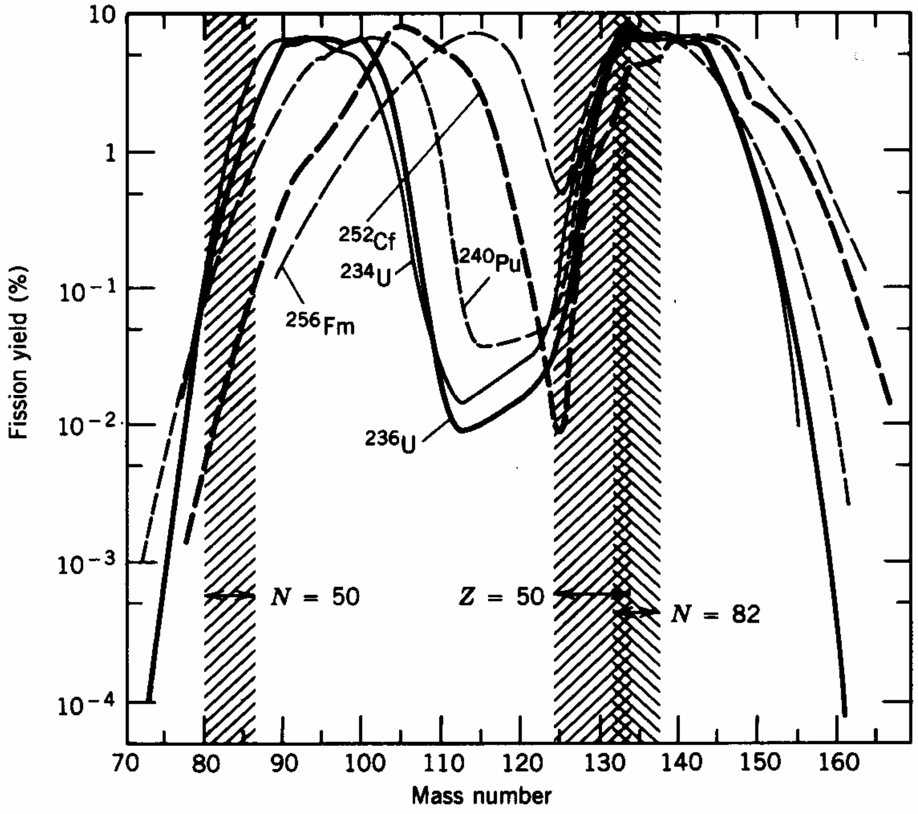

Nuclides Produced by ^{235}U Thermal N Fission

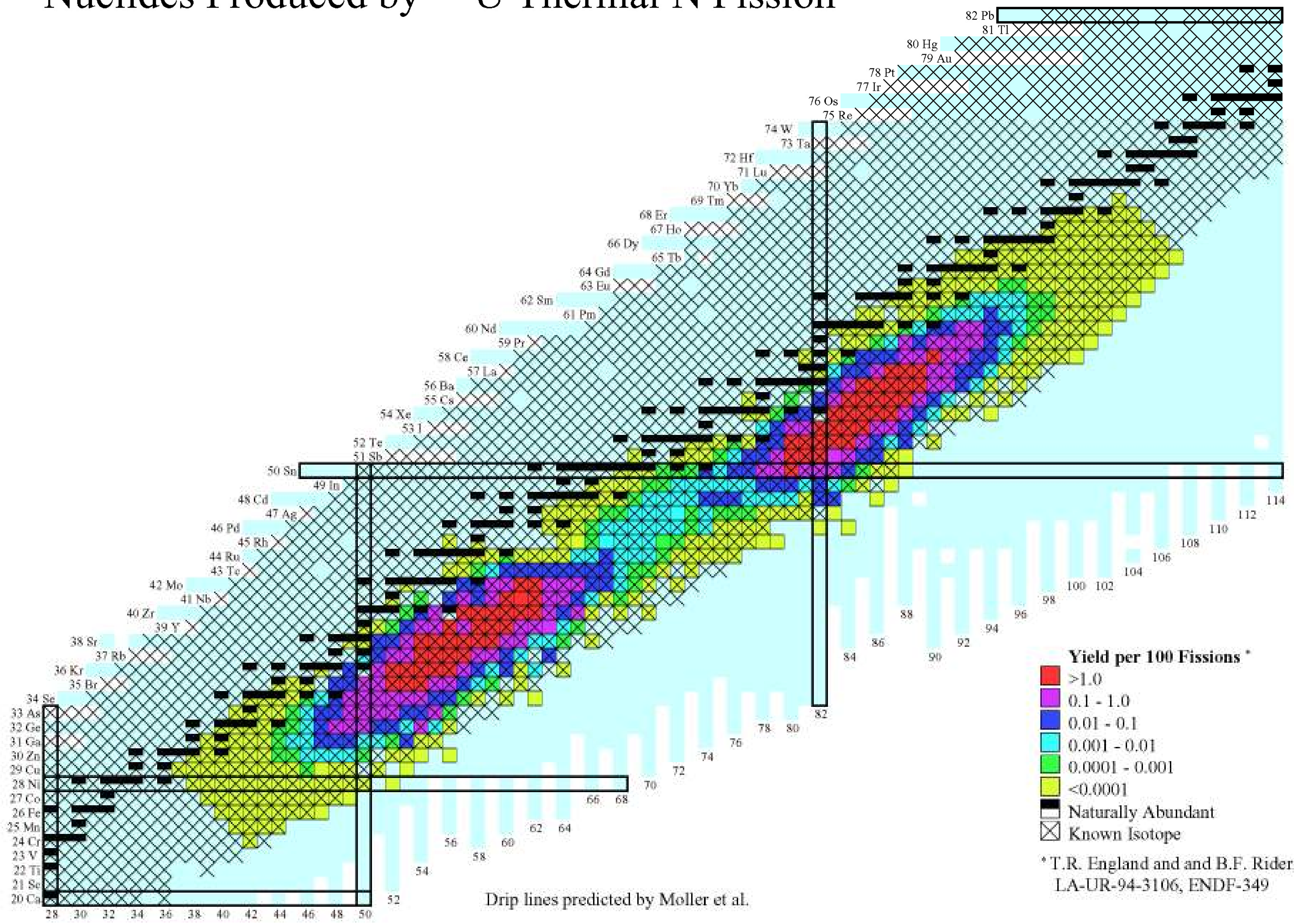

Nuclides Produced by ^{252}Cf Spontaneous Fission

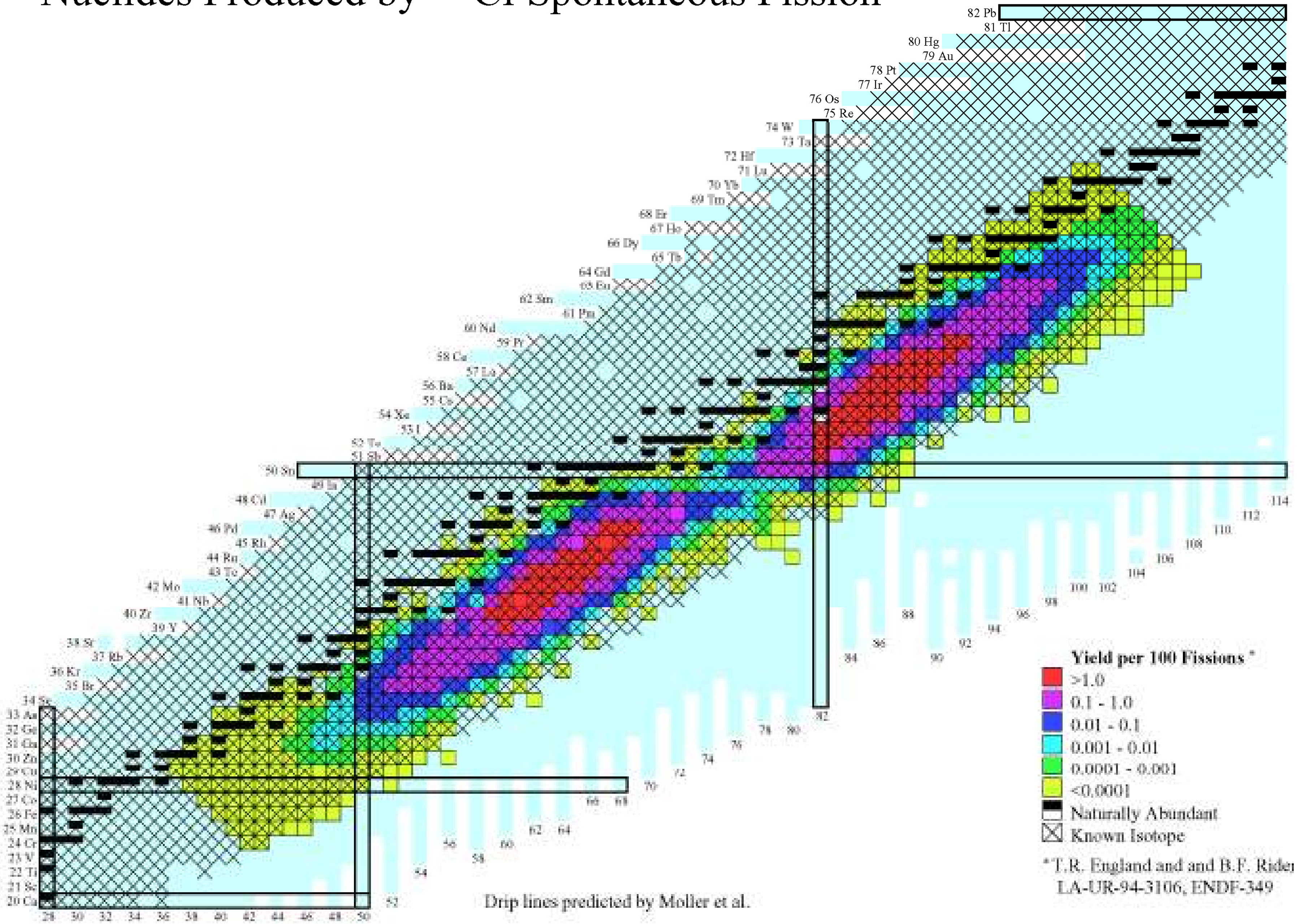

How do we measure nuclear masses ?

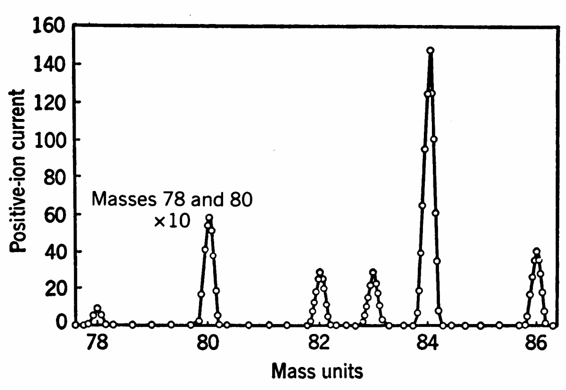

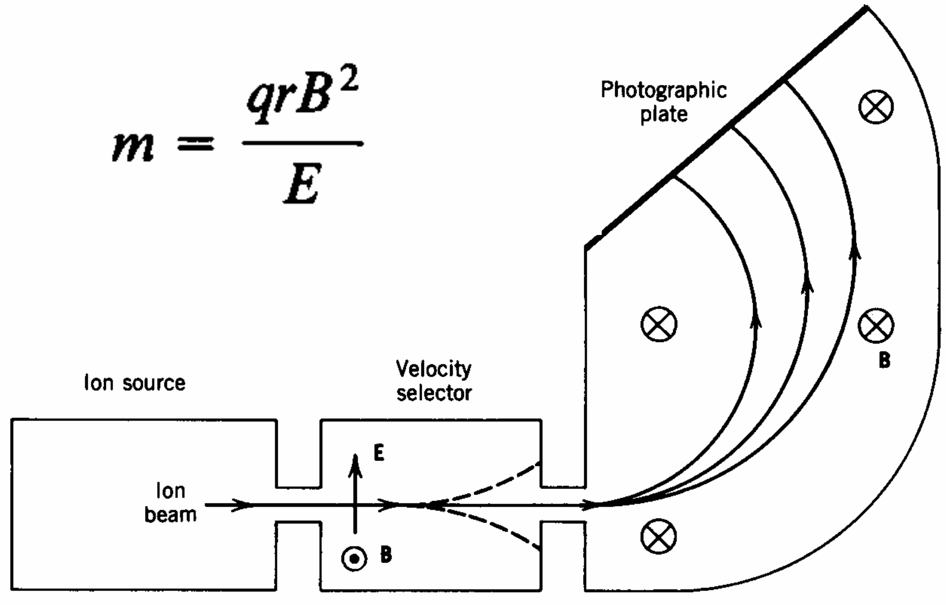

1. using magnetic spectrographs (not very precise)
2. from Qbeta measurements using beta-gamma coincidences
3. Using Penning Trap techniques, nuclear reactions...

Beta decay is one of the few possible decay channels.

Key condition: a nuclear system of lower mass.

β^- decay	$n \rightarrow p + e^- + \bar{\nu}_e$
β^+ decay	$p \rightarrow n + e^+ + \nu_e$
electron capture	$p + e^- \rightarrow n + \nu_e$

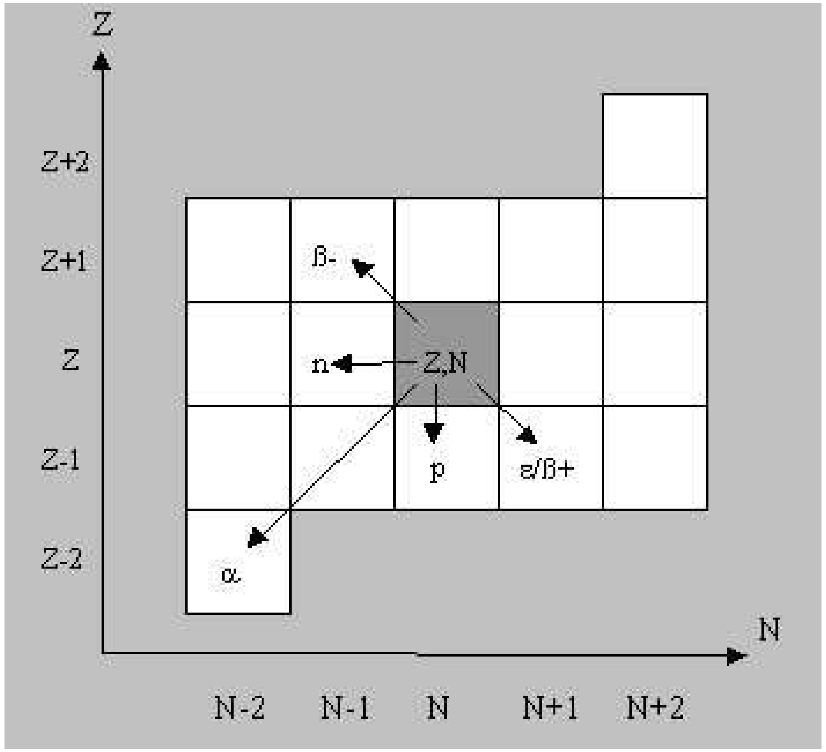

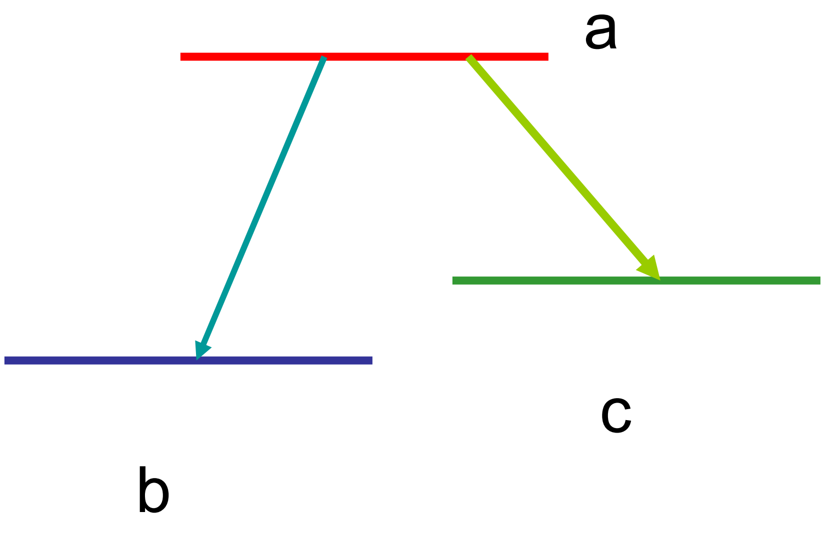

$$\lambda_a = \lambda_b + \lambda_c + \ldots \lambda_i$$

Masses of odd- and even- isobaric multiplets

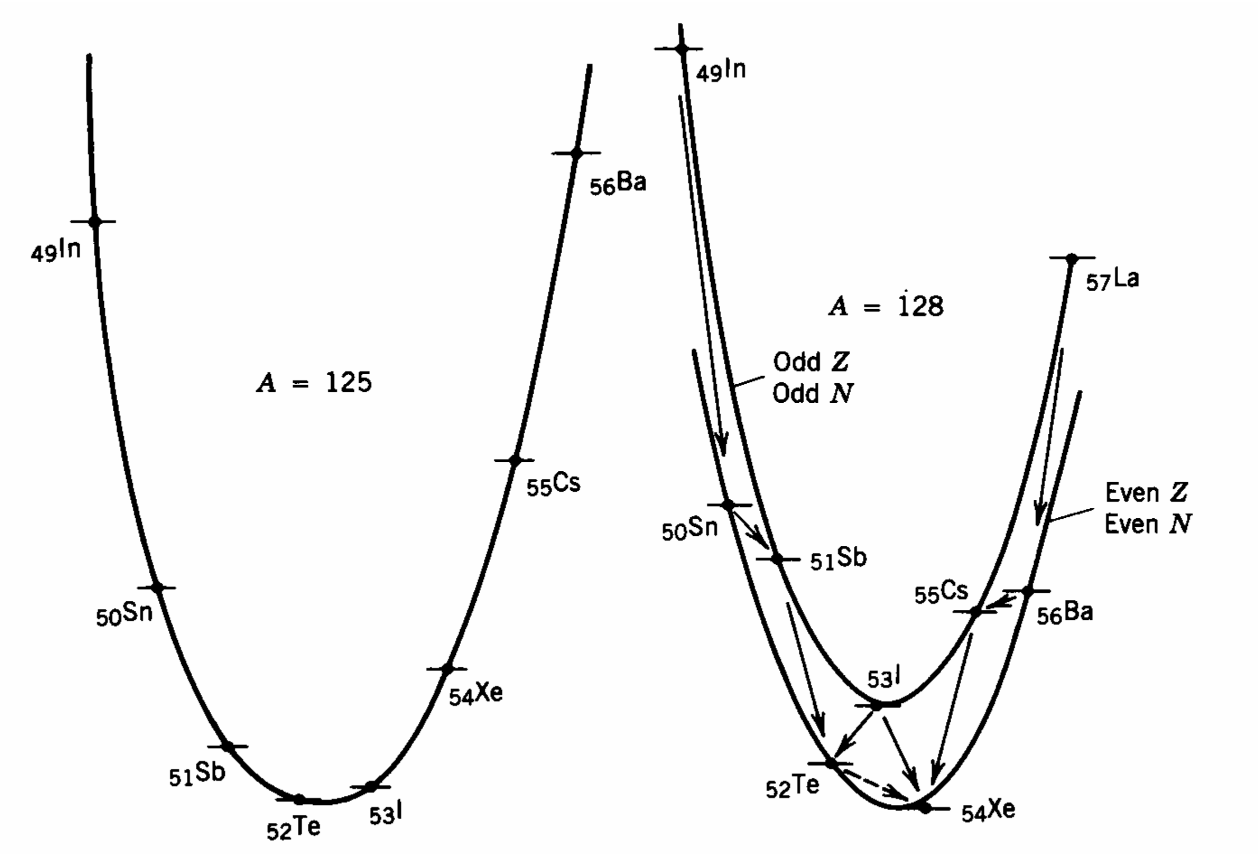

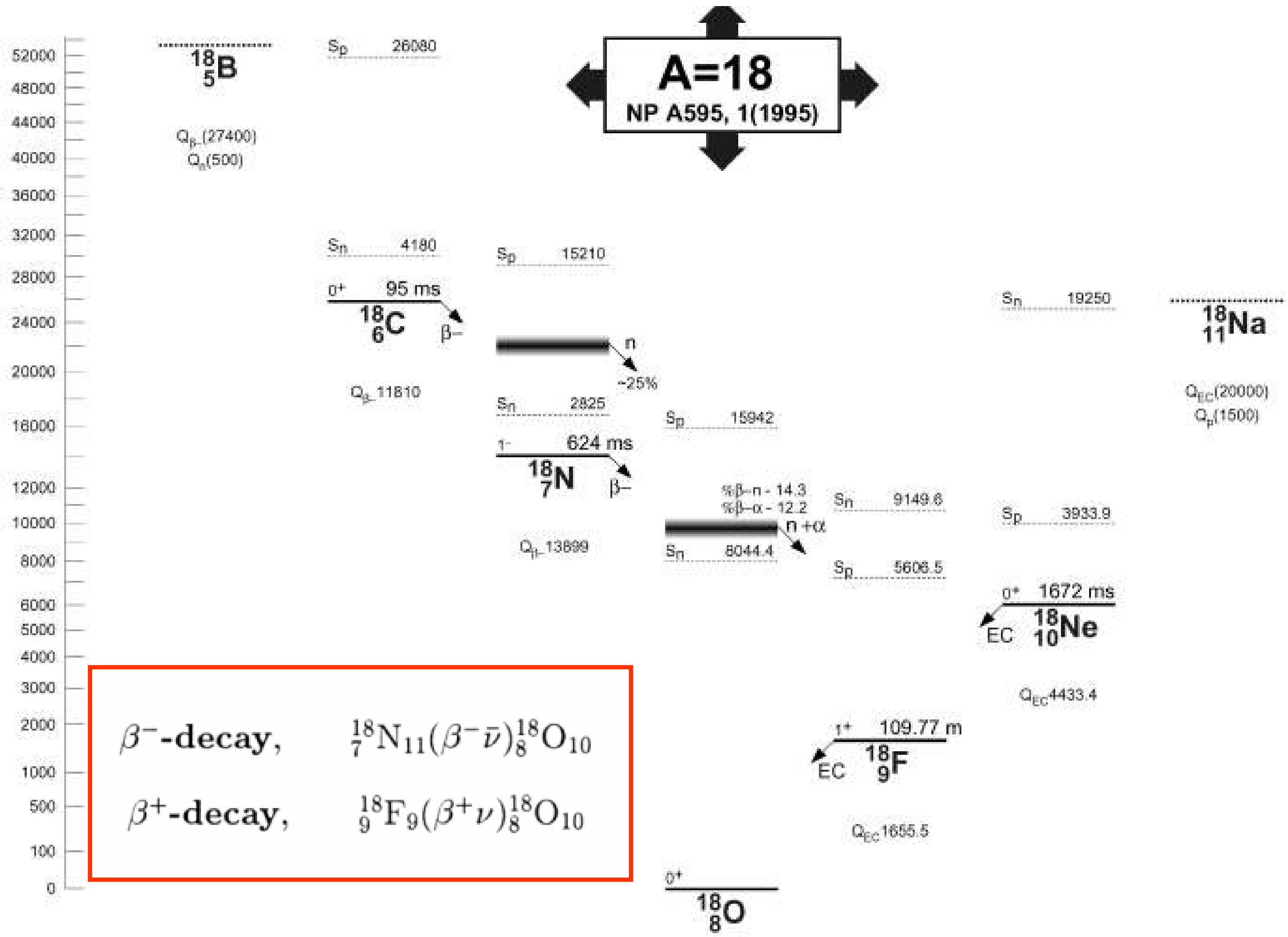

β^-**-decay,** $\quad {}^{18}_{7}\mathrm{N}_{11}(\beta^-\bar{\nu})^{18}_{8}\mathrm{O}_{10}$

β^+**-decay,** $\quad {}^{18}_{9}\mathrm{F}_{9}(\beta^+\nu)^{18}_{8}\mathrm{O}_{10}$

Beta Energy Spectra

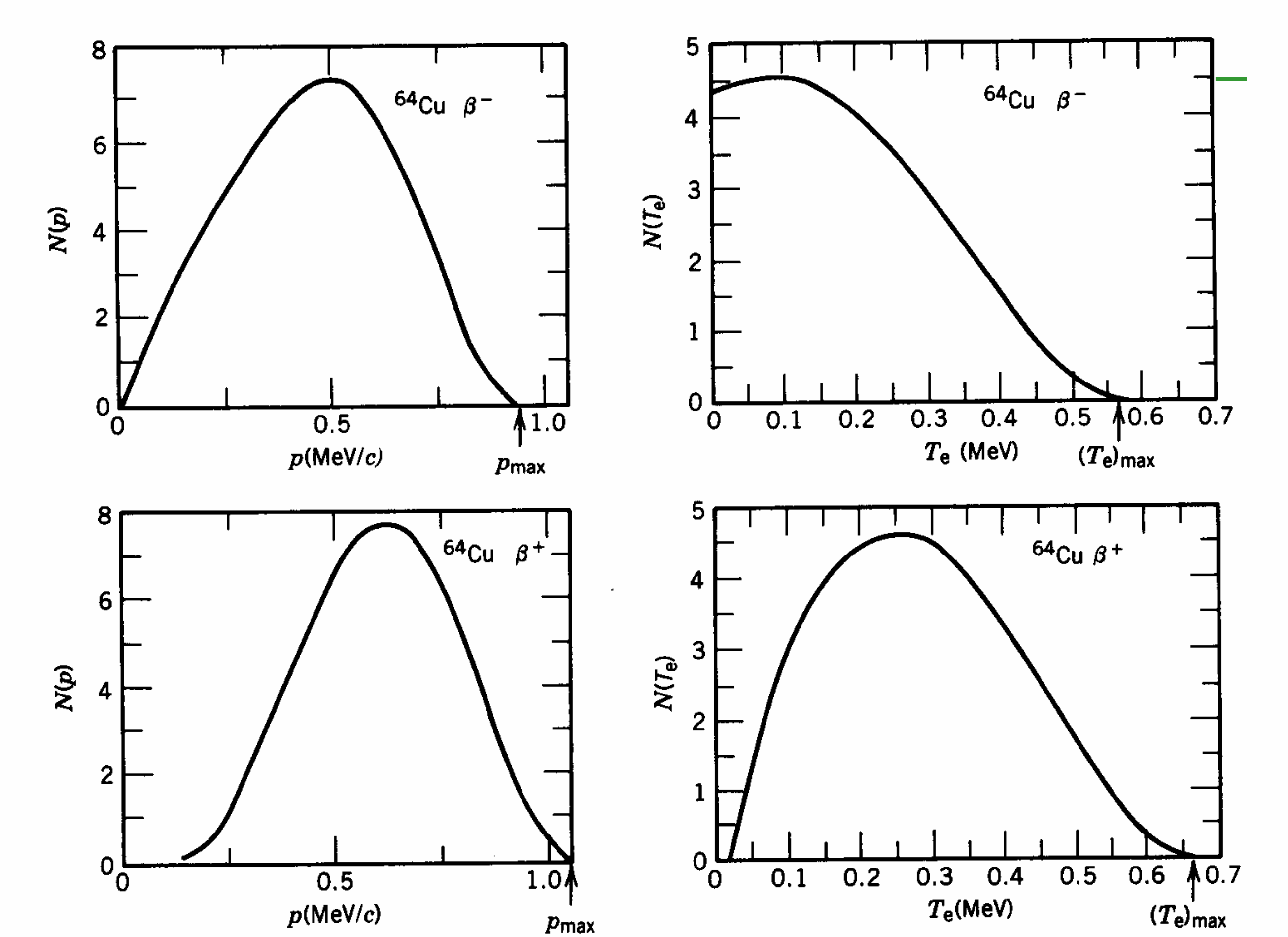

β⁻ decay $n \rightarrow p + e^- + \bar{\nu}_e$

β⁺ decay $p \rightarrow n + e^+ + \nu_e$

$$(Q - T_e) \propto \sqrt{\frac{N(p)}{p^2 F(Z', p)}}$$

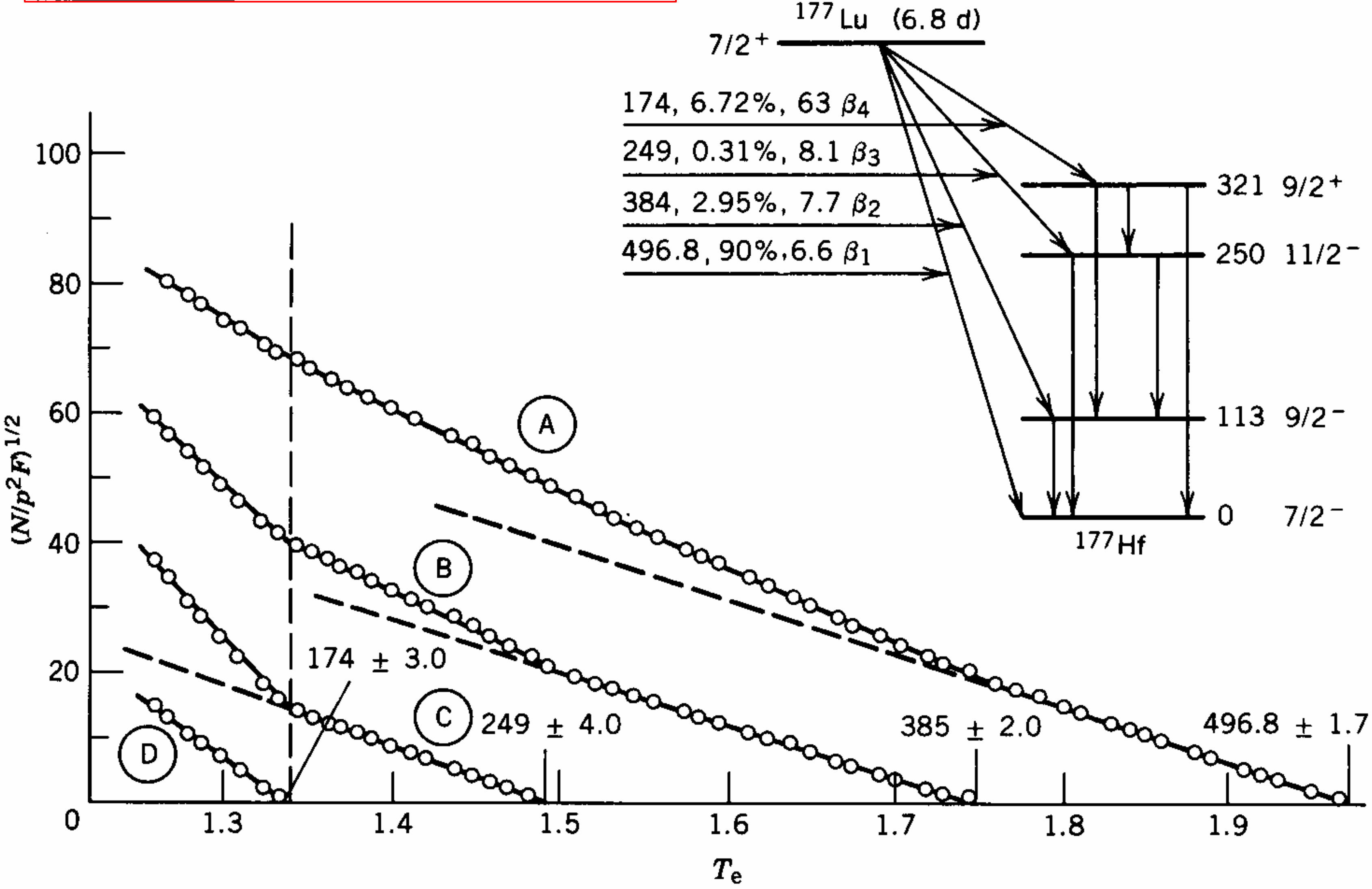

Interaction of charge particles with matter

Light charge particles (electrons)

excitation and ionization of atoms in absorber material (atomic effects)
interaction with electrons in materials (collision, scatter)
deceleration by Coulomb interaction (Bremsstrahlung)

Heavy charged particles (Z>1)

excitation and ionization of atoms in absorber material (atomic effects
Coulomb interaction with nuclei in material (collision, scatter)
(long range forces)

Neutrons:

interaction by collision with nuclei in material (short range forces)

Interaction of Charged Particles with Matter

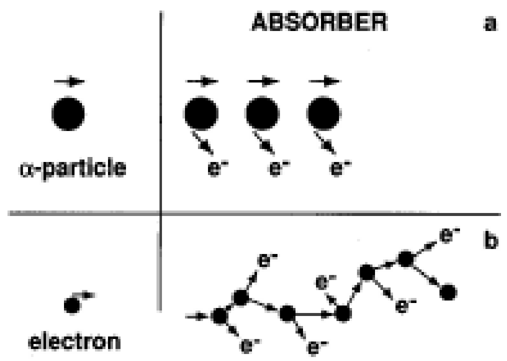

Interaction of gamma-rays with matter

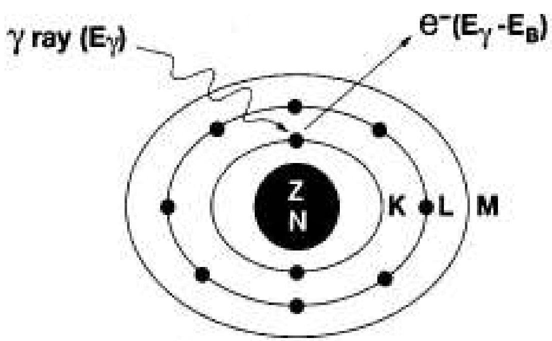

Photoelectric Effect

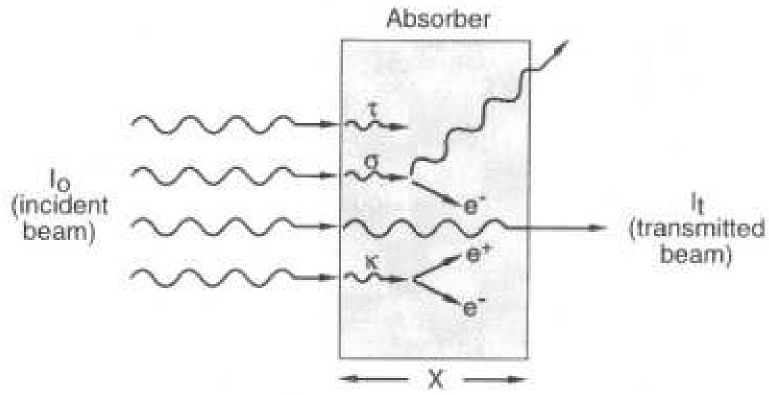

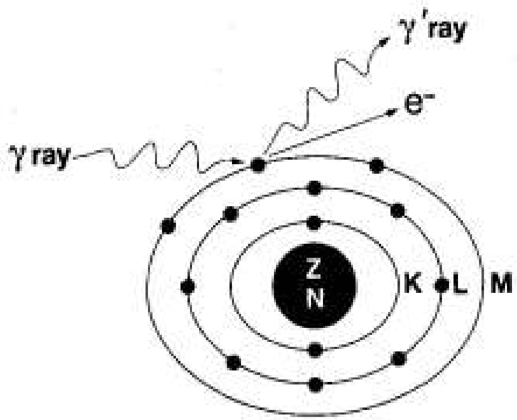

Compton Scattering

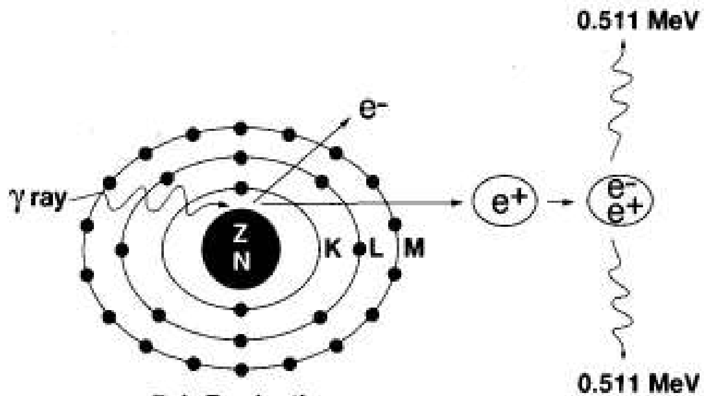

Pair Production

Compton scattering

$$E'_\gamma = \frac{E_\gamma}{1 + (E_\gamma/mc^2)(1 - \cos\theta)}$$

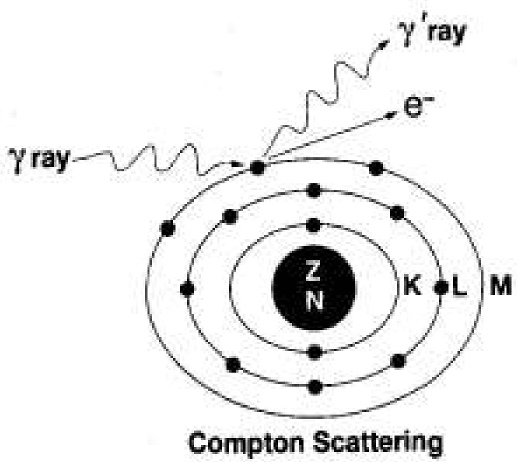

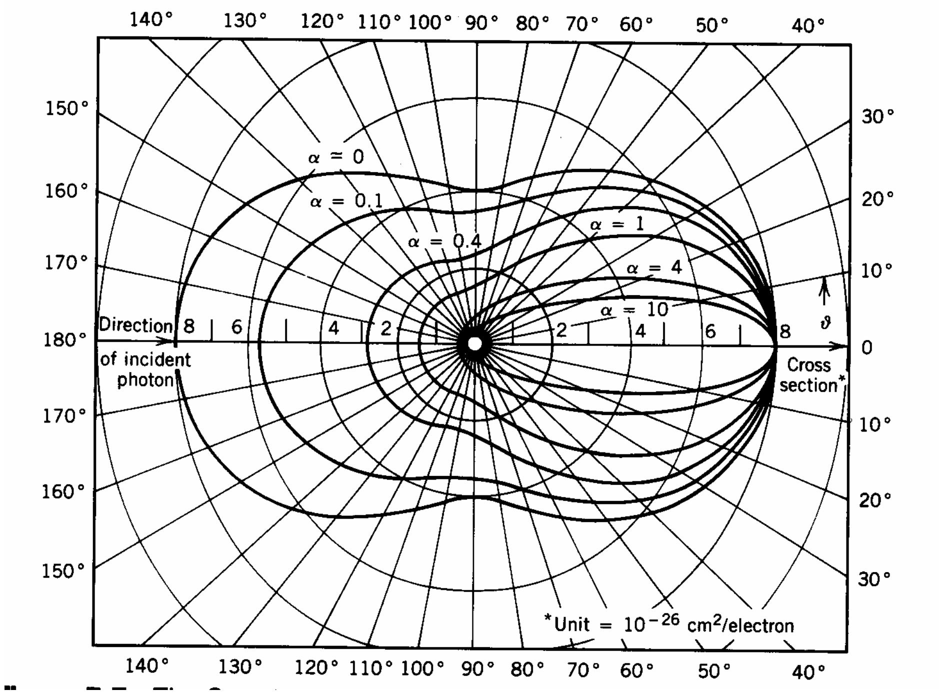

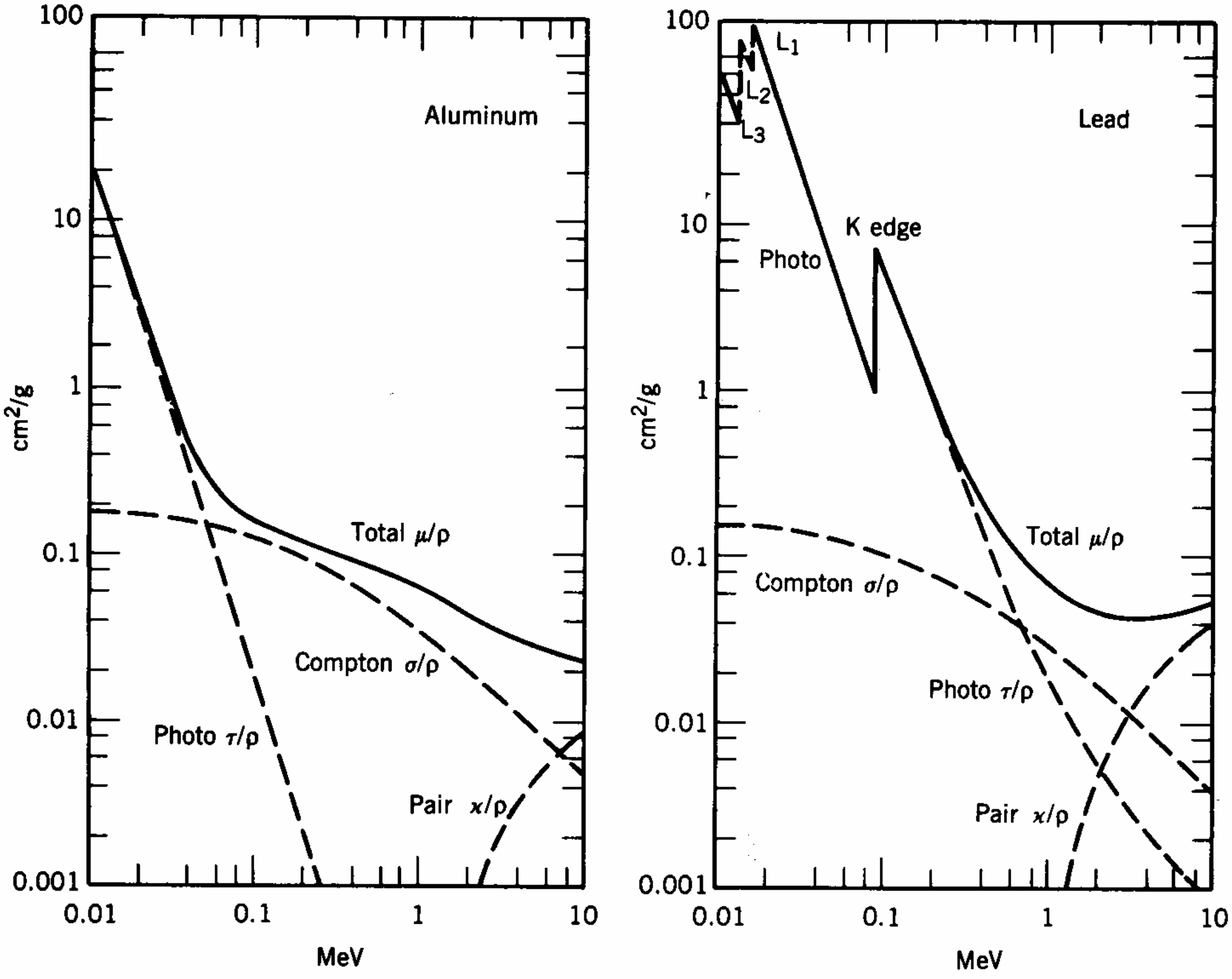
Aluminum
100
10
1
0.1
0.01
0.001
cm²/g
0.01
0.1
1
10
MeV
Total μ/ρ
Compton σ/ρ
Photo τ/ρ
Pair κ/ρ
Lead
L1
L2
L3
K edge
Photo
Total μ/ρ
Compton σ/ρ
Photo τ/ρ
Pair κ/ρ

Space inside an atom is empty !

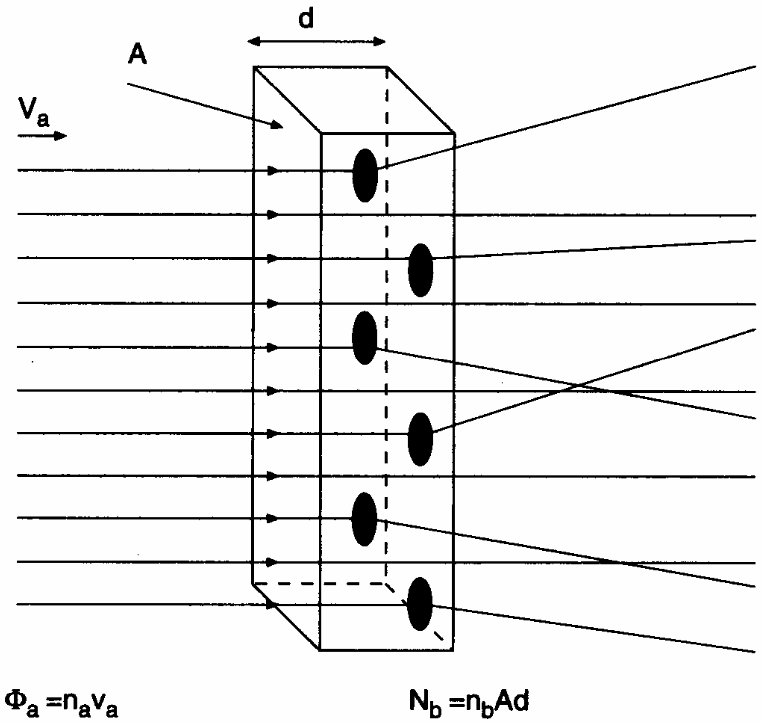

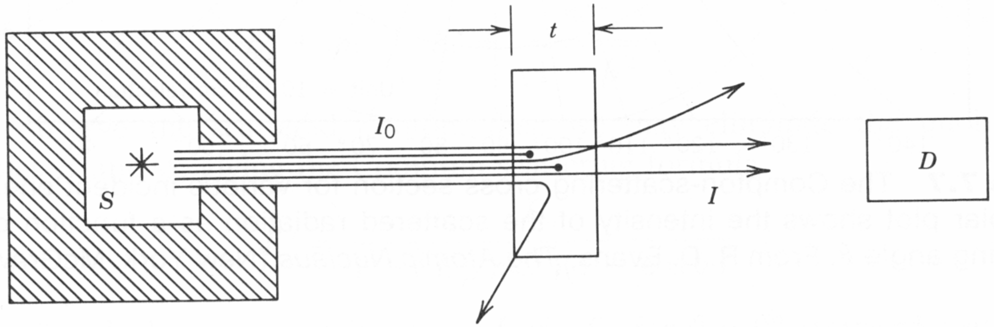

Detectors for nuclear radiation

Scintillators:	gamma, beta, charged particles
	poor energy resolution
	excellent time resonse
Semiconductors HPGe:	gamma, beta
	excellent energy resolution
	poor time response

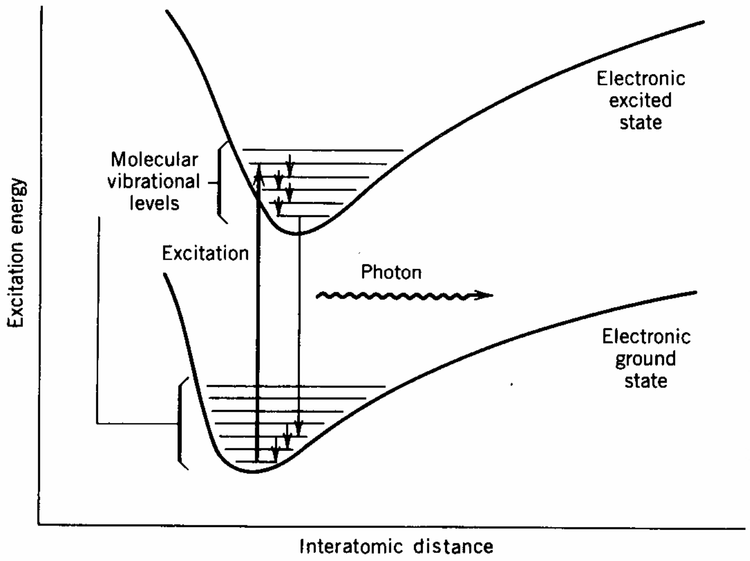

Organic scintillators

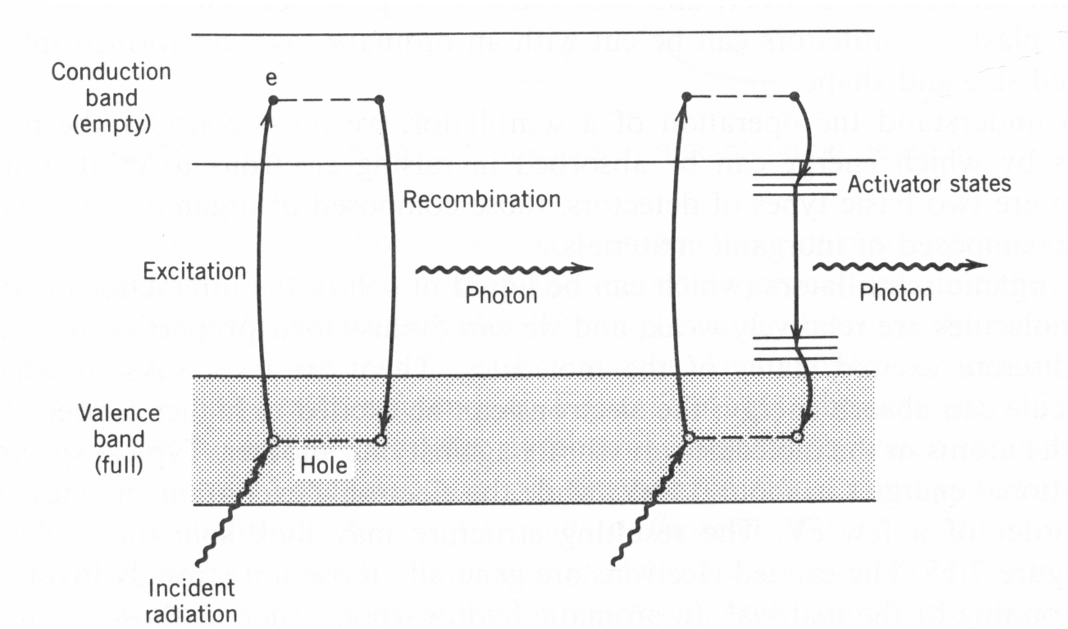

Crystals

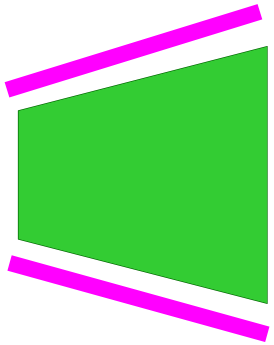

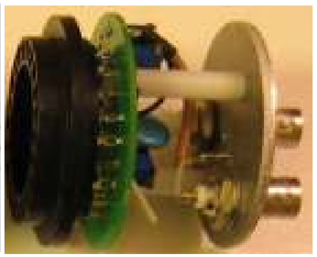

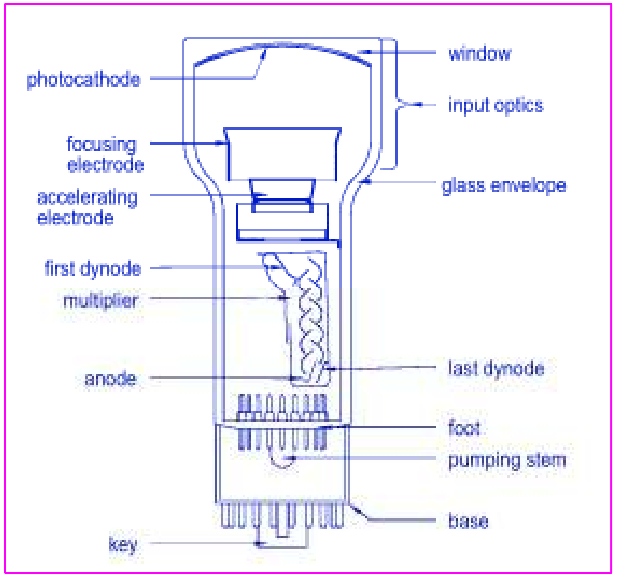
photocathode
window
input optics
focusing electrode
accelerating electrode
glass envelope
first dynode
multiplier
last dynode
anode
foot
pumping stem
base
key

Key aspects of fast response phototubes

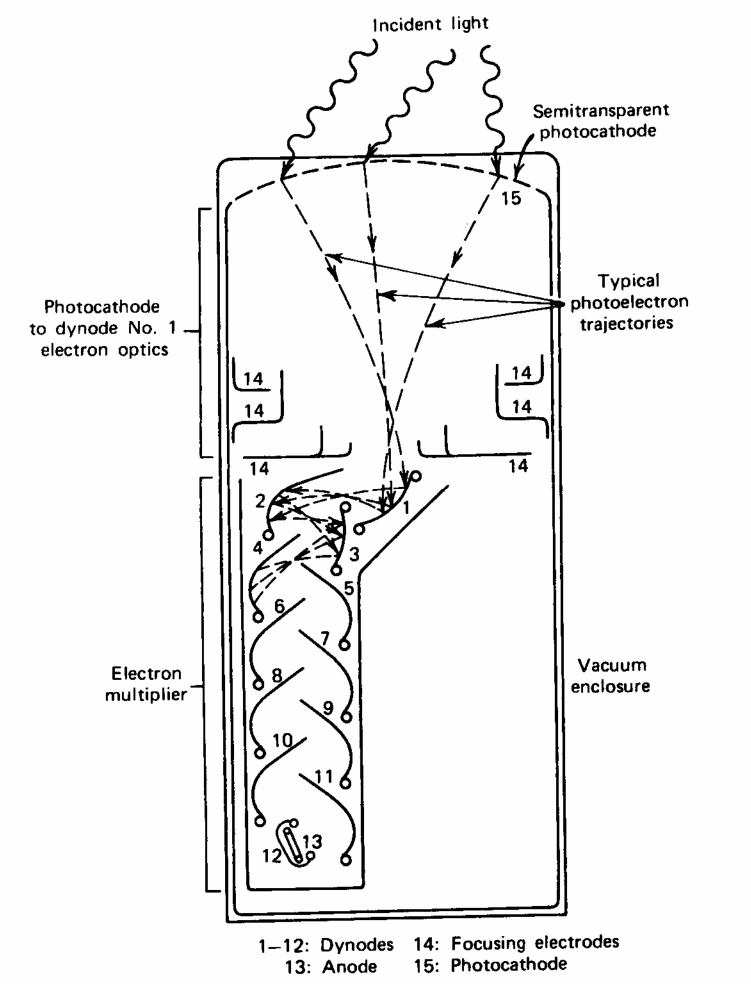

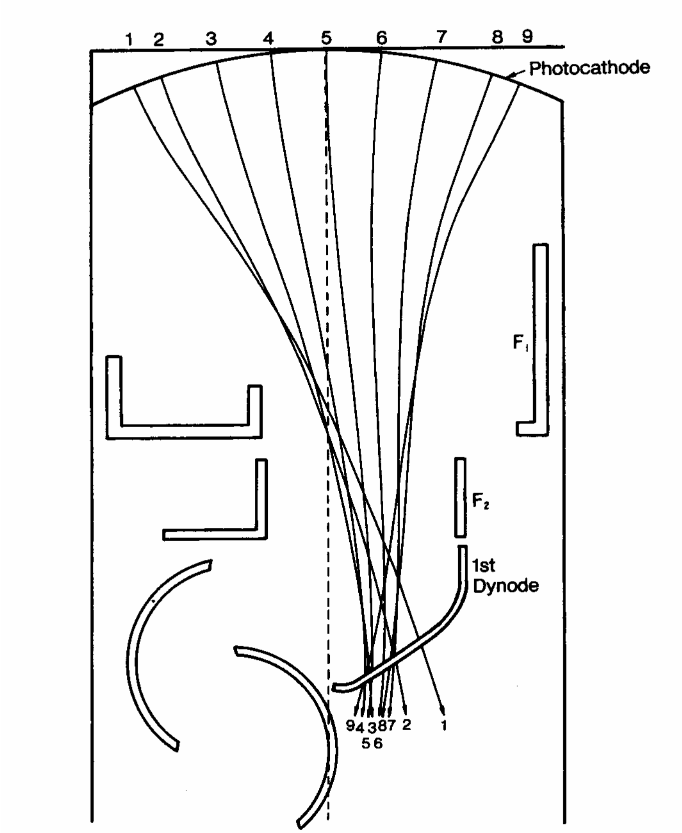

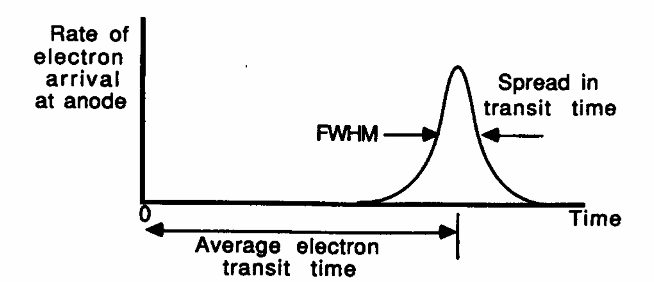

HPGe

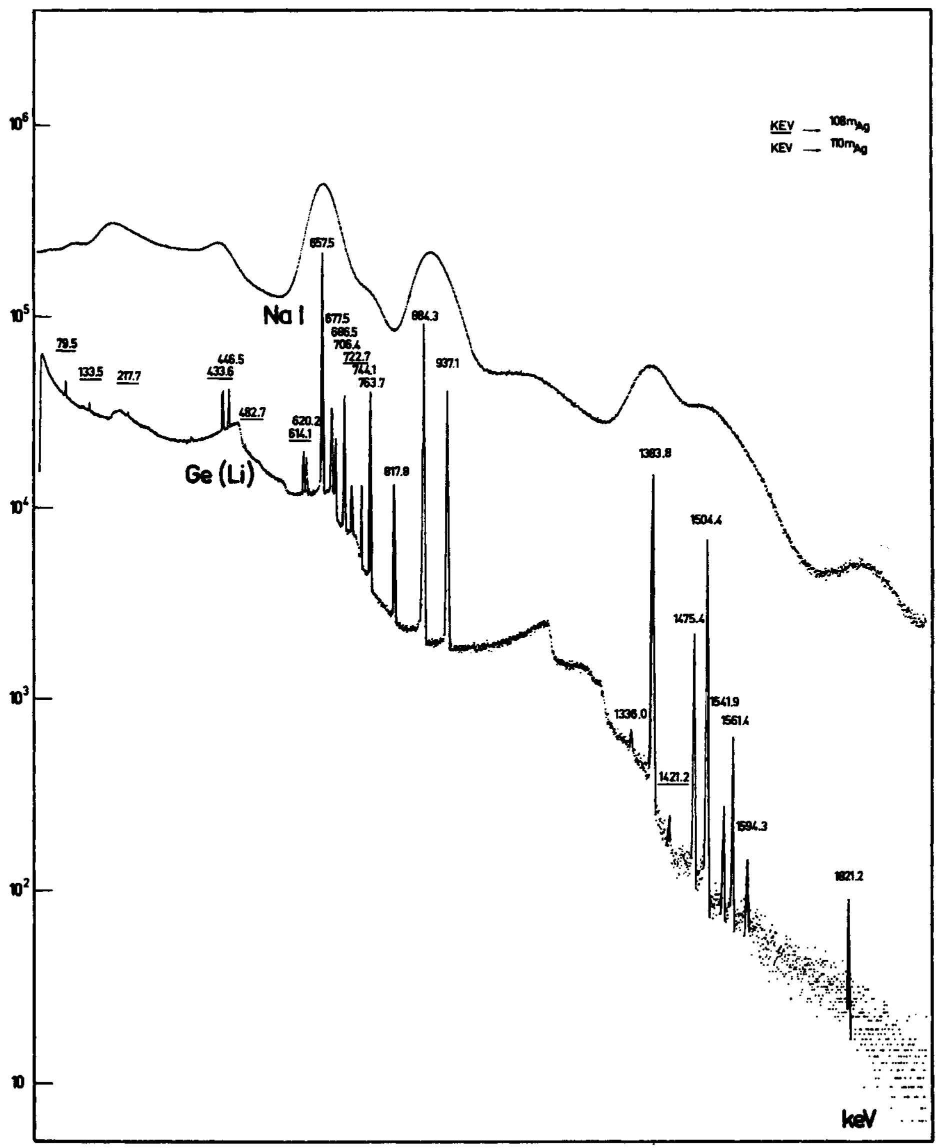

KEV → 108mAg
KEV → 110mAg
10^6
10^5
10^4
10^3
10^2
10
Na I
Ge (Li)
79.5
133.5
217.7
446.5
433.6
482.7
620.2
614.1
657.5
677.5
686.5
706.4
722.7
744.1
763.7
817.9
884.3
937.1
1383.8
1336.0
1421.2
1475.4
1504.4
1541.9
1561.4
1594.3
1821.2
keV

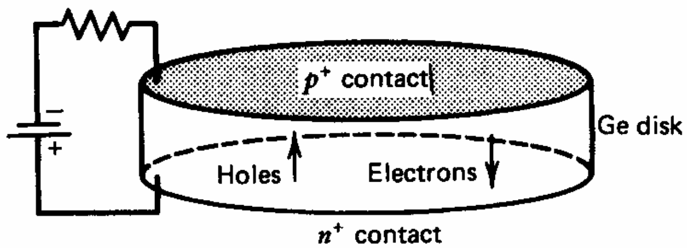

p^+ contact
Ge disk
Holes
Electrons
n^+ contact
−
+

Signal processing: the amplifier

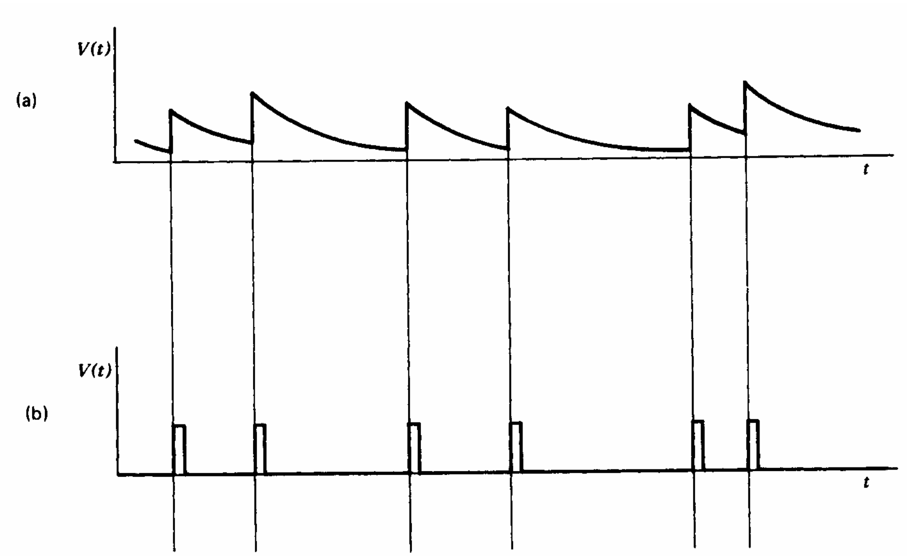

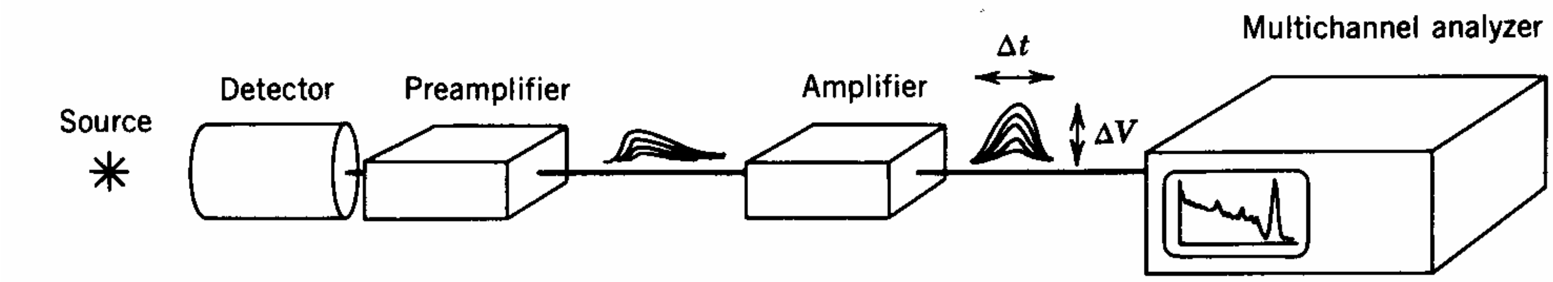

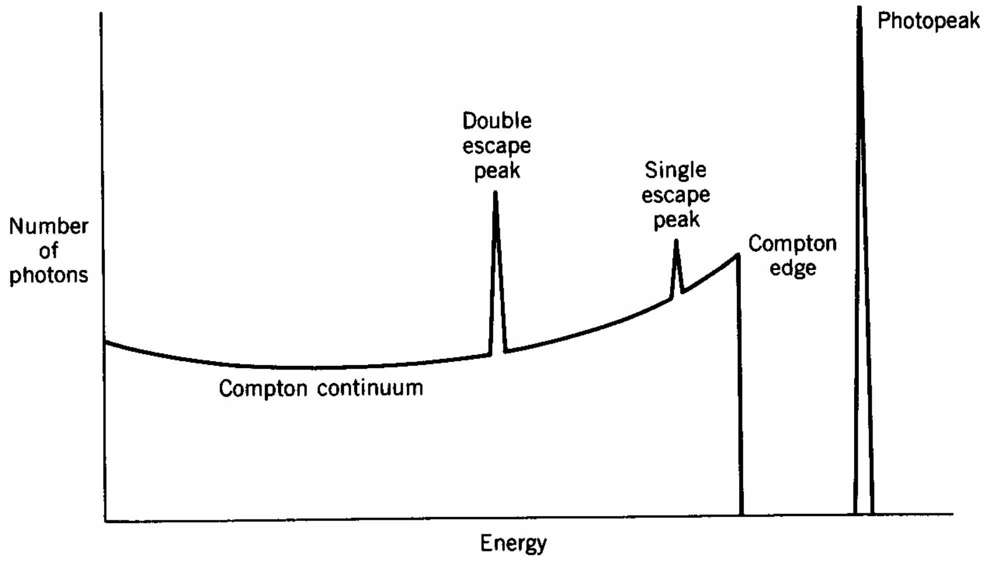

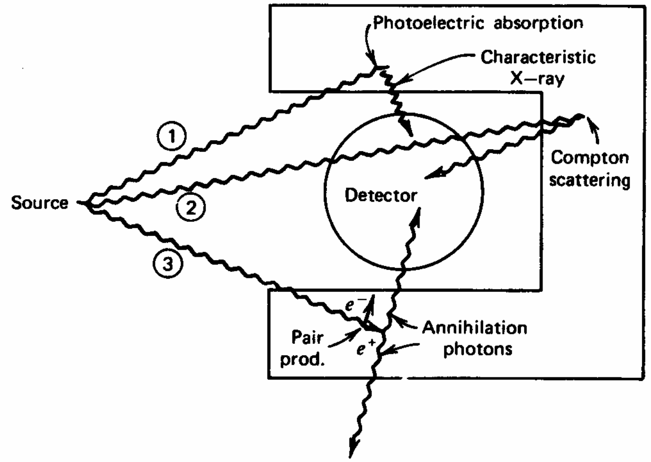

Schematic energy spectra in HPGe

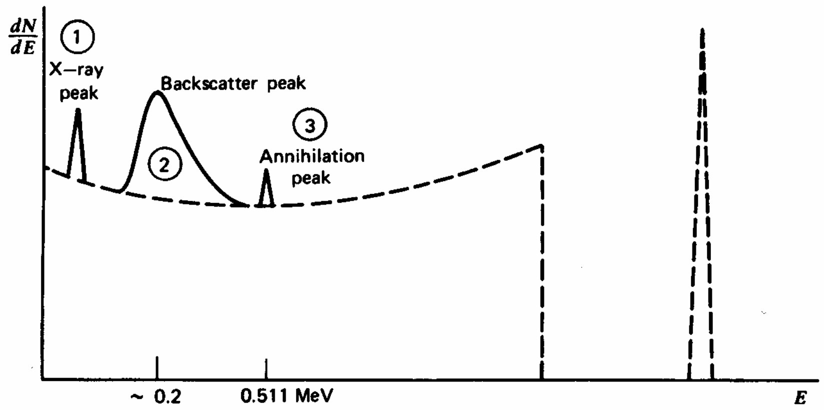

Signal processing: coincidence circuit

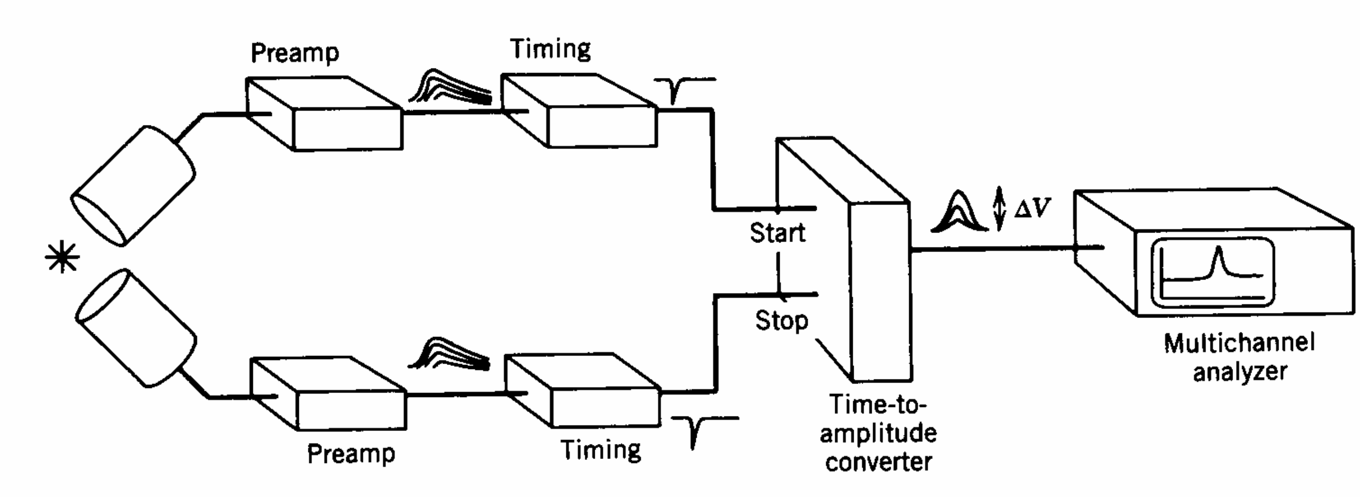

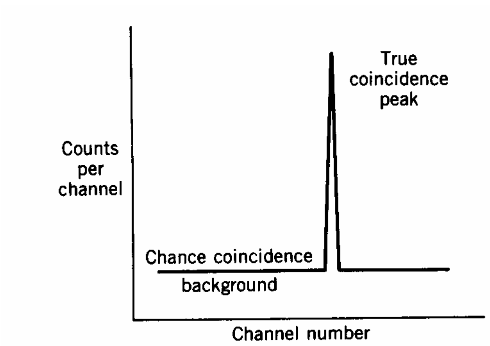

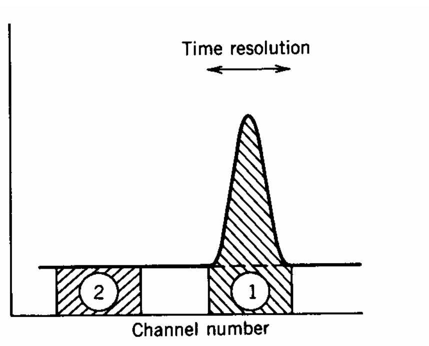

Random or true events?

Detectors are mostly idle!

True time determination of a hit in a detector

Trigger level

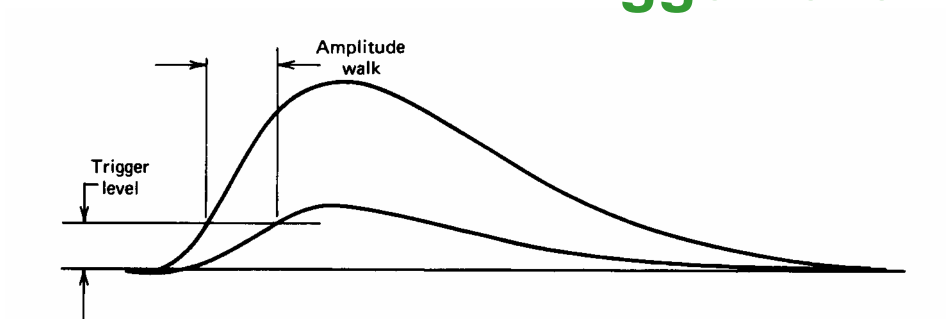

Noise issue

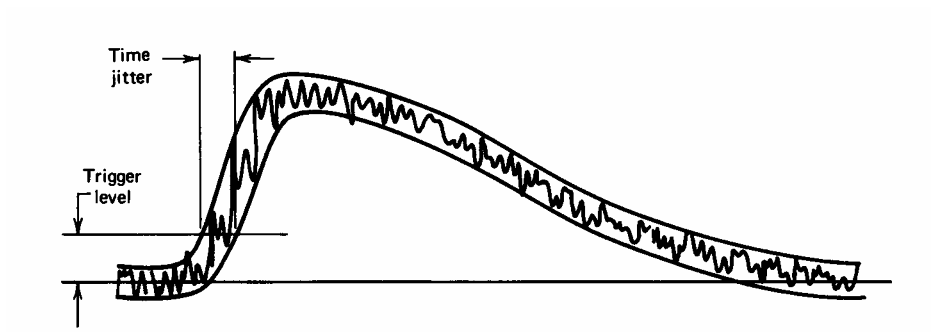

CFD solution

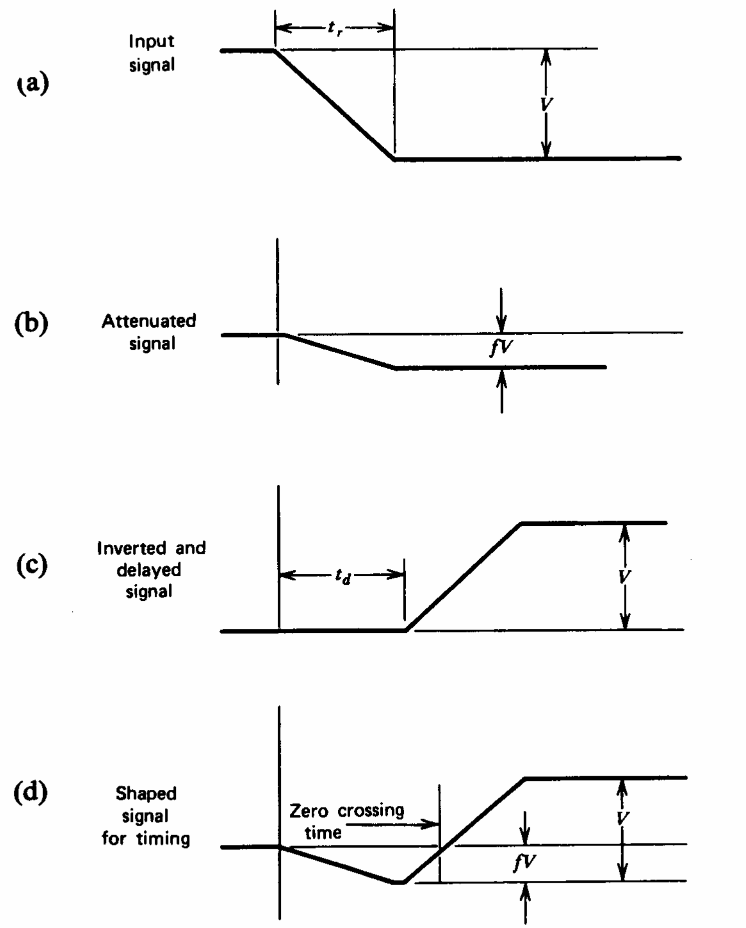

Random events

- Random events ("randoms") are γ-events uncorrelated to the β-decay.

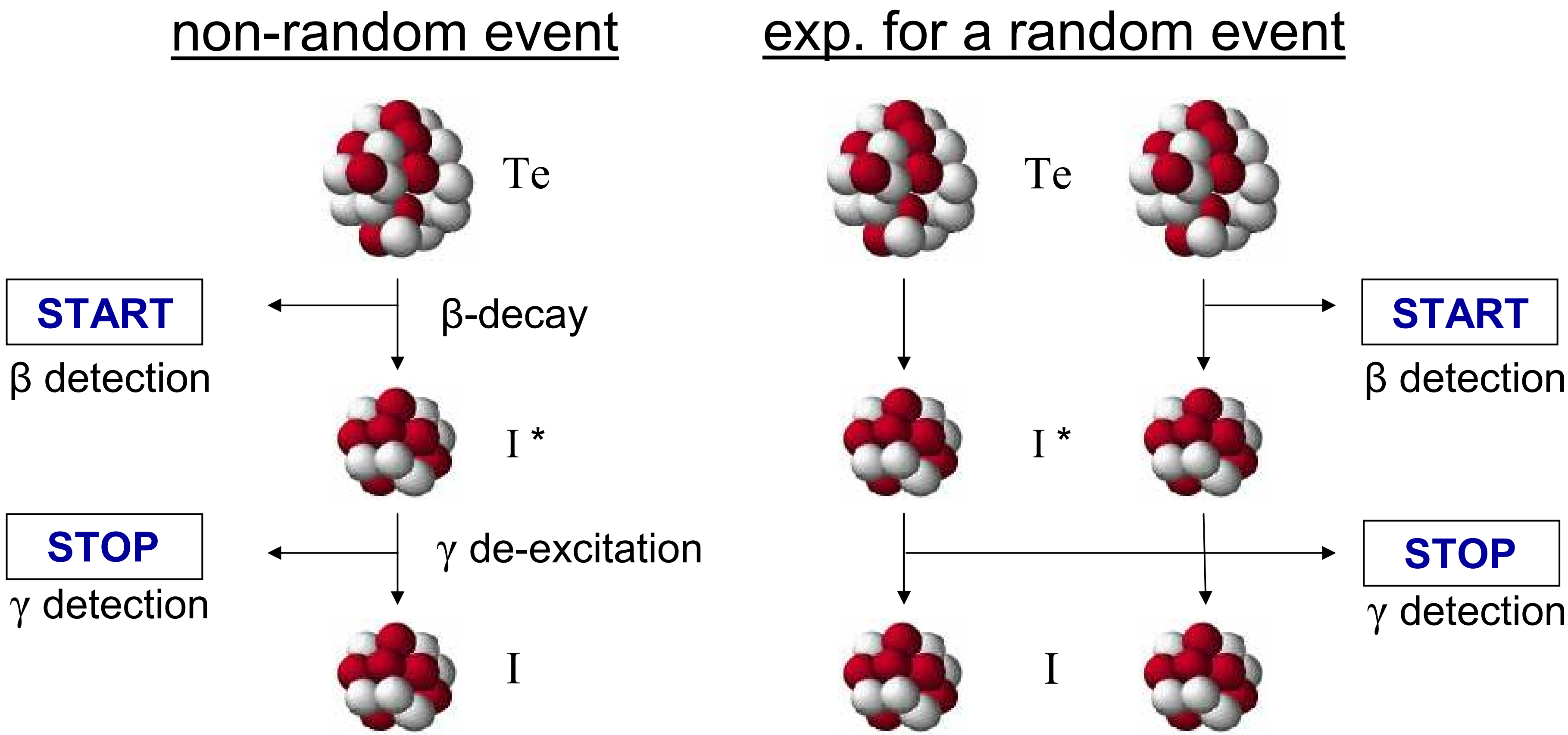

From Ralf Schuber

Constructing a level scheme

total Ge energy spectrum

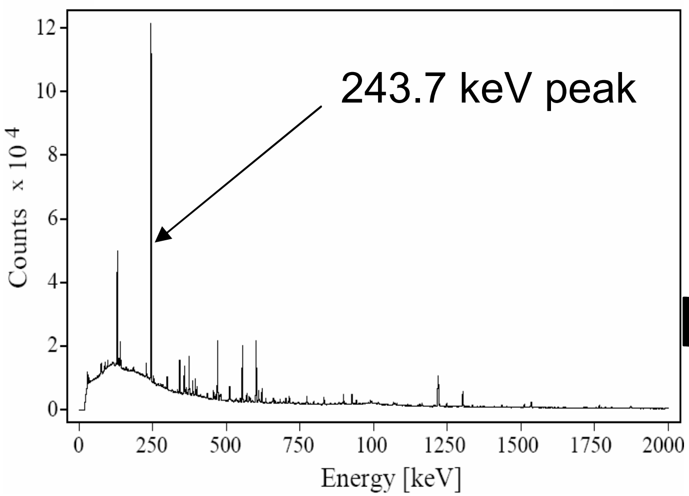

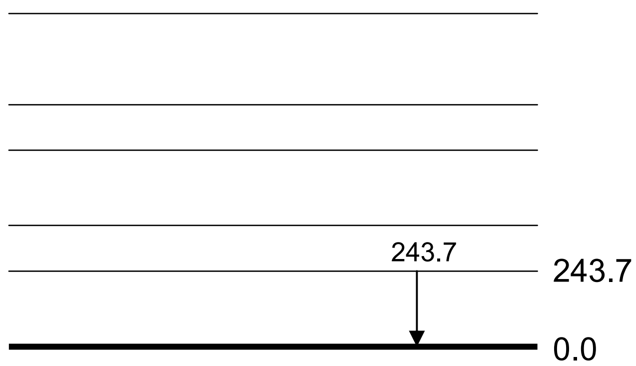

Set gates on full energy peak in the Ge spectrum. When viewing the gated spectrum, coincident γ–rays can be seen.

gated spectrum on '243.7'

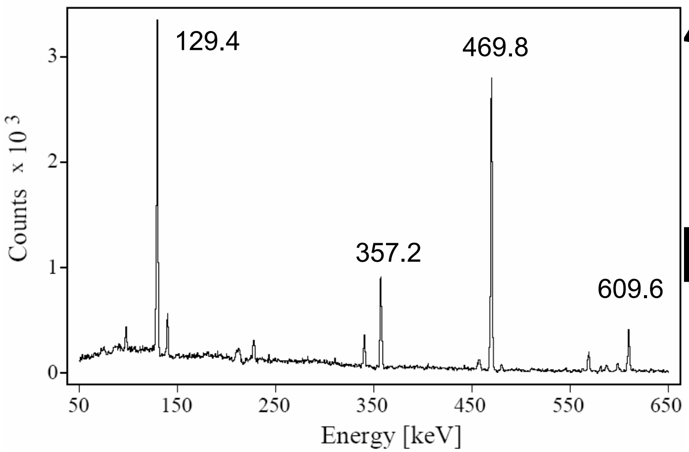

Strong γ–rays in coincidence

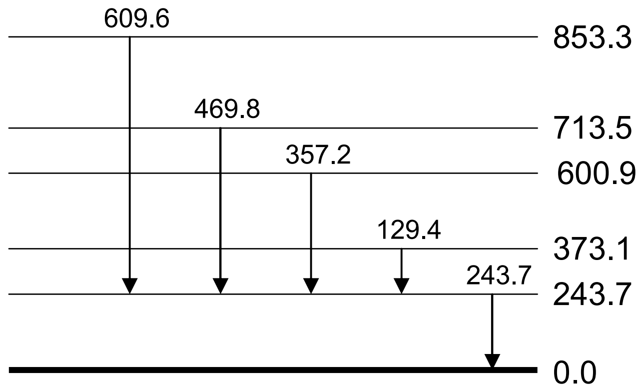

part of the decay scheme of ^{137}I

Inverting the gate of one of the γ–rays in coincident with the 243.7 keV peak

total Ge spectrum

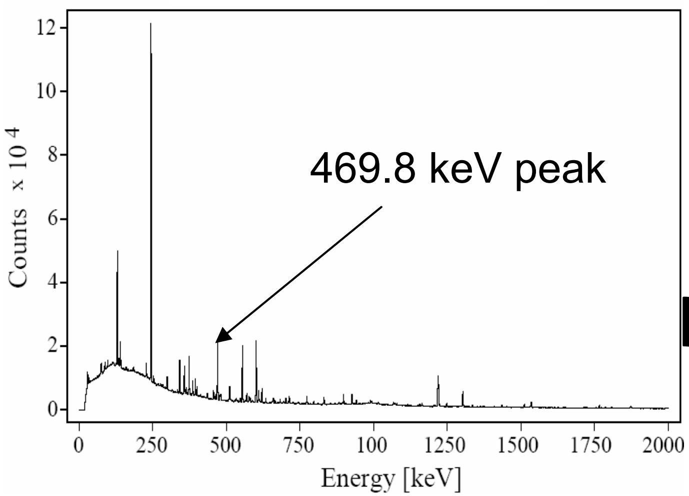

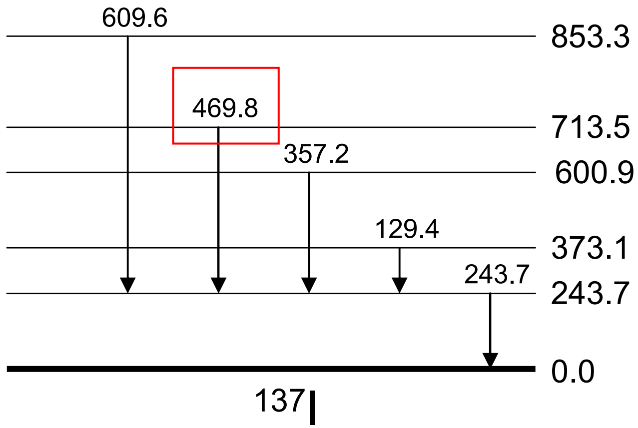

By selecting the 469.8 keV peak one should see the 243.7 keV peak along with other energy peaks with which the 469.8-γ-ray is in coincidence.

gated spectrum on '469.8'

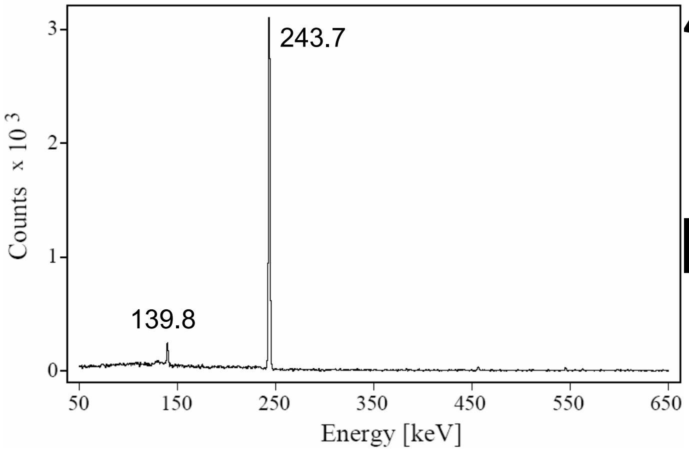

Strong γ–rays in coincidence

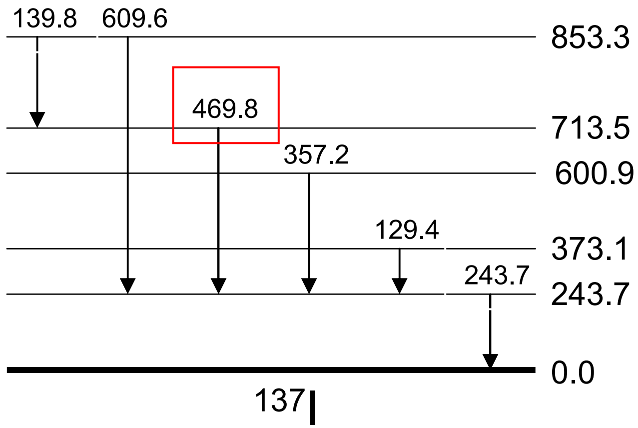

Pause !

The position of the $h_{11/2}$ neutron hole state in ^{131}Sn

The origin of the problem is related to the very special decay properties of the three isomers of ^{131}In.

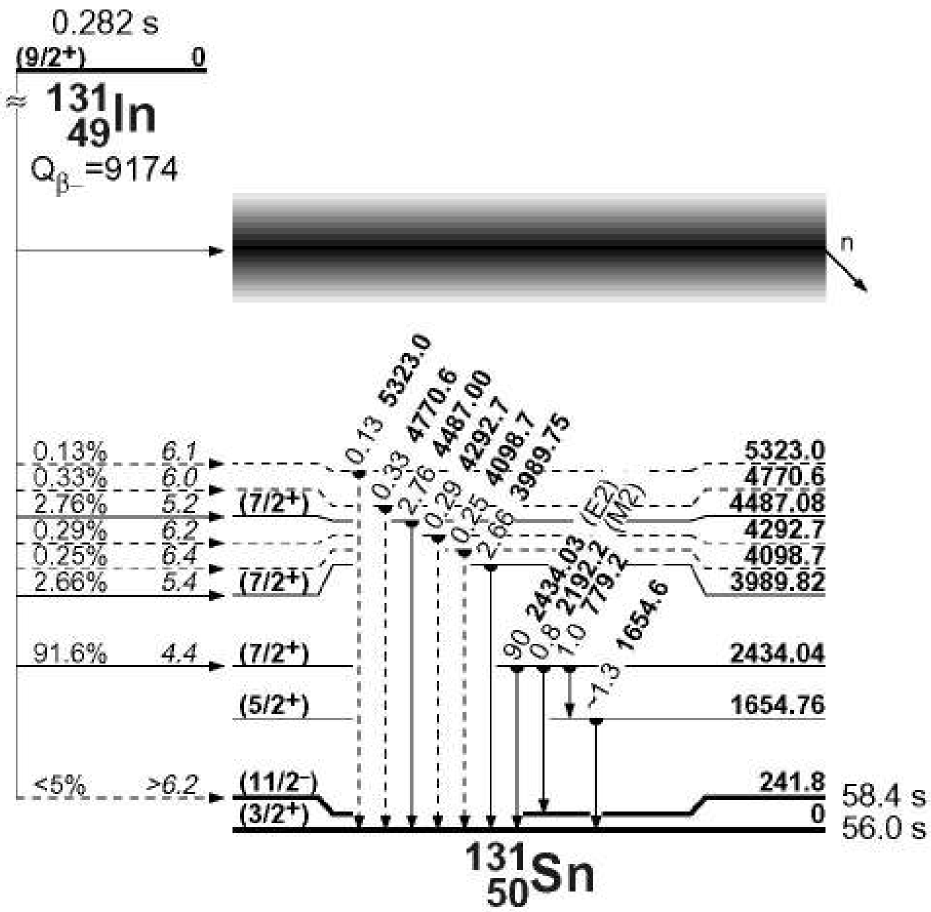

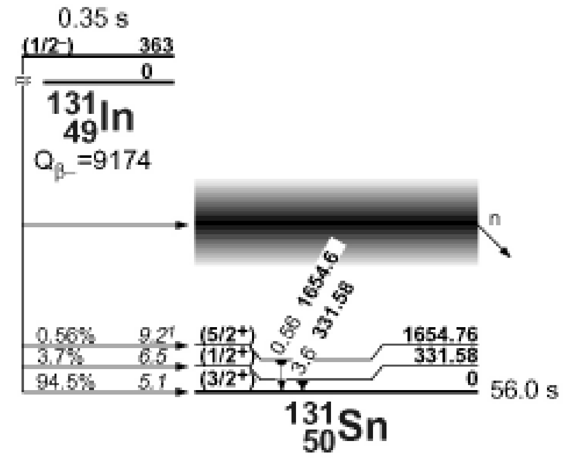

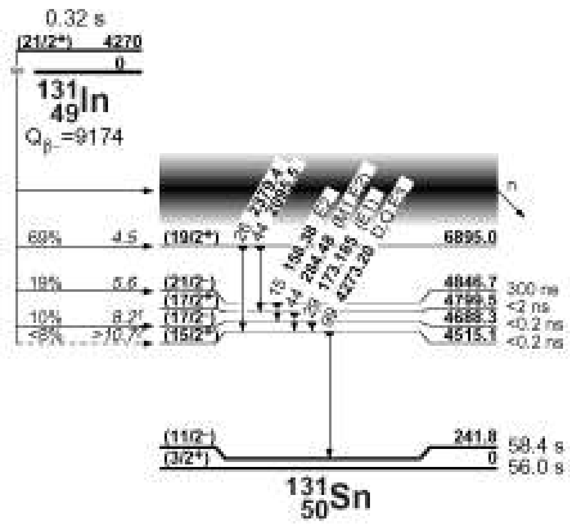

Table of Isotopes 1998, R.B. Firestone et al.

B.Fogelberg and J. Blomqvist, Phys.Lett. B137 (1984) 20, also Nucl.Phys. A429 (1984) 205

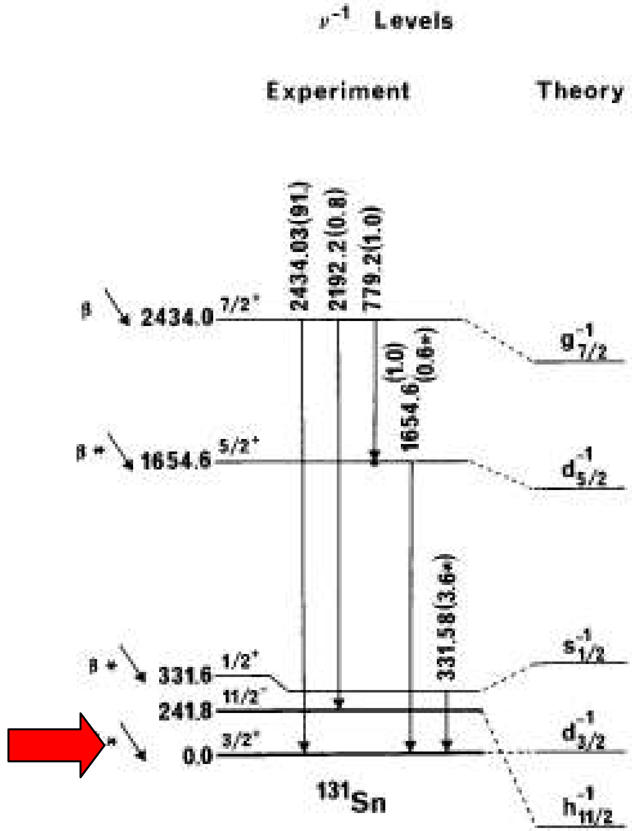

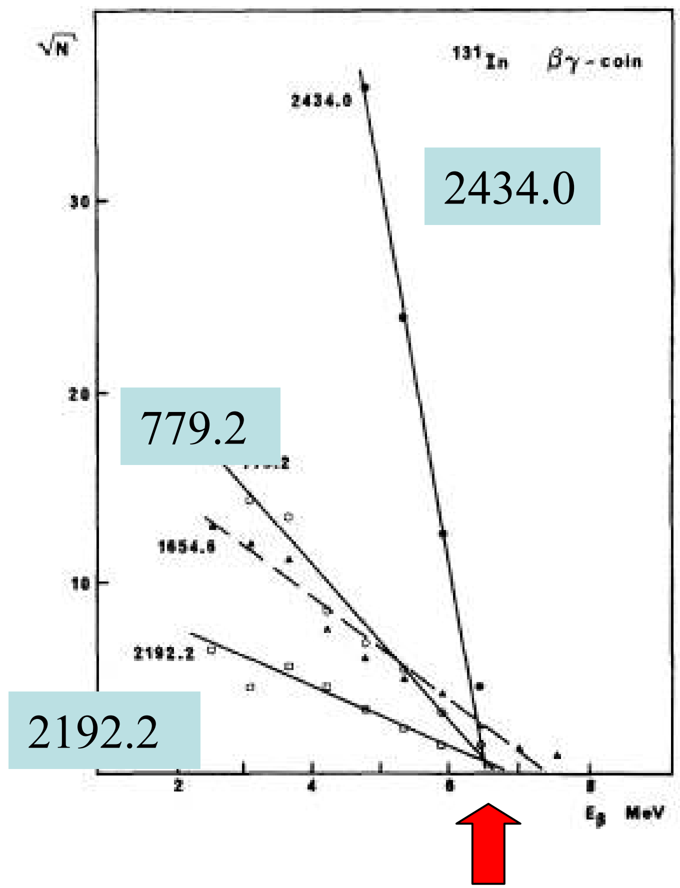

The Qbeta end-point energies shown here suggest strongly that both the 779.2 and 2192.2 keV gamma rays follow the decay of the 2434.0 keV level in ^{131}Sn.

The excitation energy of the 11/2 state in ^{131}Sn was consistently found troublesome !

$$\pi g_{7/2}\nu(f_{7/2}h^{-1}_{11/2})$$

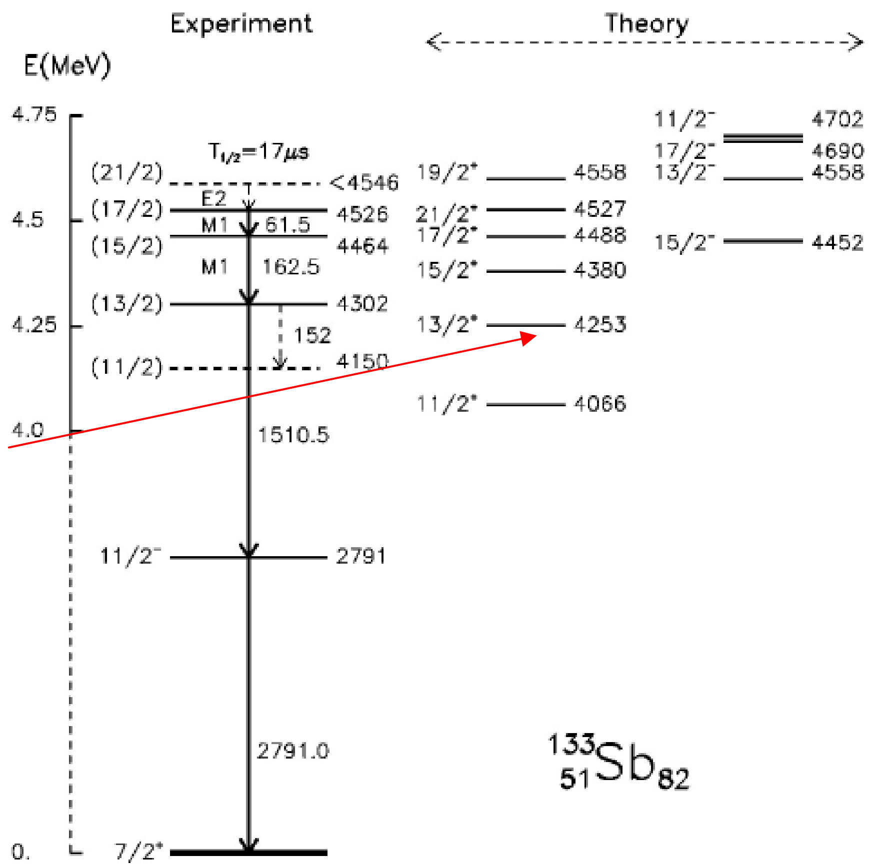

The single-particle energies are also taken from experiment. However, we think that the experimental energy difference $\epsilon h^{-1}_{11/2} - \epsilon d^{-1}_{3/2}$=241.8 keV, measured for ^{131}Sn is very likely uncorrect. We have used in this calculation a more realistic value of 110 keV

J. Genevey et al, Eur. Phys. J. A7 (2000) 463

It followed from their shell model interpretation of the structures in ^{123}Sn-^{129}Sn and $^{124\text{-}130}$Sn that the excitation energy is lower than 140 keV.

The OSIRIS fission product separator was located at the Studsvik Laboratory in Sweden.

Thermal neutrons were provided by the R2-0 600 kW reactor, which was a movable reactor.

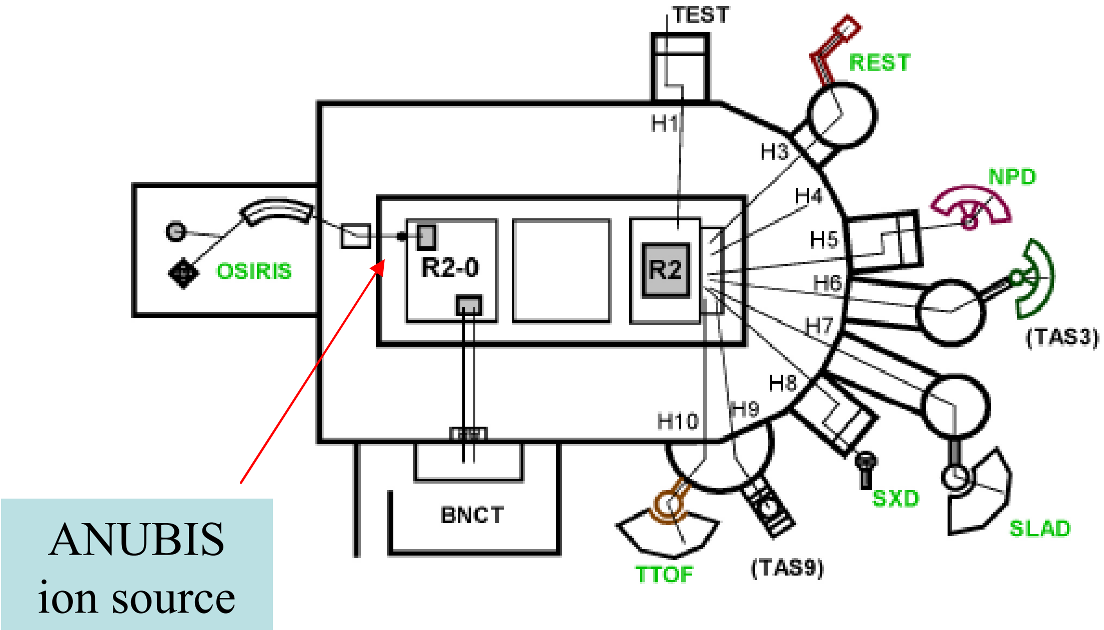

It utilizes a high temperature ANUBIS-type integrated target-ion-source with typically a target of about 1 g of ^{235}U

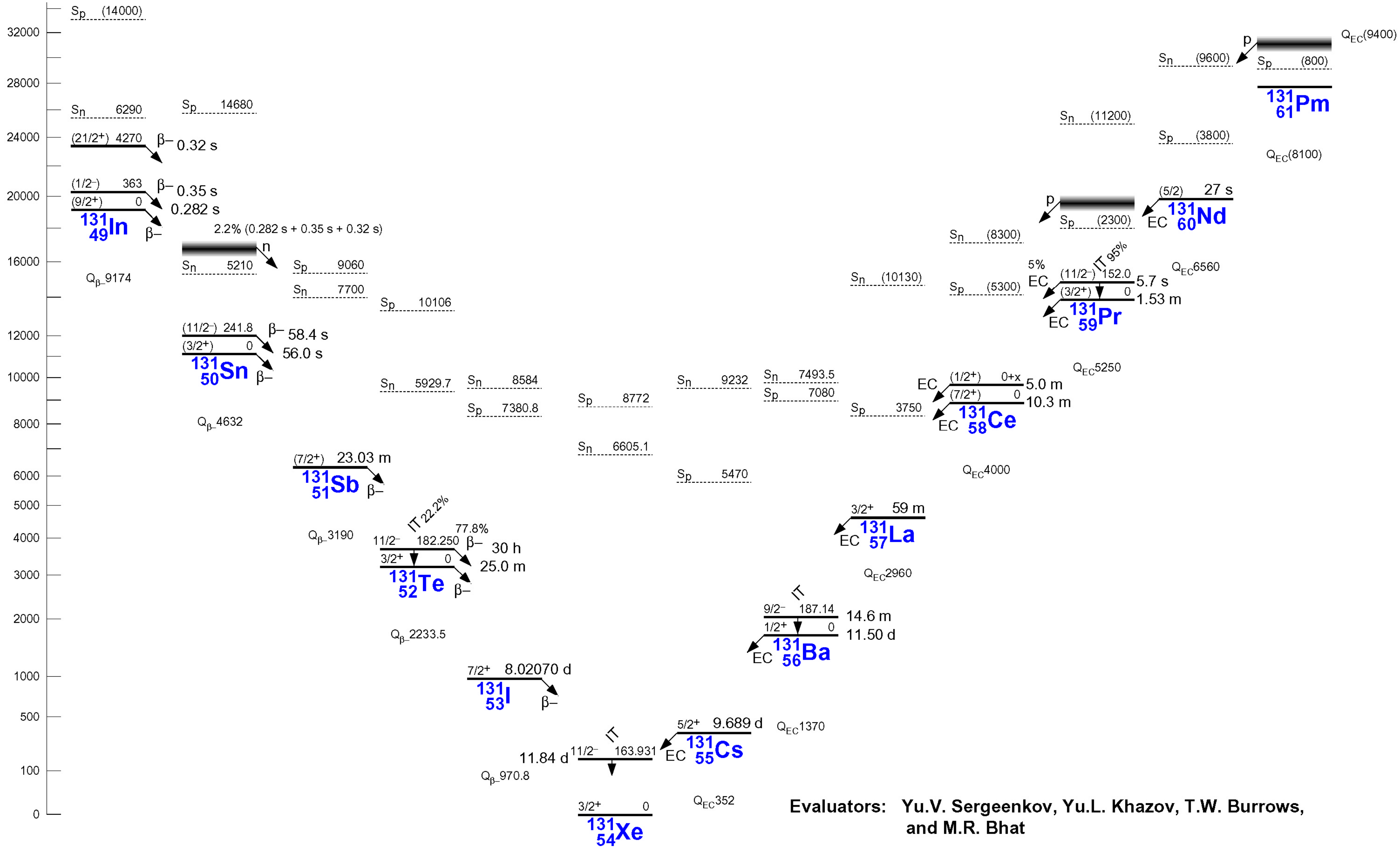

Evaluators: Yu.V. Sergeenkov, Yu.L. Khazov, T.W. Burrows, and M.R. Bhat

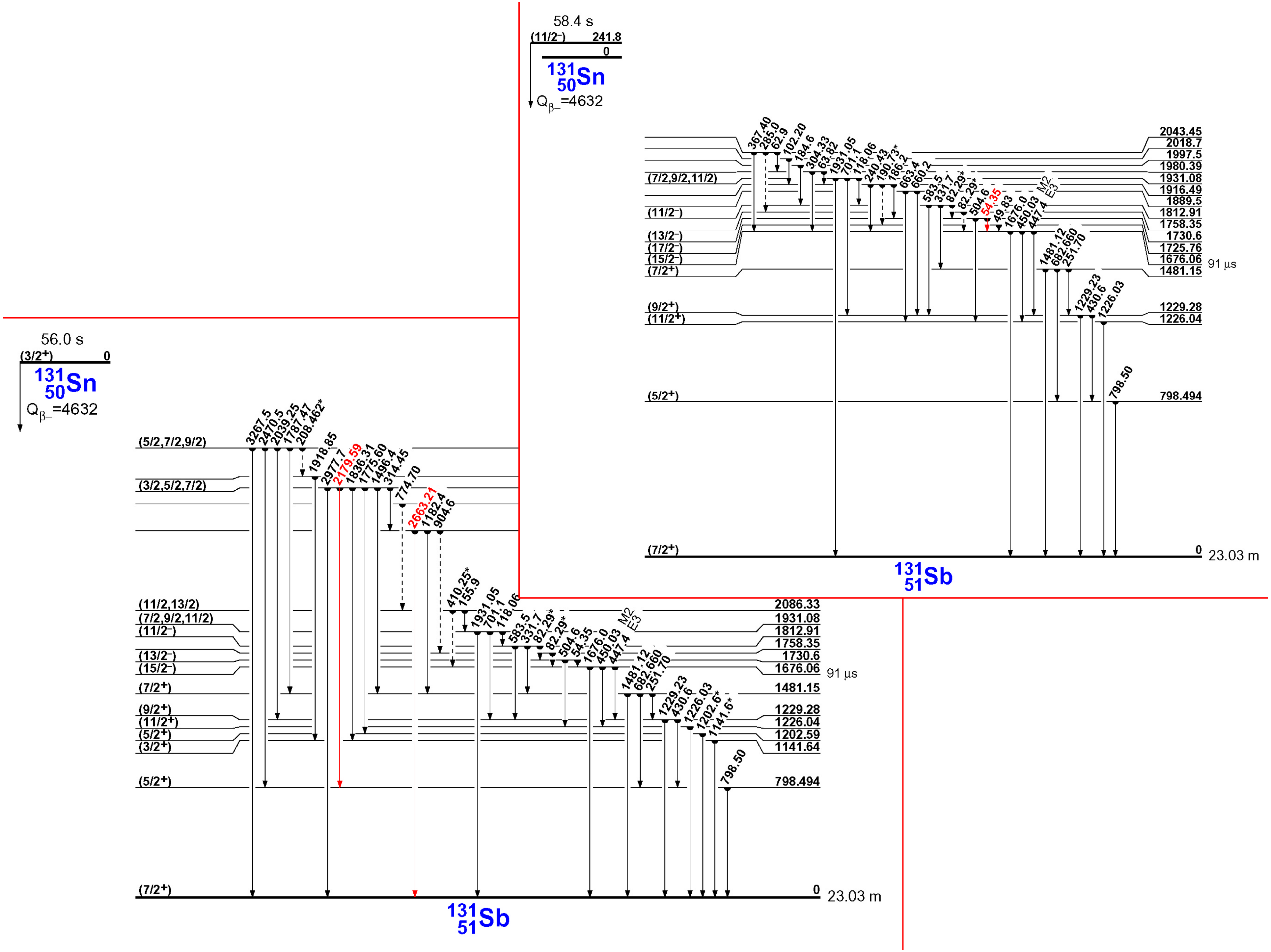

58.4 s
(11/2−) 241.8
0
131 50 Sn
Qβ− =4632
2043.45
2018.7
1997.5
1980.39
(7/2,9/2,11/2) 1931.08
1916.49
1889.5
(11/2−) 1812.91
1758.35
(13/2−) 1730.6
(17/2−) 1725.76
(15/2−) 1676.06 91 µs
(7/2+) 1481.15
(9/2+) 1229.28
(11/2+) 1226.04
(5/2+) 798.494
(7/2+) 0 23.03 m
131 51 Sb
56.0 s
(3/2+) 0
131 50 Sn
Qβ− =4632
(5/2,7/2,9/2)
(3/2,5/2,7/2)
(11/2,13/2) 2086.33
(7/2,9/2,11/2) 1931.08
(11/2−) 1812.91
1758.35
(13/2−) 1730.6
(15/2−) 1676.06 91 µs
(7/2+) 1481.15
(9/2+) 1229.28
(11/2+) 1226.04
(5/2+) 1202.59
(3/2+) 1141.64
(5/2+) 798.494
(7/2+) 0 23.03 m
131 51 Sb
M2
E3

A number of experiments have been performed at the OSIRIS fission product mass separator at Studsvik and included gamma-gamma coincidences using Ge spectrometers and beta-gamma Qbeta measurements using a thin HPGe spectrometer for beta detection and a well shielded Ge detector.

To start with, no trace of the previously observed 2192 keV gamma line was found !

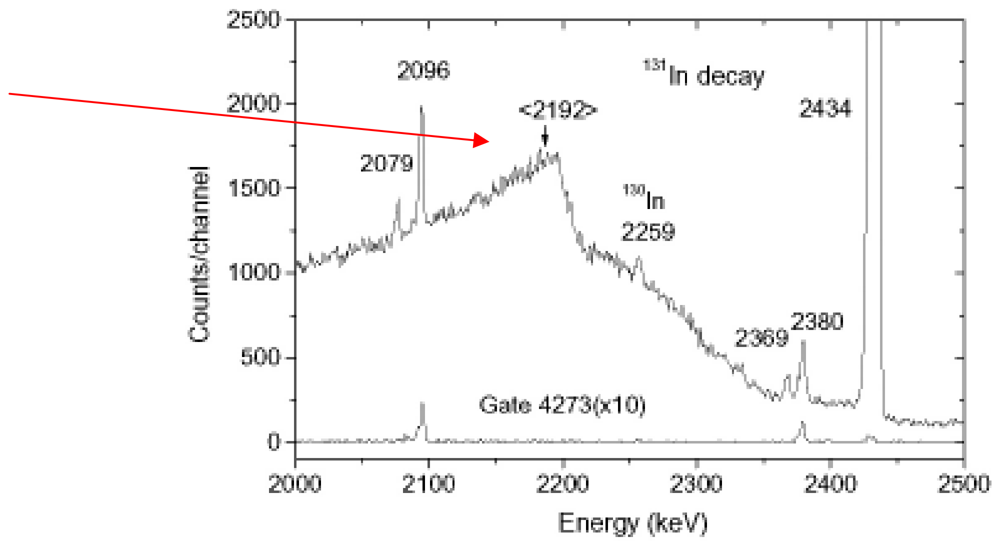

Beta-particle-gated gamma-ray spectrum obtained for the decays of the three isomers of ^{131}In. Data from the new experiment.

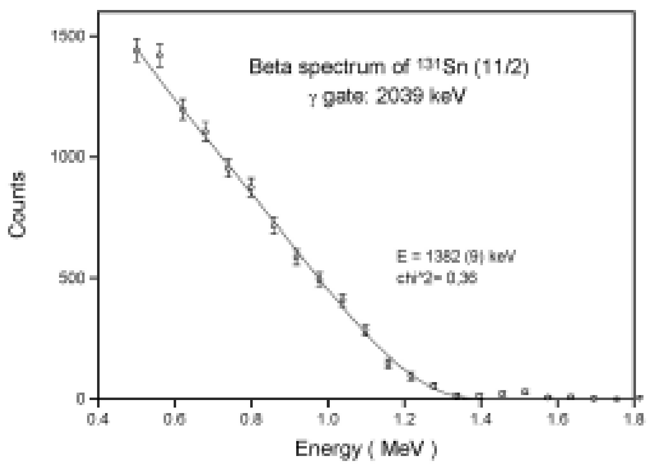

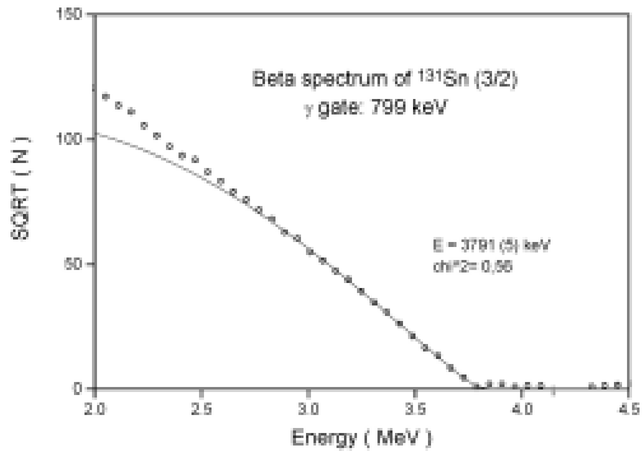

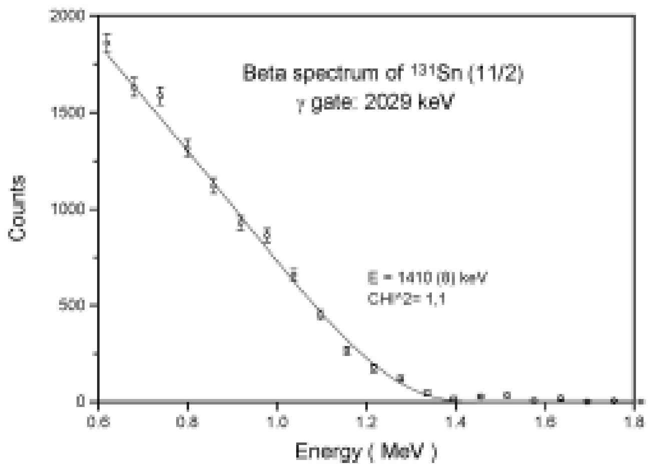

Excitation energy of the 11/2- state in ^{131}Sn is:

69(14) keV

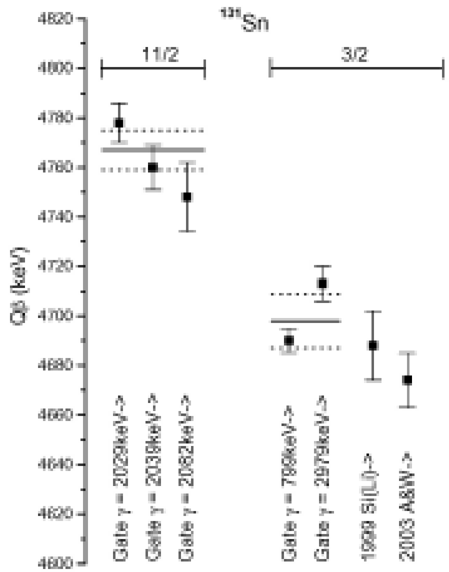

Beta energy spectra gated by respective gamma-rays from the two isomers of ^{131}Sn; data from the beta-gamma Qbeta measurements at OSIRIS.

B. Fogelberg et al. PRC70, 034312 (2004)

A more precise value of 65.1 keV may be deduced from the level scheme of ^{131}Sn obtained currently, however without firm support from gamma-gamma coincidence data.

The new value of 69(14) keV, which is relatively low, is in agreement with systematics and in disagreement with the previous determination.

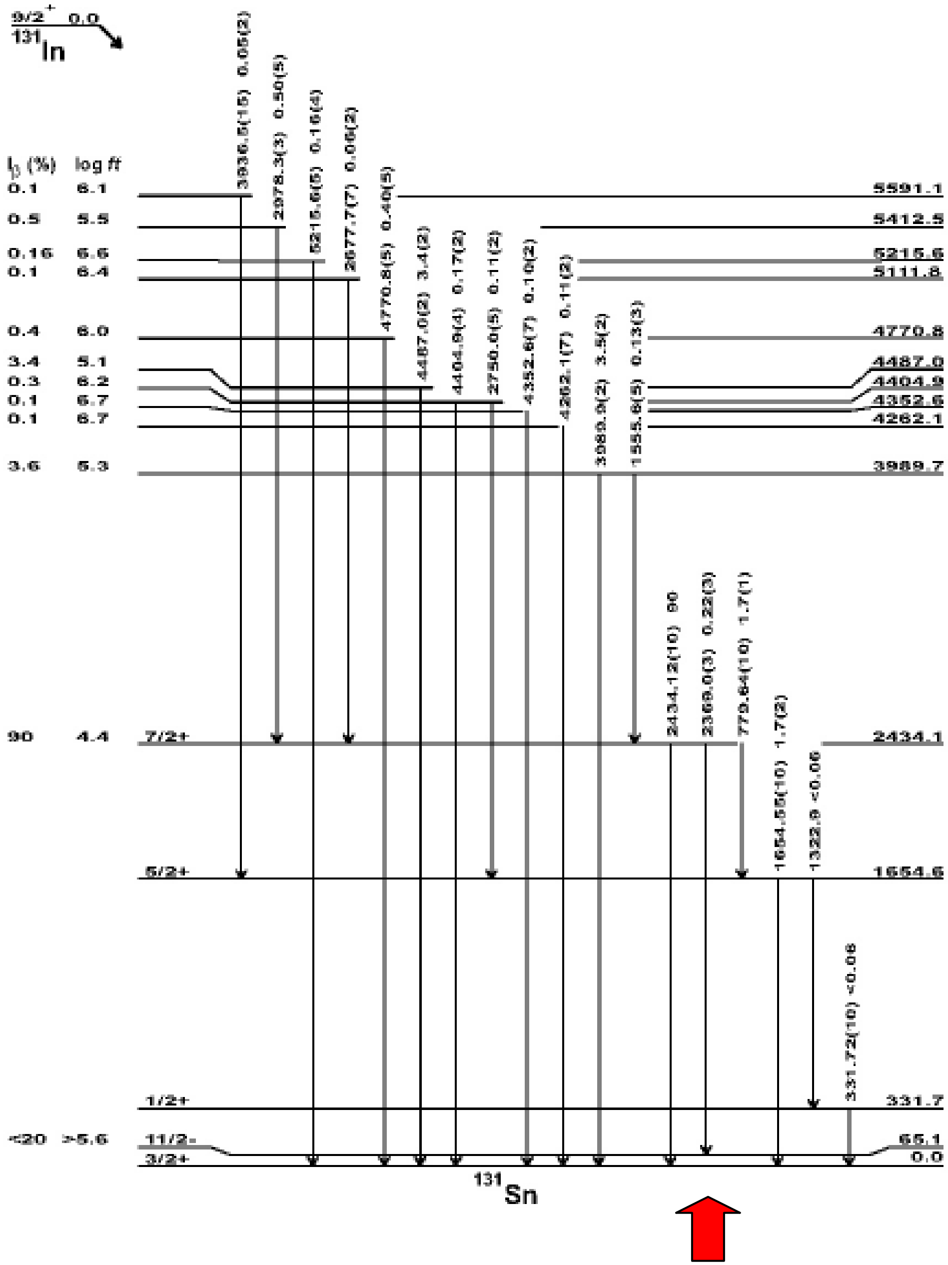

Ultra fast timing and transition rates

Transition matrix elements

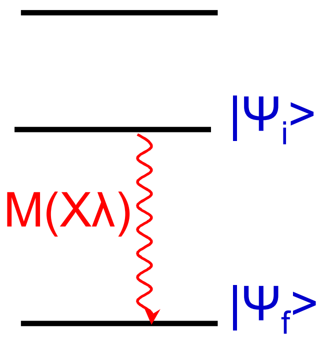

J_i π_i

$$B\left(X\lambda; I_i \to I_f\right) = (2I_i + 1)^{-1} \left| \left\langle \psi_f \| M(X\lambda) \| \psi_i \right\rangle \right|^2$$

J_f π_f

Selection rules for some electromagnetic transitions.

Multi-polarity	Electric			Magnetic		
	$E\ell$	$\lvert\Delta J\rvert$	ΔP	$M\ell$	$\lvert\Delta J\rvert$	ΔP
Dipole	E1	1	−	M1	1	+
Quadrupole	E2	2	+	M2	2	−
Octupole	E3	3	−	M3	3	+

Variety of cases

$$B(^M_E\lambda; I_i \rightarrow I_f) = \frac{L[(2L+1)!!]^2\hbar}{8\pi(L+1)}\left(\frac{\hbar c}{E_\gamma}\right)^{2L+1} \quad P_\gamma(^M_E\lambda; I_i \rightarrow I_f)$$

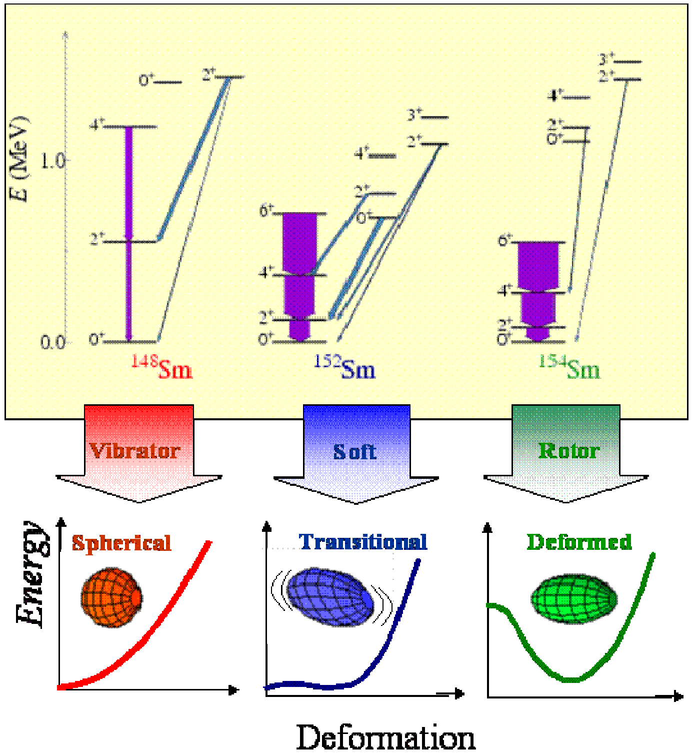

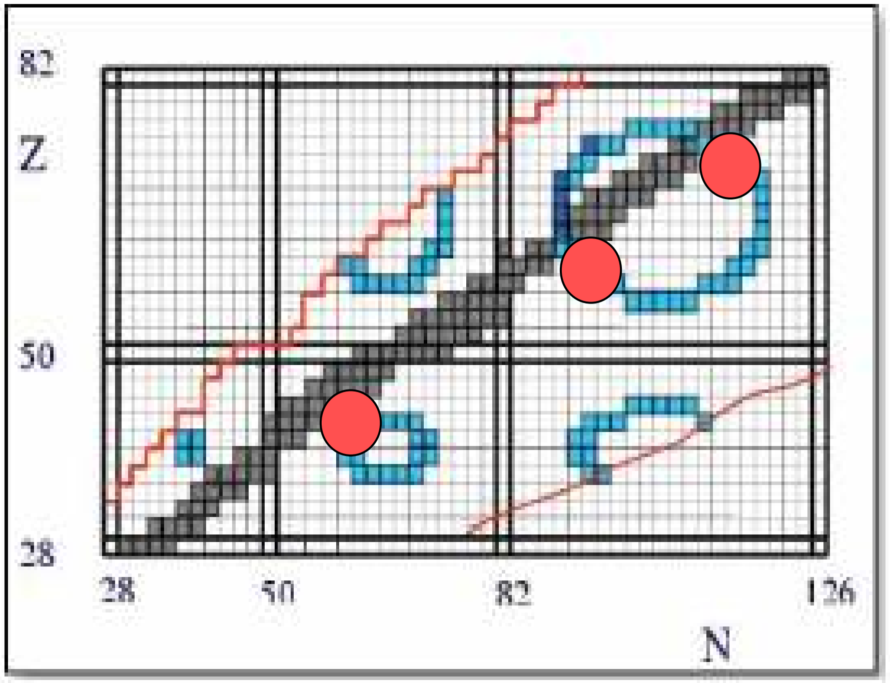

$B_W(E1) =$	6.446×10^{-2}	$A^{2/3}$	$e^2 fm^2$
$B_W(E2) =$	5.940×10^{-2}	$A^{4/3}$	$e^2 fm^4$
$B_W(E3) =$	5.940×10^{-2}	A^{2}	$e^2 fm^6$
$B_W(E4) =$	6.285×10^{-2}	$A^{8/3}$	$e^2 fm^8$
$B_W(M1) =$	1.790		μ_N^2
$B_W(M2) =$	1.650	$A^{2/3}$	$\mu_N^2 fm^2$
$B_W(M3) =$	1.650	$A^{4/3}$	$\mu_N^2 fm^4$
$B_W(M4) =$	1.746	A^{2}	$\mu_N^2 fm^6$

E_γ (MeV), τ_γ (s)

$B(E1)\downarrow =$	6.29×10^{-16}	E_γ^{-3}	τ_γ^{-1}	$e^2 fm^2$
$B(E2) =$	8.20×10^{-10}	E_γ^{-5}	τ_γ^{-1}	$e^2 fm$
$B(E3) =$	1.76×10^{-3}	E_γ^{-7}	τ_γ^{-1}	$e^2 fm$
$B(E4) =$	5.92×10^{3}	E_γ^{-9}	τ_γ^{-1}	$e^2 fm$
$B(M1) =$	5.68×10^{-14}	E_γ^{-3}	τ_γ^{-1}	μ_N^2
$B(M2) =$	7.41×10^{-8}	E_γ^{-5}	τ_γ^{-1}	$\mu_N^2 fm$
$B(M3) =$	1.59×10^{-1}	E_γ^{-7}	τ_γ^{-1}	$\mu_N^2 fm$
$B(M4) =$	5.34×10^{5}	E_γ^{-9}	τ_γ^{-1}	$\mu_N^2 f$

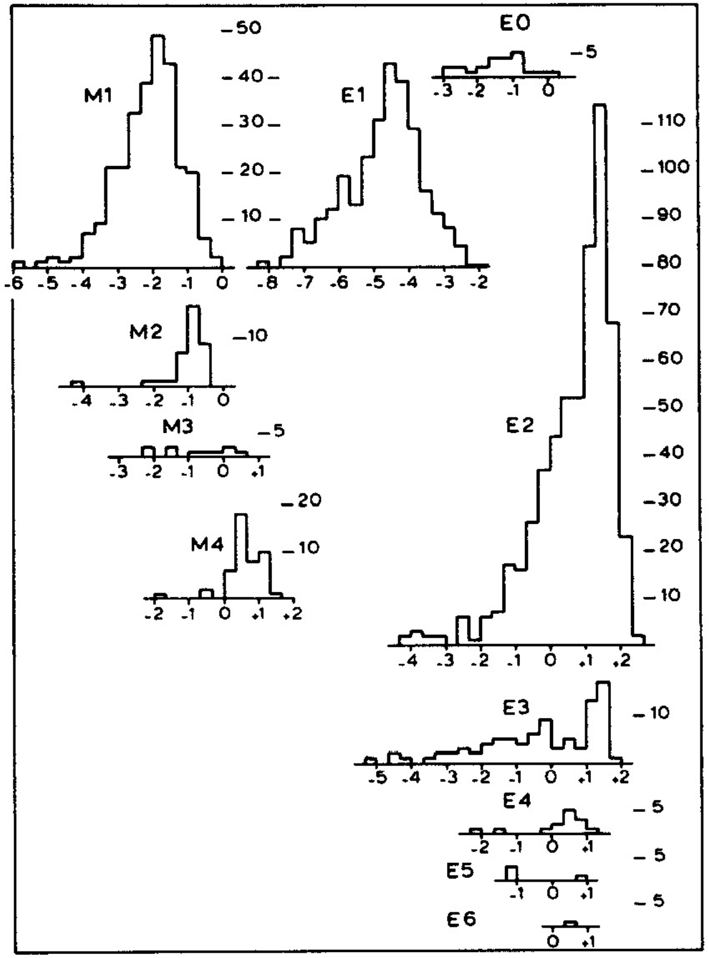

Fig. 1. Gamma-ray strength distributions in the $A = 91$–150 region for transitions of different character ($E0$–$E6$, $M1$–$M4$). The logarithmic abscissa scale indicates the strength in Weisskopf units, except for $E0$ transitions which are in Wilkinson units.

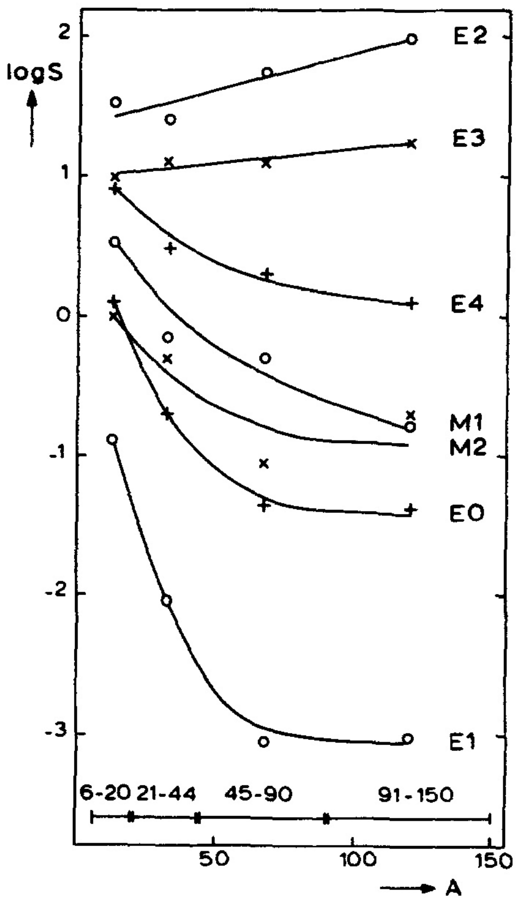

Fig. 7. Average strengths of strongest transitions as a function of A; for $E1$, $E2$, and $M1$ averages are taken of the strongest 10%, for $E3$ and $M2$ of the strongest 50%, and for $E0$ and $E4$ of all transitions. Strengths are

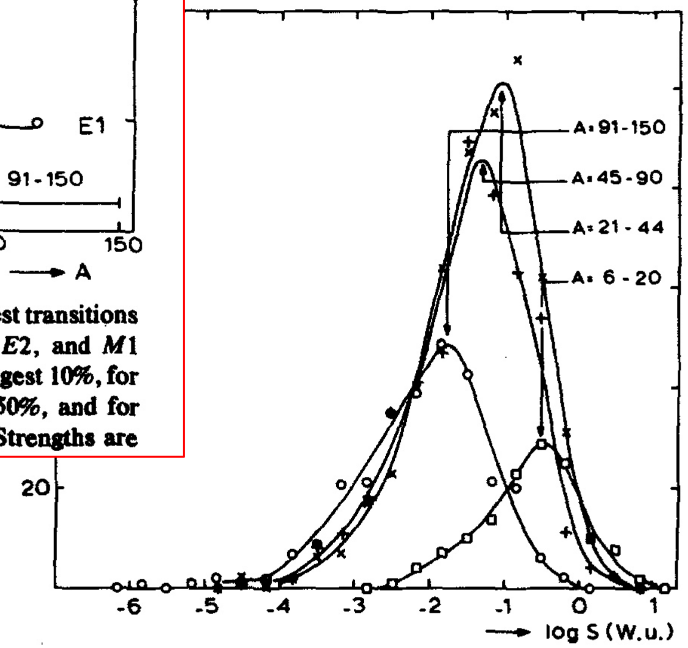

Fig. 6. Comparison of $M1$ strength distributions for different A-regions. Data for $A = 6$–44 and $A = 45$–90 are from Refs. 1 and 2, respectively.

P.M. Endt, ADNDT 26(1981) 47

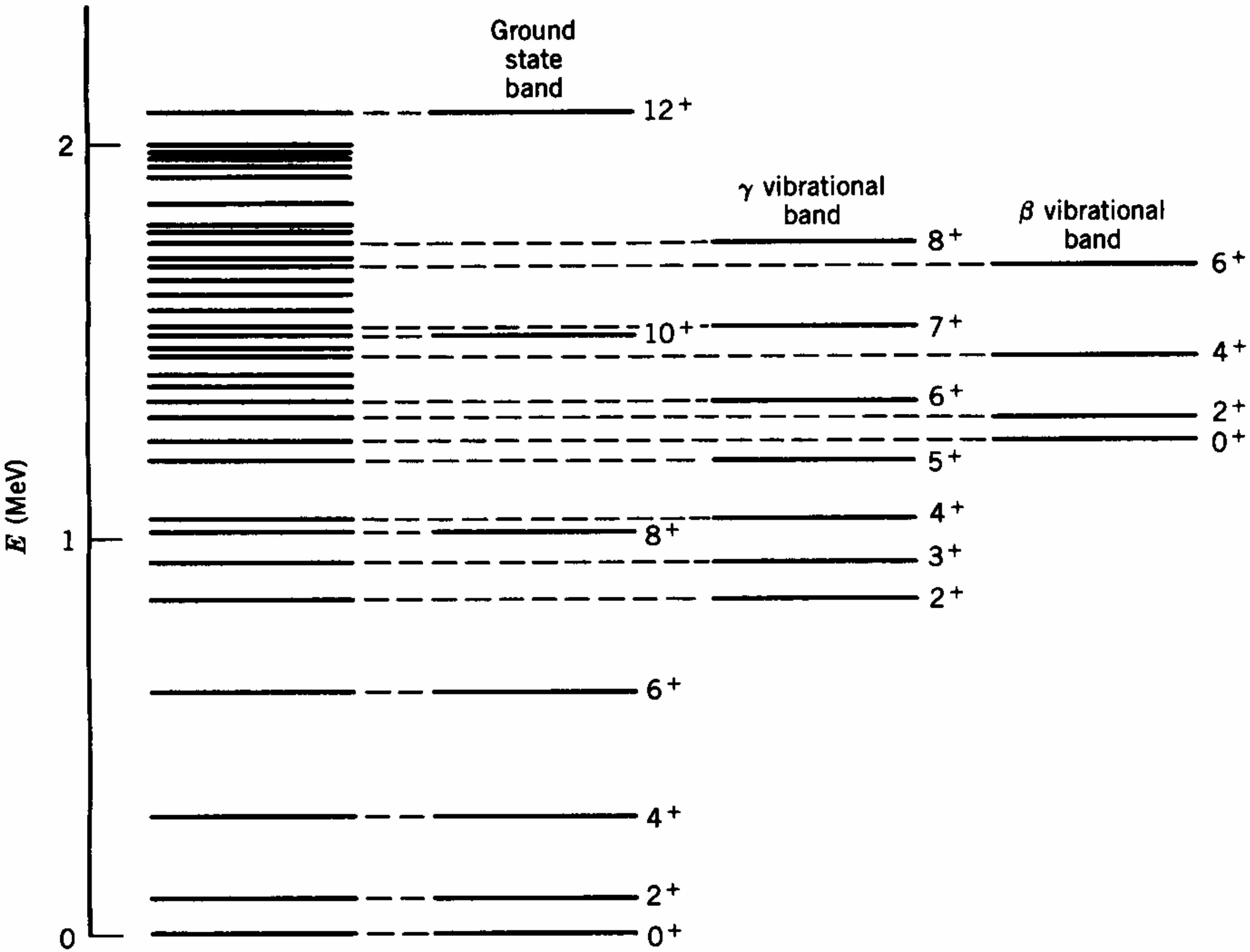

E (MeV)
0
1
2
Ground state band
0+
2+
4+
6+
8+
10+
12+
γ vibrational band
2+
3+
4+
5+
6+
7+
8+
β vibrational band
0+
2+
4+
6+

Measurement techniques of nuclear half lives

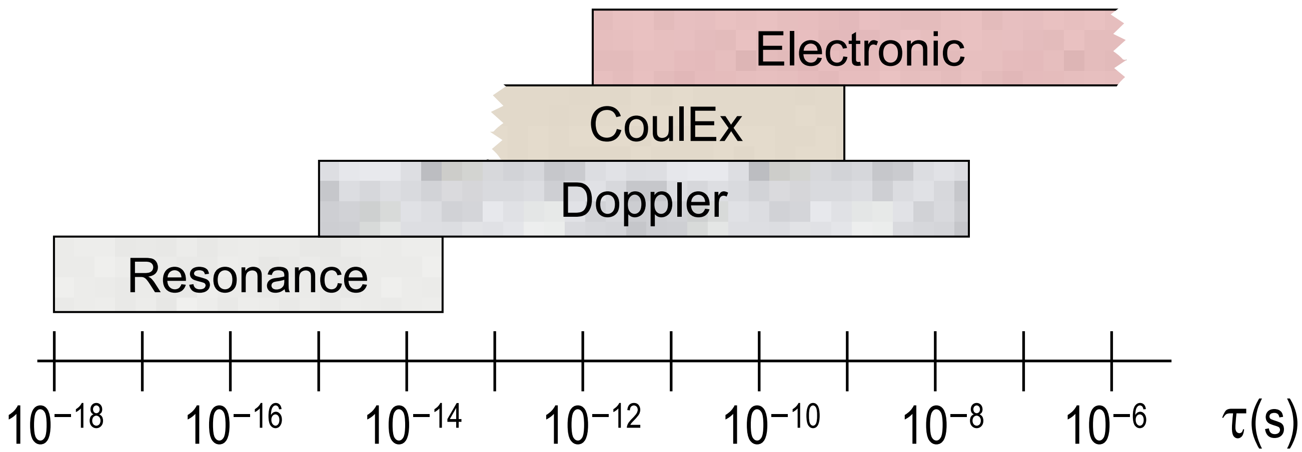

L.M. Fraile

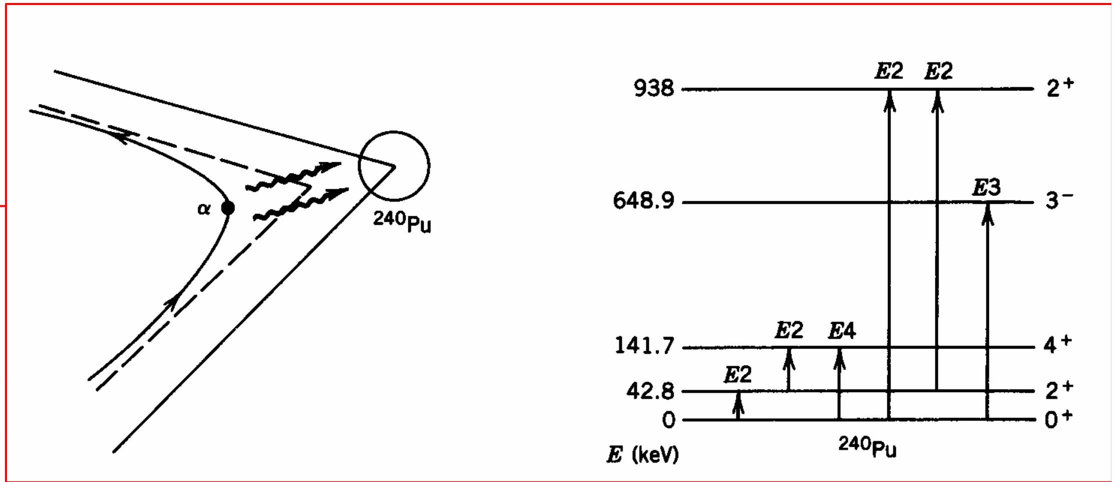

Coulomb excitation

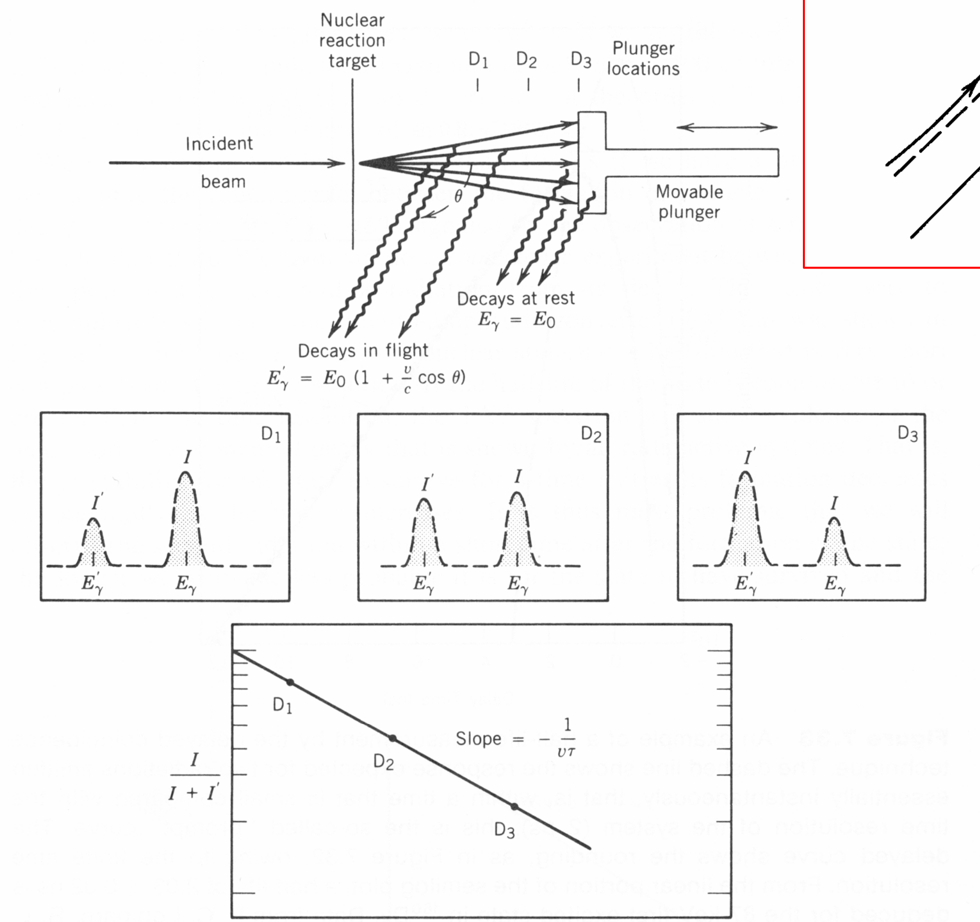

Figure 7.34 Schematic views of the Doppler-recoil method of lifetime measurement. Decaying nuclei are observed by a detector whose axis makes an angle θ with the recoil direction. Moving the plunger changes the relative numbers of decays in flight and at rest, which can be used to determine the mean life of the decay.

Doppler-recoil method

The region NE of ^{132}Sn

$\pi\ (0g_{7/2}, 1d_{5/2}, 1d_{3/2}, 2s_{1/2}, 0h_{11/2})^{Z-50}$

	Cs 127	Cs 128	Cs 129	Cs 130	Cs 131	Cs 132	Cs 133	Cs 134	Cs 135	Cs 136	Cs 137	Cs 138	Cs 139	Cs 140	Cs 141	Cs 142	Cs 143	Cs 144	Cs 145	Cs 146	Cs 147	Cs 148	Cs 149	Cs 150	Cs 151	Cs 152
54	Xe 126	Xe 127	Xe 128	Xe 129	Xe 130	Xe 131	Xe 132	Xe 133	Xe 134	Xe 135	Xe 136	Xe 137	Xe 138	Xe 139	Xe 140	Xe 141	Xe 142	Xe 143	Xe 144	Xe 145	Xe 146	Xe 147	94		96	
	I 125	I 126	I 127	I 128	I 129	I 130	I 131	I 132	I 133	I 134	I 135	I 136	I 137	I 138	I 139	I 140	I 141	I 142	I 143	I 144	92					
52	Te 124	Te 125	Te 126	Te 127	Te 128	Te 129	Te 130	Te 131	Te 132	Te 133	Te 134	Te 135	**Te 136**	Te 137	Te 138	Te 139	Te 140	Te 141	Te 142							
	Sb 123	Sb 124	Sb 125	Sb 126	Sb 127	Sb 128	Sb 129	Sb 130	Sb 131	Sb 132	Sb 133	**Sb 134**	**Sb 135**	Sb 136	Sb 137	Sb 138	Sb 139		90							
50	Sn 122	Sn 123	Sn 124	Sn 125	Sn 126	Sn 127	Sn 128	Sn 129	Sn 130	Sn 131	**Sn 132**	Sn 133	Sn 134	Sn 135	Sn 136	Sn 137										
	In 121	In 122	In 123	In 124	In 125	In 126	In 127	In 128	In 129	In 130	In 131	In 132	In 133	In 134	In 135		88									
48	Cd 120	Cd 121	Cd 122	Cd 123	Cd 124	Cd 125	Cd 126	Cd 127	Cd 128	Cd 129	Cd 130	Cd 131	Cd 132		86											
	Ag 119	Ag 120	Ag 121	Ag 122	Ag 123	Ag 124	Ag 125	Ag 126	Ag 127	Ag 128	Ag 129	Ag 130	84													
46	Pd 118	Pd 119	Pd 120	Pd 121	Pd 122	Pd 123	Pd 124		80		82															
	72		74		76		78																			

^{132}Sn *core*

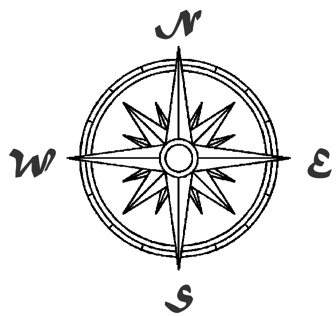

^{132}Sn *core*

$\nu\ (1f_{7/2}, 0h_{9/2}, 1f_{5/2}, 2p_{3/2}, 2p_{1/2}, 0i_{13/2})^{N-82}$

L.M. Fraile

CERN Accelerator Complex

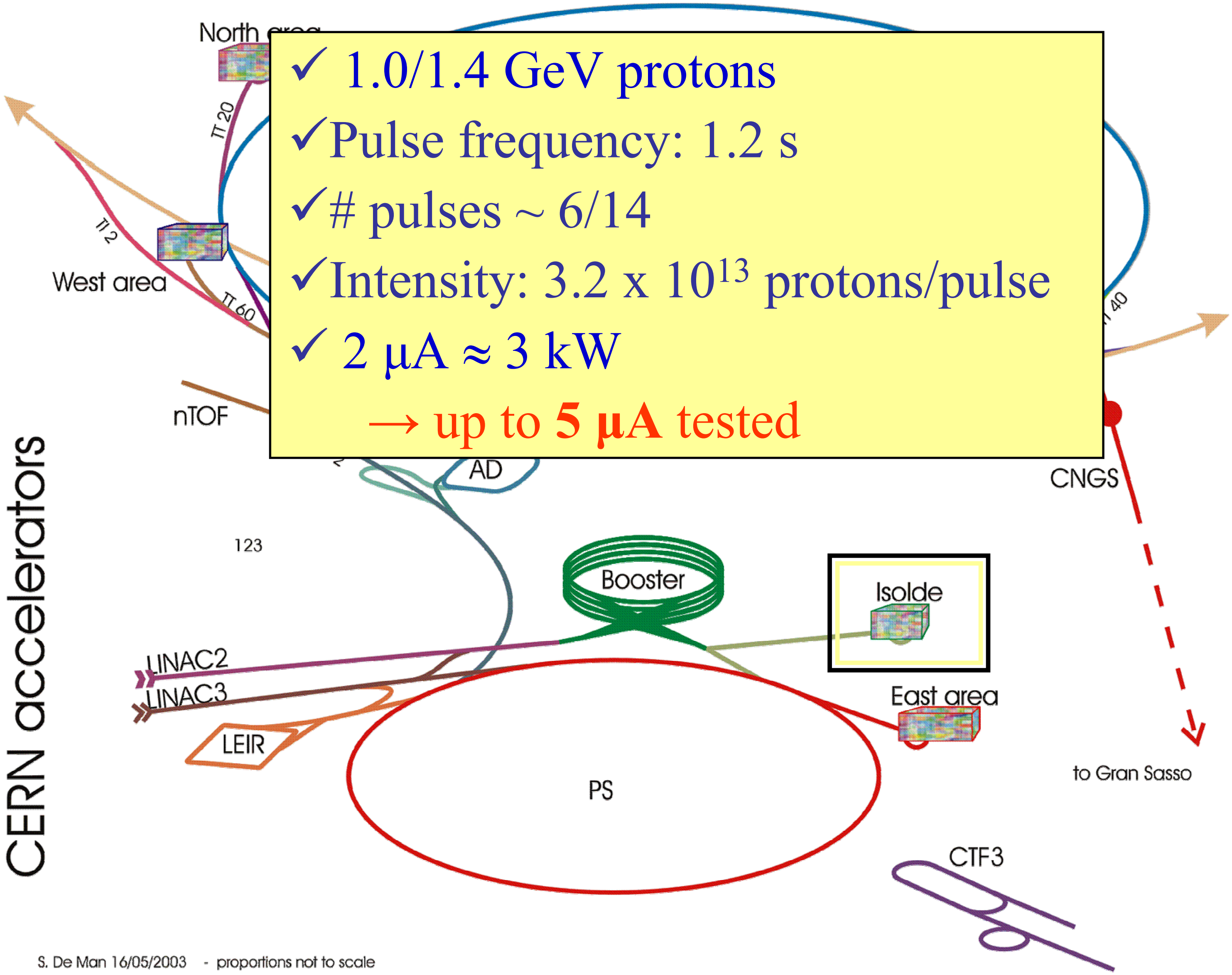

- ✓ 1.0/1.4 GeV protons
- ✓ Pulse frequency: 1.2 s
- ✓ # pulses ~ 6/14
- ✓ Intensity: 3.2 x 10^{13} protons/pulse
- ✓ 2 μA ≈ 3 kW
  - → up to **5 μA** tested

ISOLDE

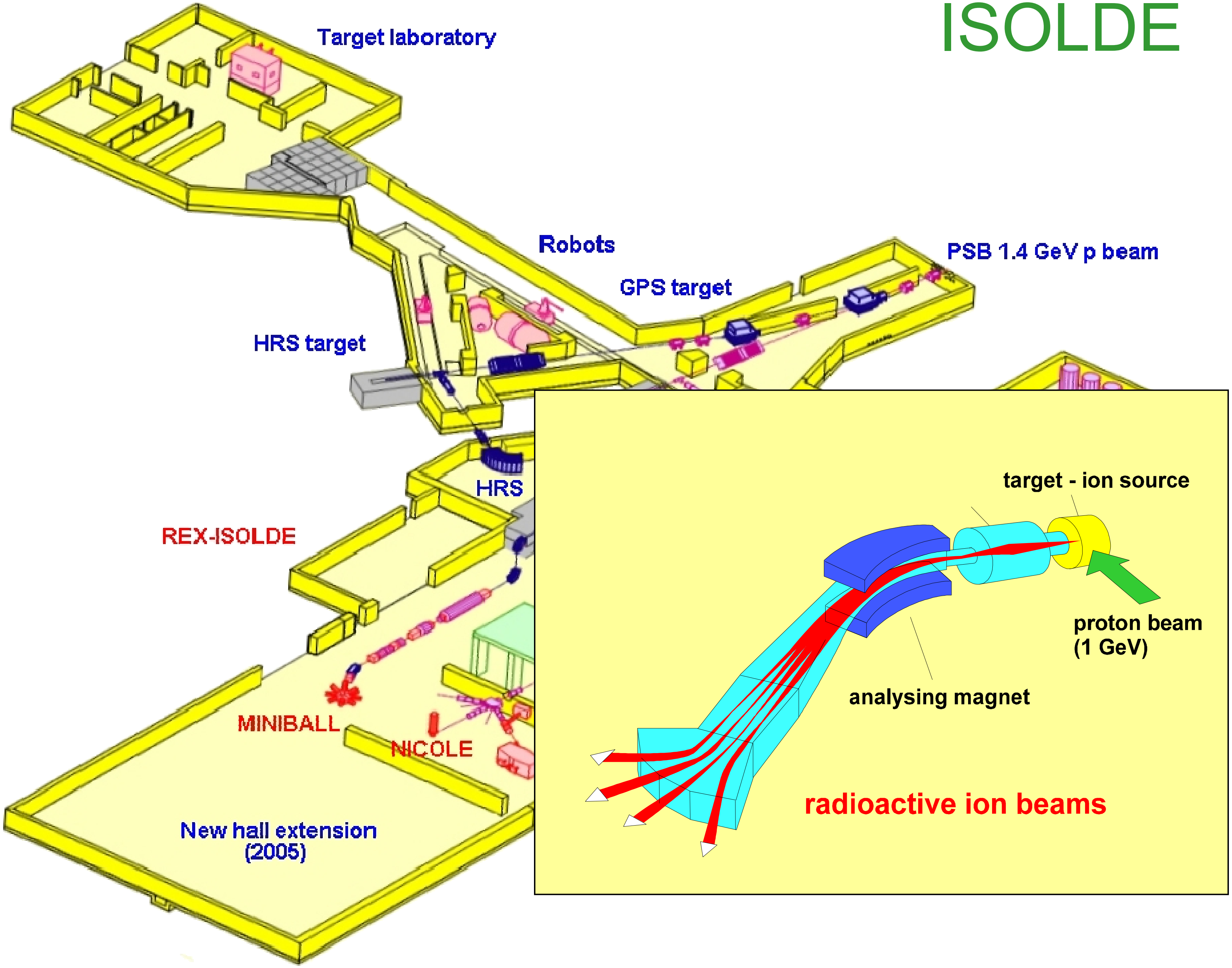

Target laboratory
Robots
GPS target
PSB 1.4 GeV p beam
HRS target
HRS
REX-ISOLDE
MINIBALL
NICOLE
New hall extension
(2005)
target - ion source
proton beam
(1 GeV)
analysing magnet
radioactive ion beams

Production

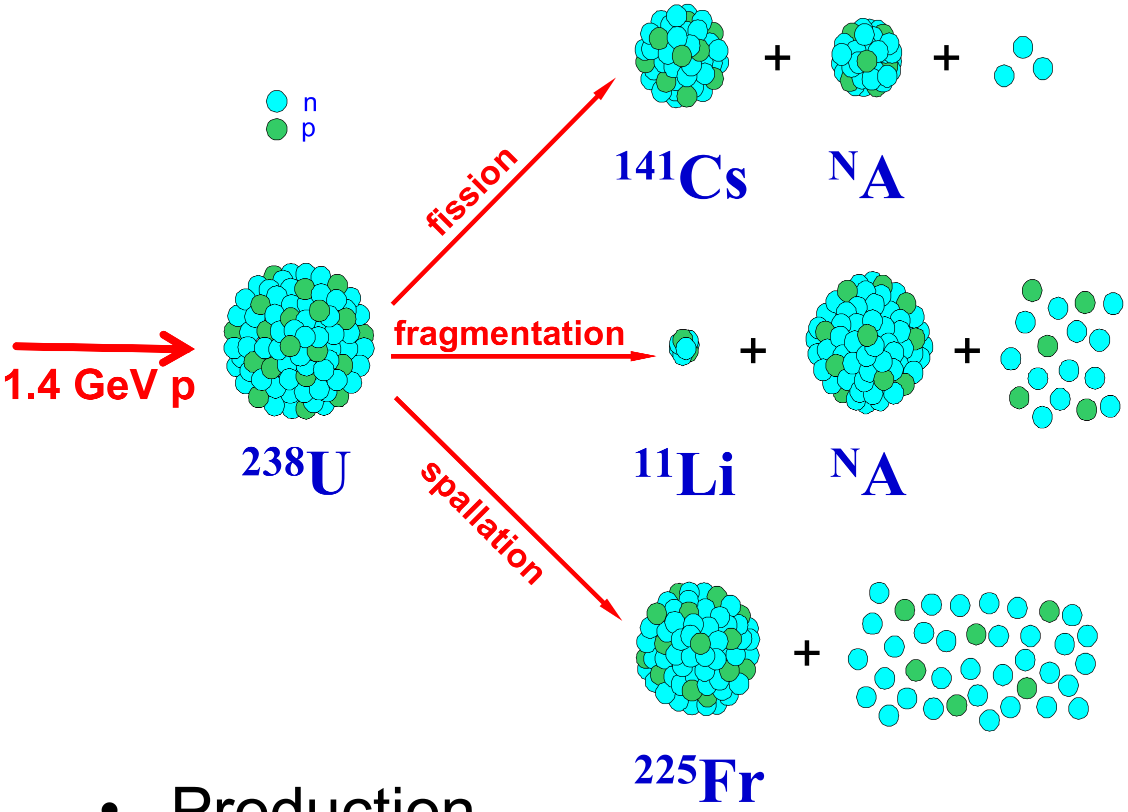

- Production
- Diffusion
- Effusion
  - **http://www.targisol.csic.es/**

Measurement Station

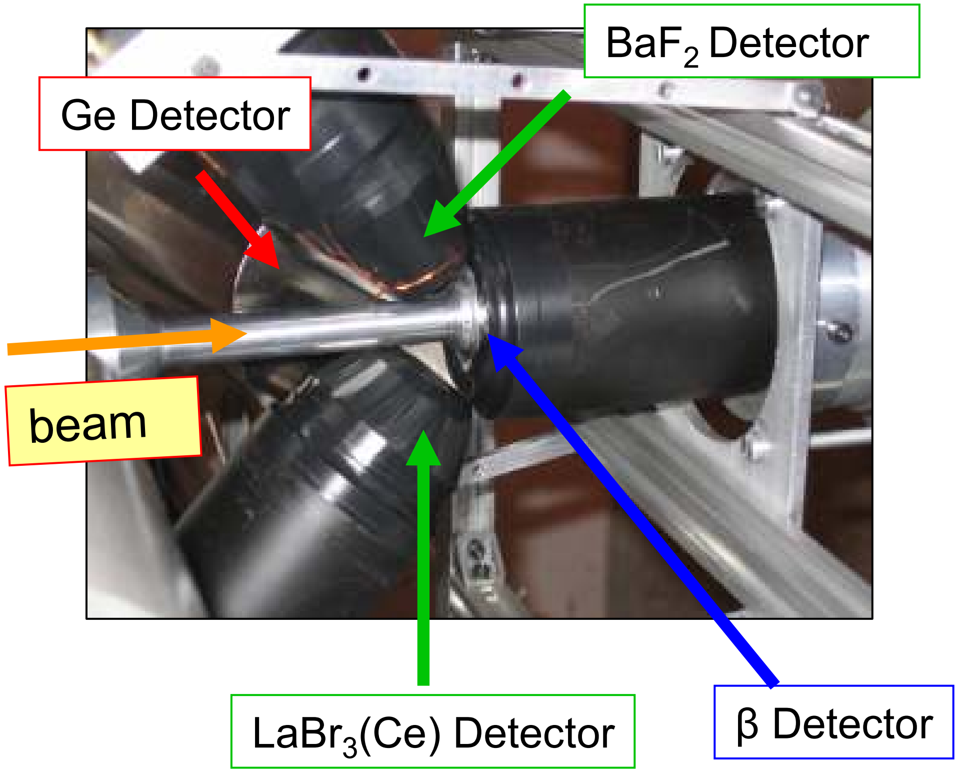

Ge: Used to detect γ-rays, characterized by high energy resolution but poor time response

LaBr$_3$(Ce)/BaF$_2$: Fast response γ-detectors but having poor energy resolution; they are used as our stop watch detectors.

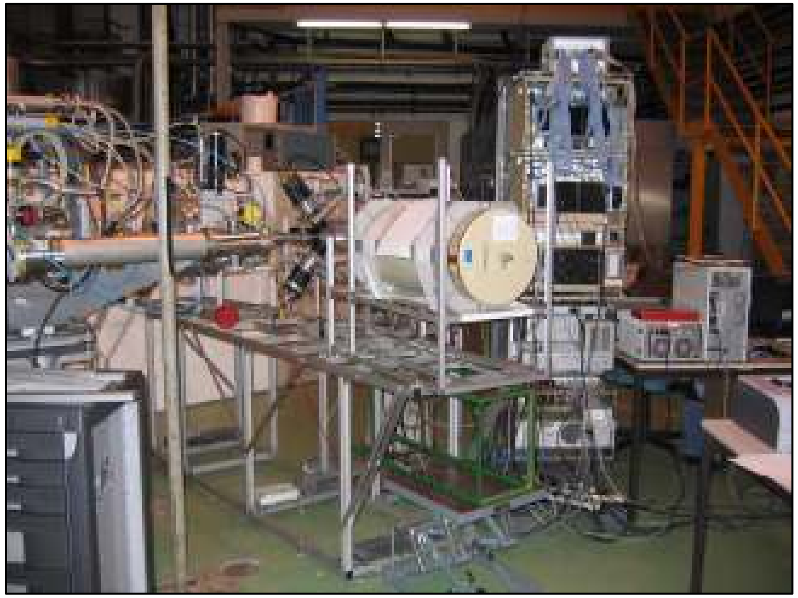

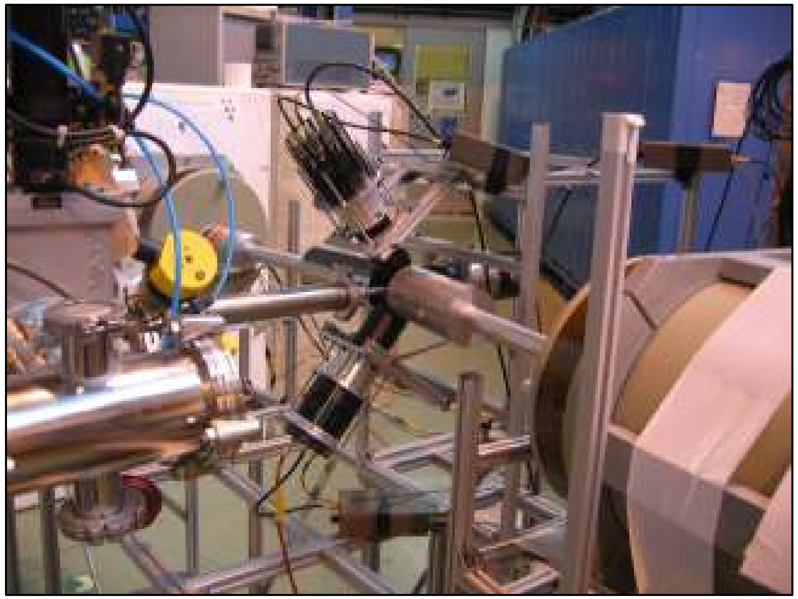

Experimental setup

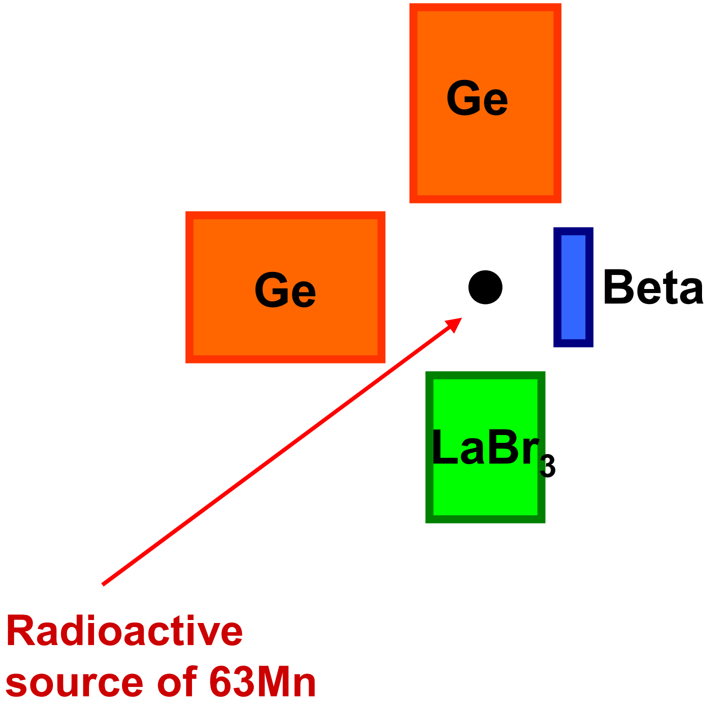

- Double coincidences between beta- and gamma-rays (beta-Ge and beta-$LaBr_3$ detectors)
- Triple coincidences of the beta-gamma-gamma type involving beta-Ge-Ge and Beta-Ge-$LaBr_3$ detectors.

A. Baluyut COS-JAM 2008

Basic Principles of Ultra Fast Timing (Advanced Time-Delayed Method)

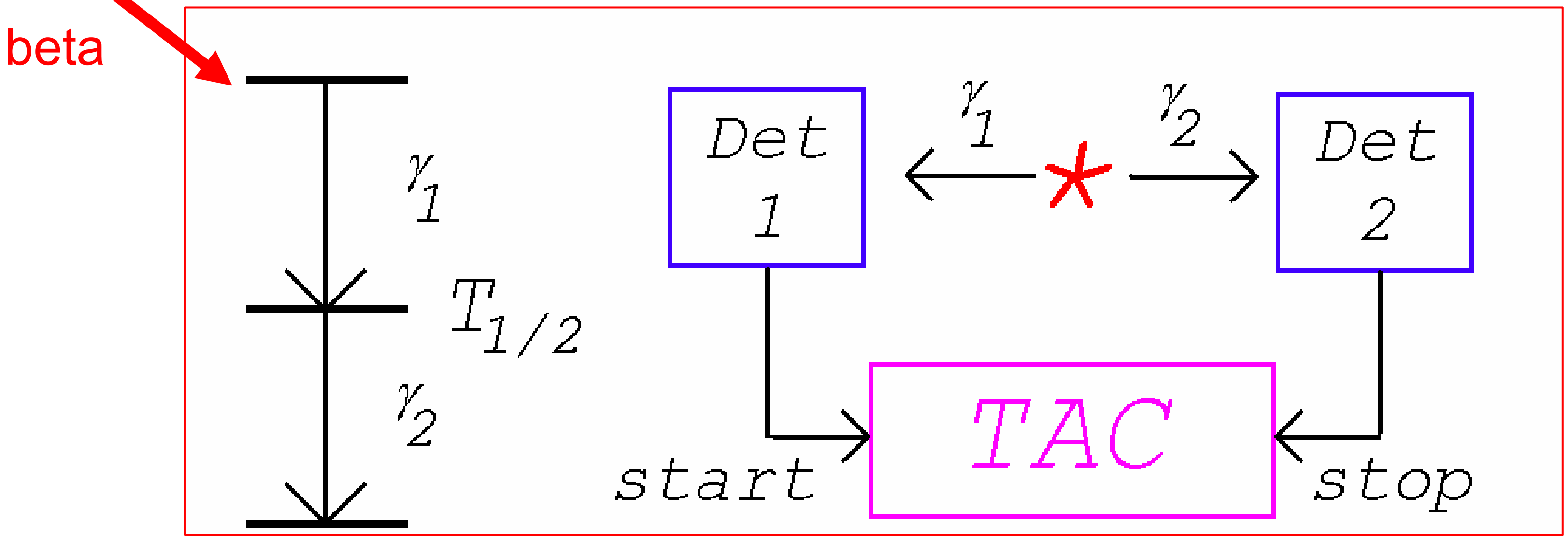

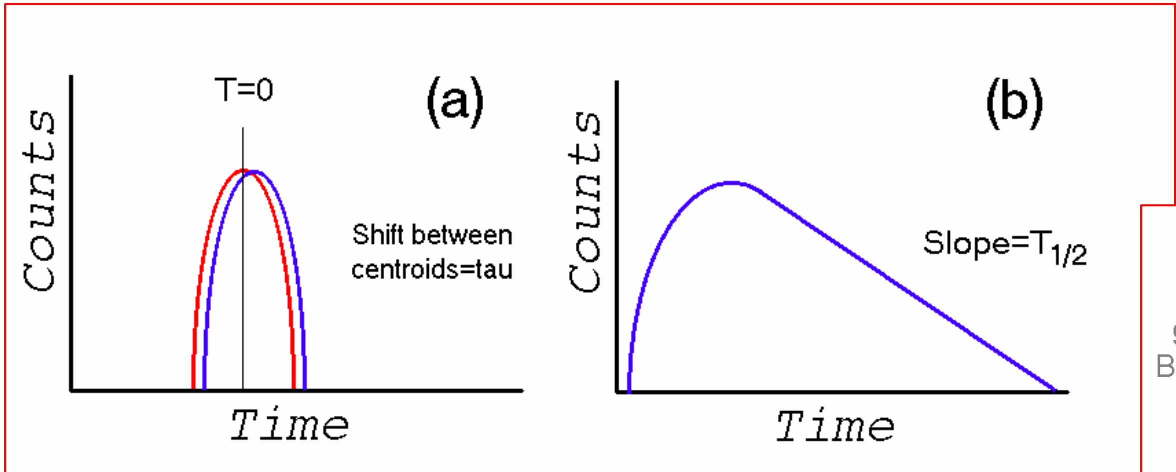

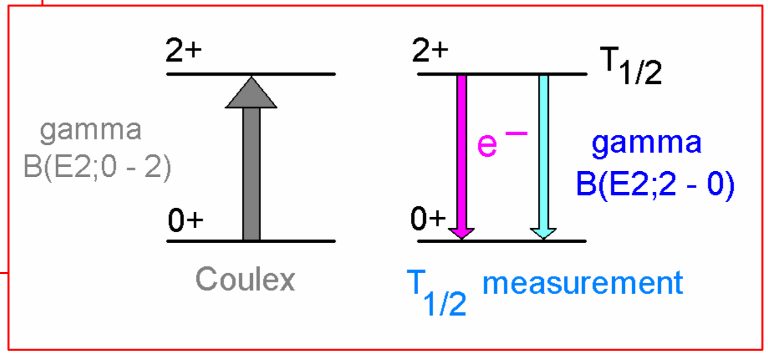

The range for the measurements is from 30 ps to 30 ns (or longer) by the slope method and down to about 5-10 ps by the centroid shift method, see H.Mach et al. Nucl. Phys. A523 (1991) 197.

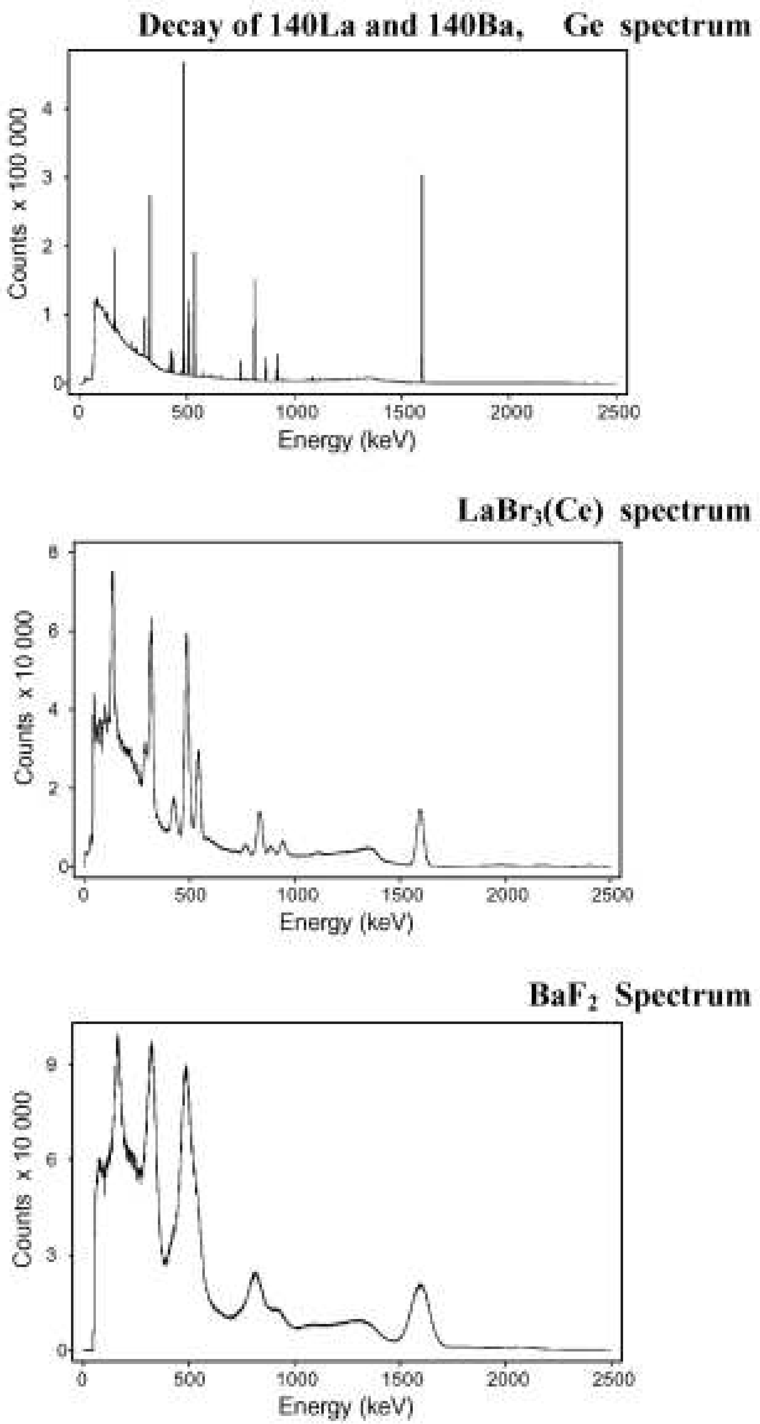

Our experiment represented one of the first applications of $LaBr_3(Ce)$ to fast timing

$LaBr_3(Ce)$ has much better energy resolution than BaF_2 (a factor of ~3) and currently very similar time resolutions, with a strong potential for an improvement.

Observe better energy resolution and also much improved peak to Compton ratio critical in Fast Timing

Core and valence particles

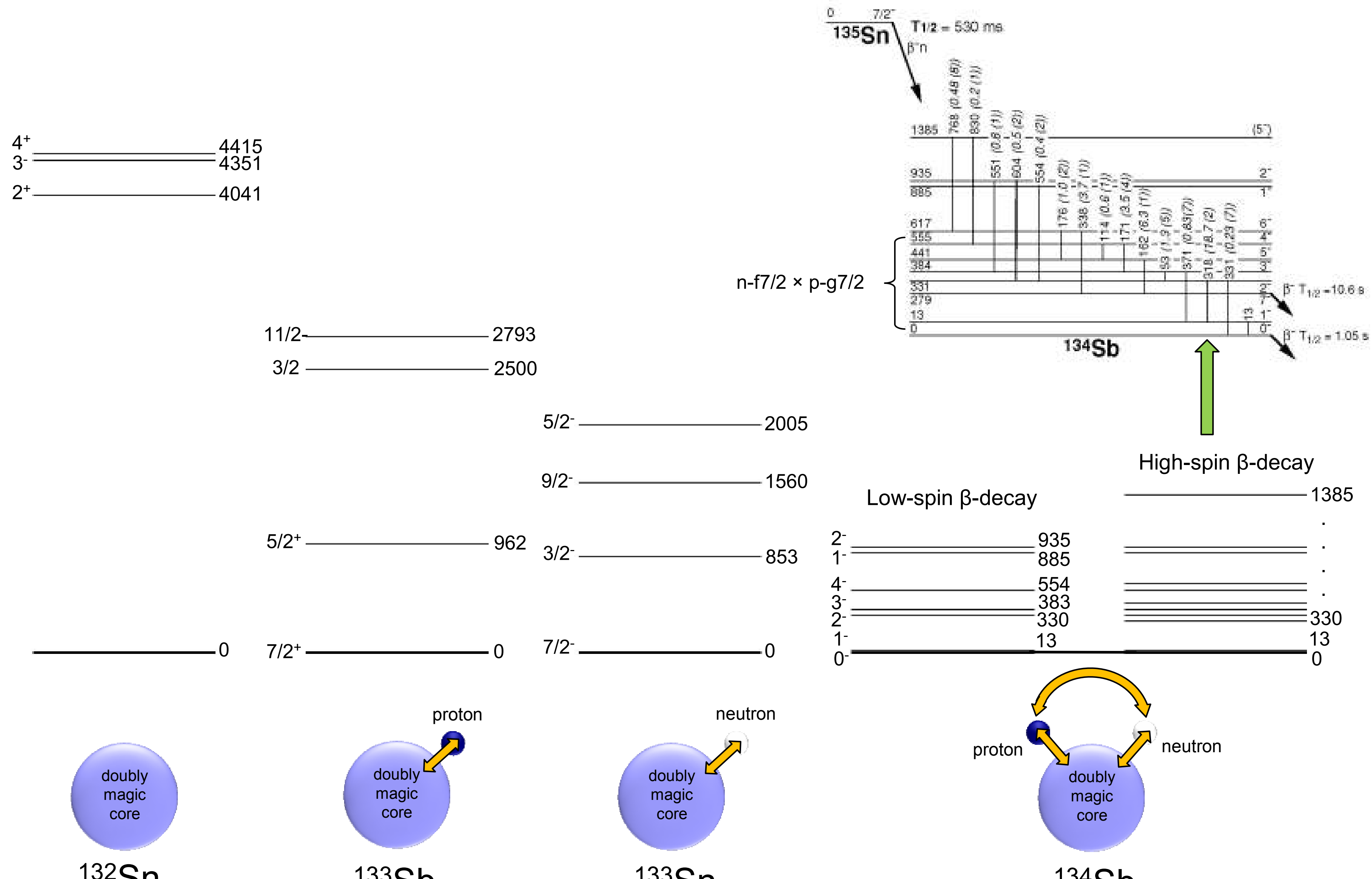

From E.White

Results on ^{134}Sb from the beta decay of ^{134}Sn

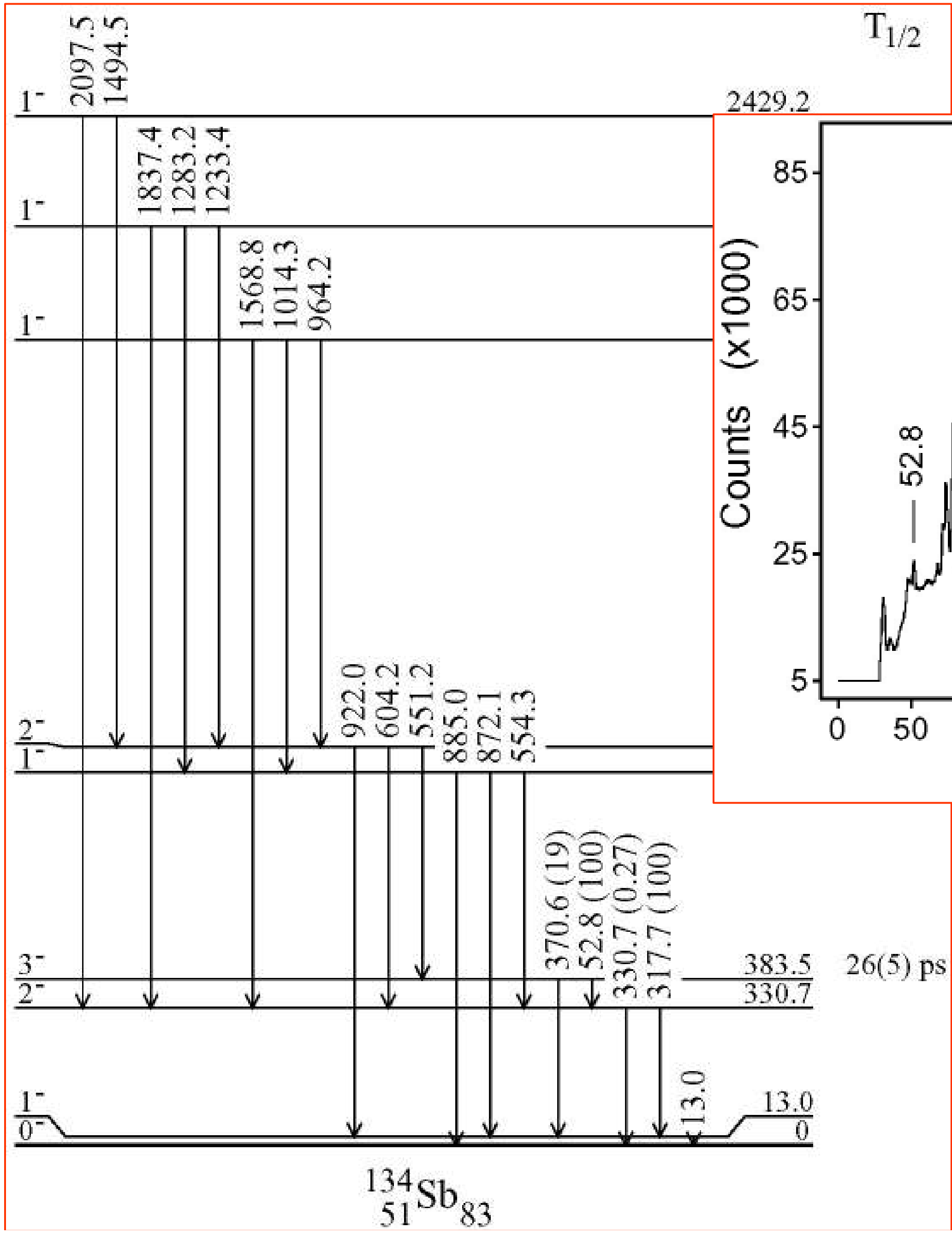

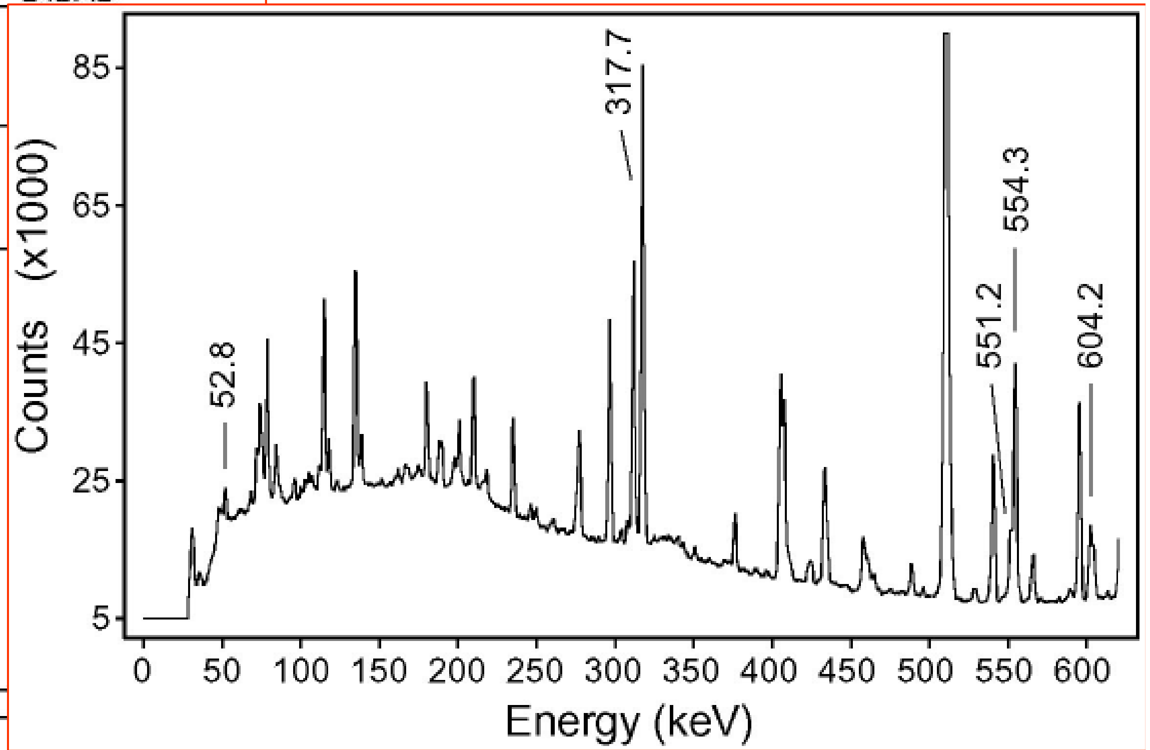

Very strong production of ^{134}Sn

Beta-gamma-gamma coincidences using Beta-Ge-Ge detectors

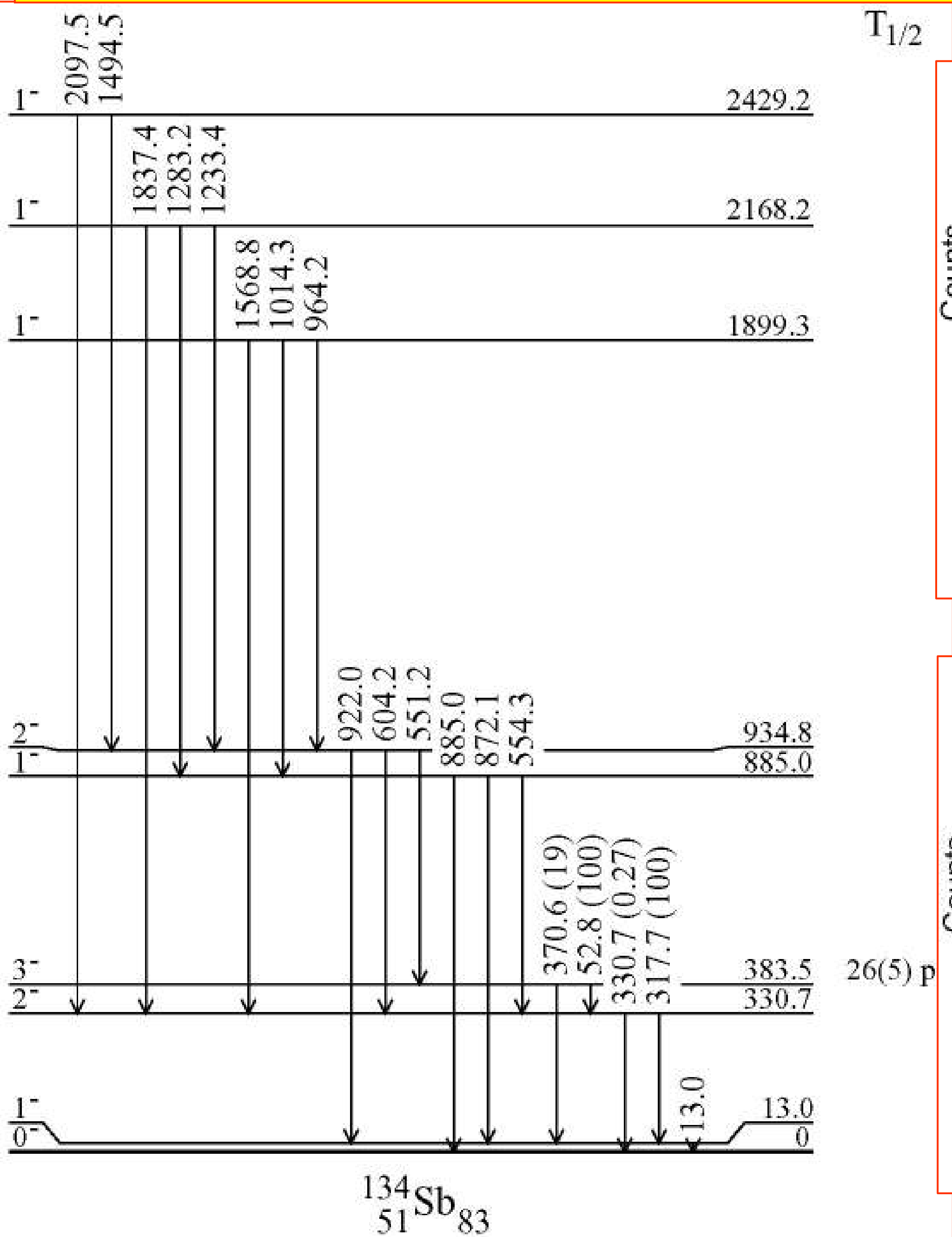

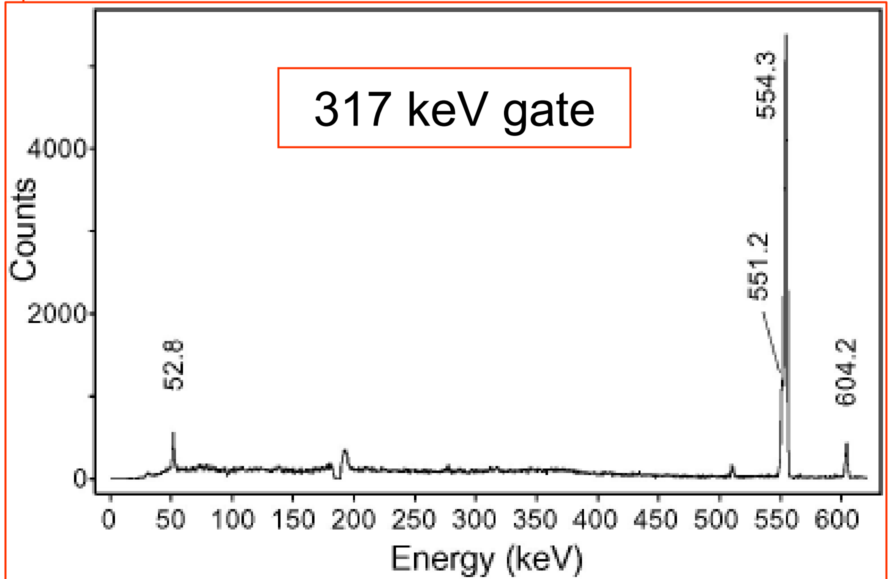

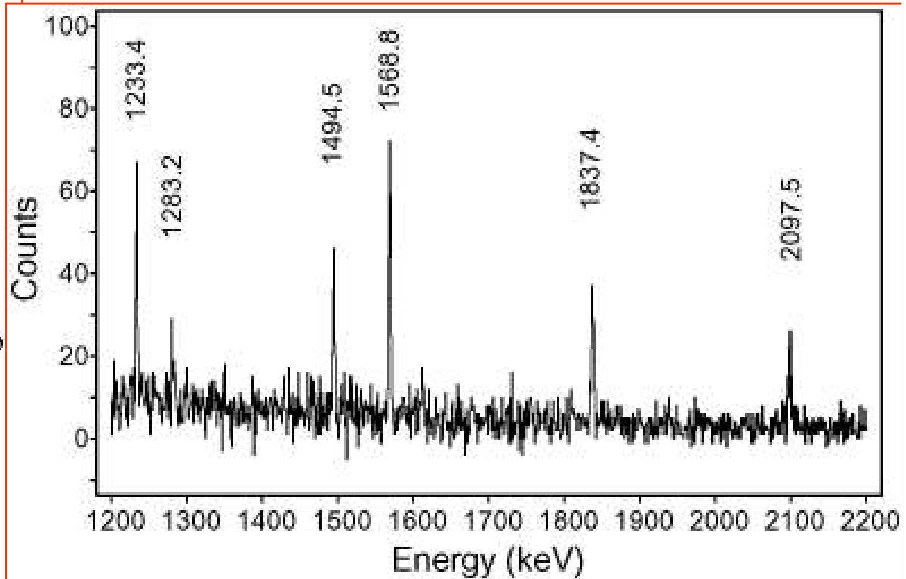

Weak gamma branches

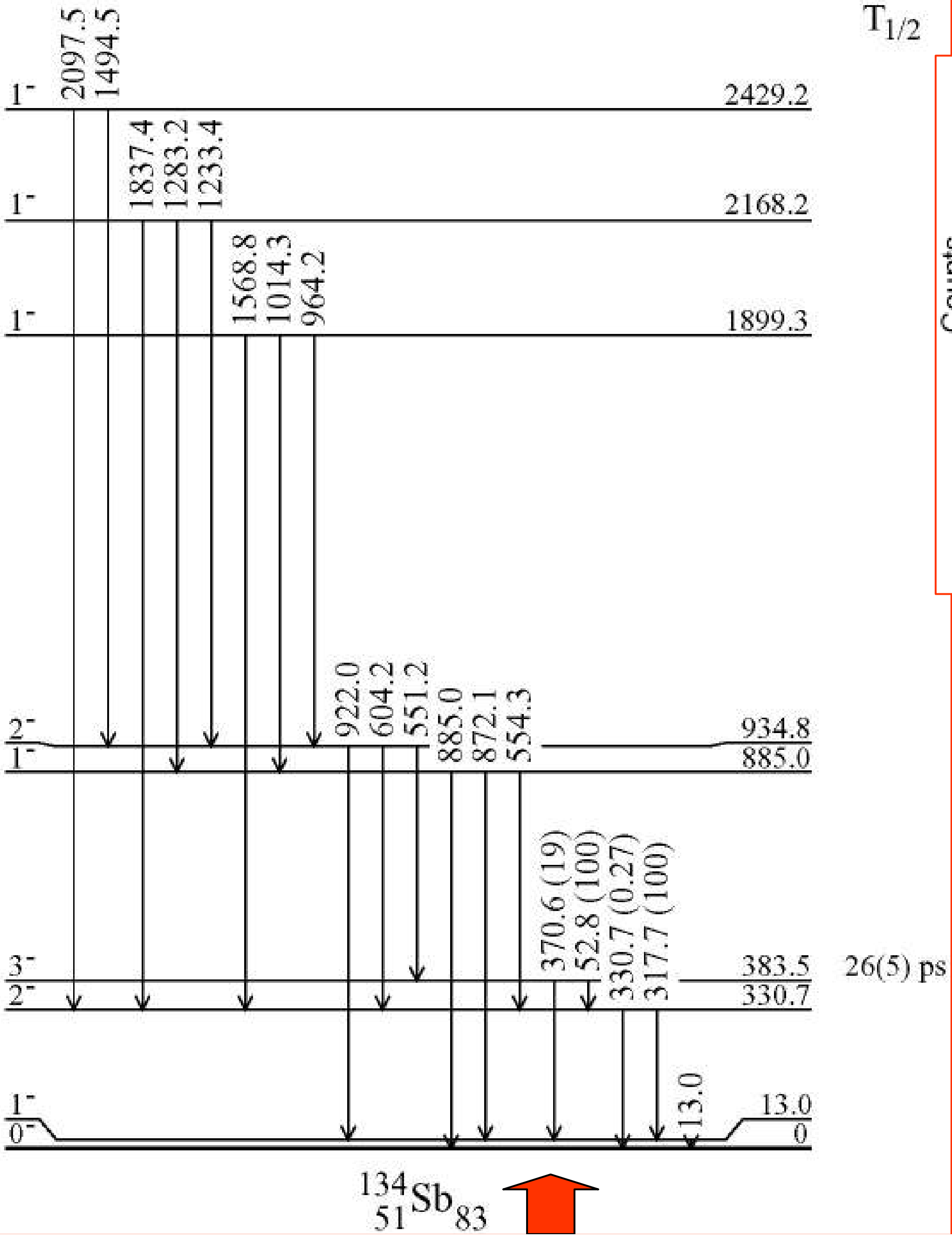

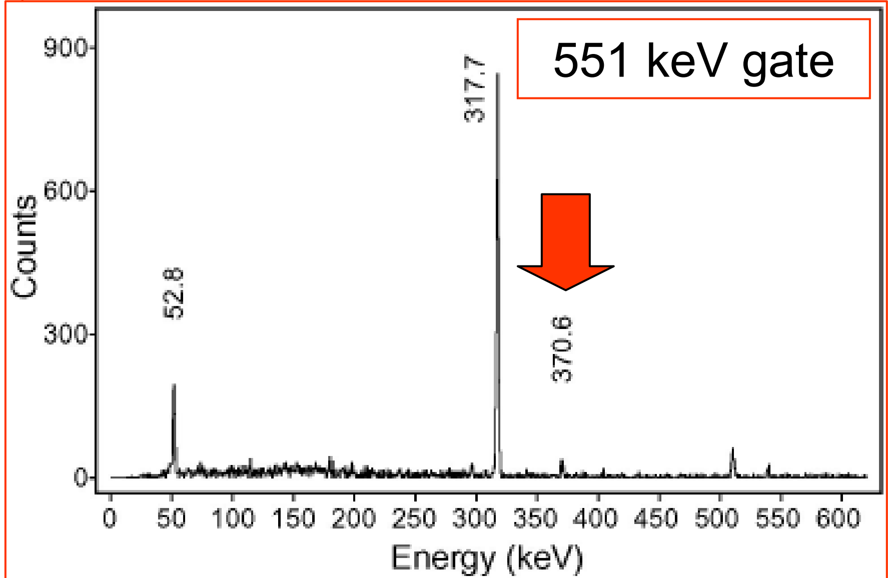

Weak gamma branches

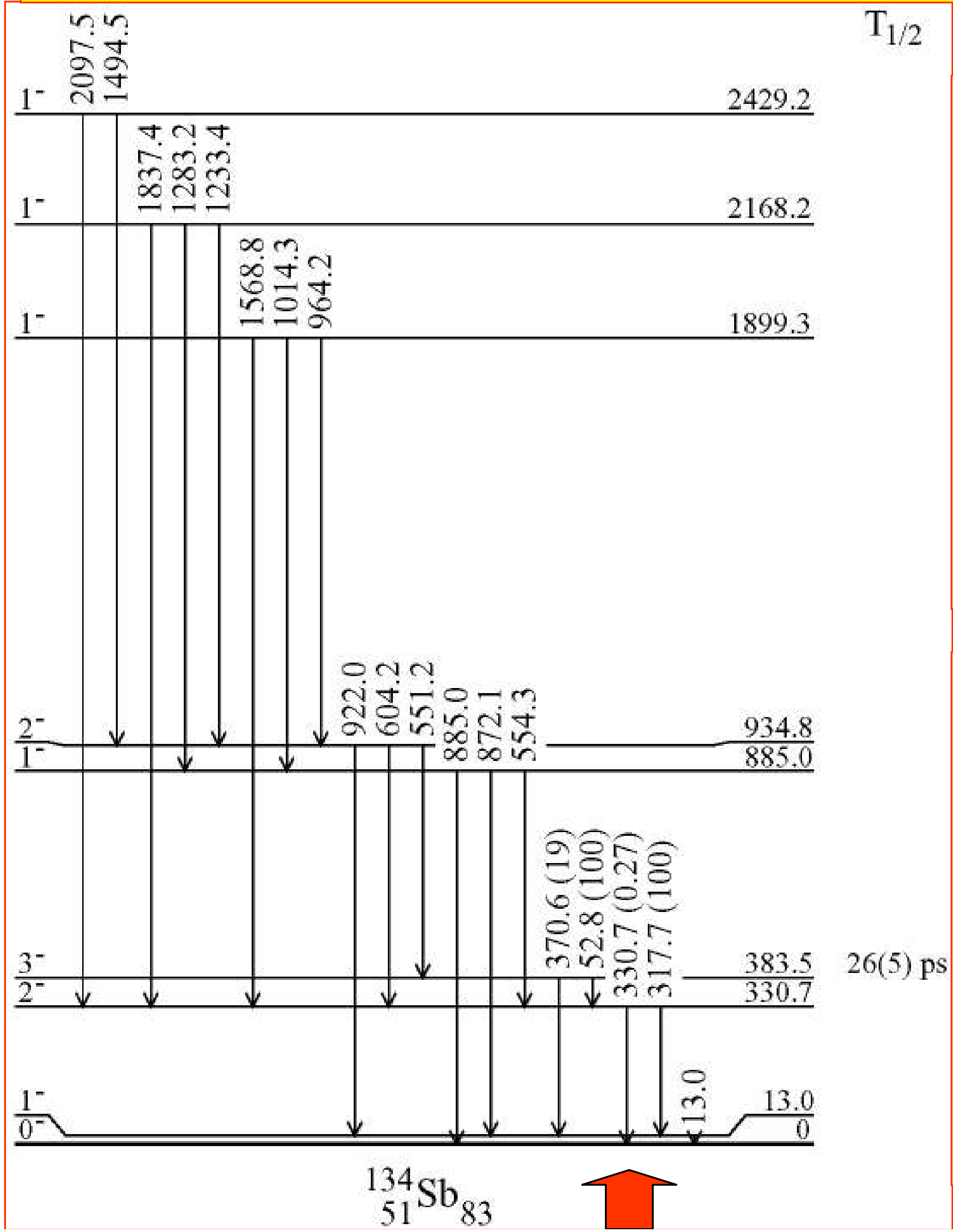

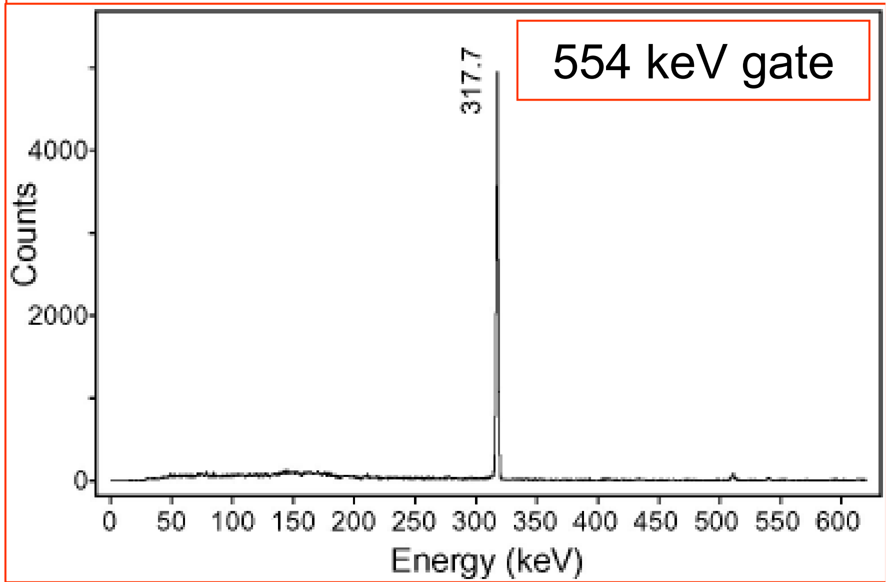

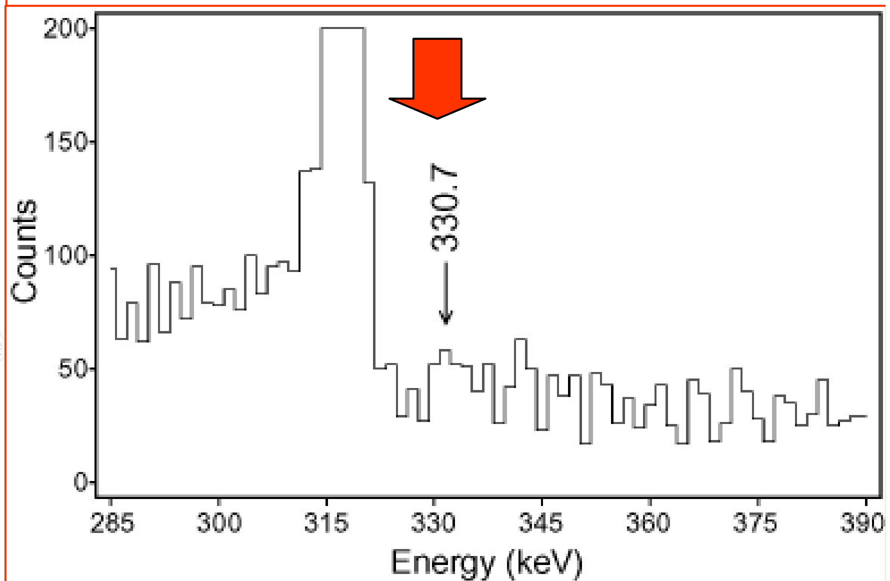

Lifetime measurement of the 383 keV level

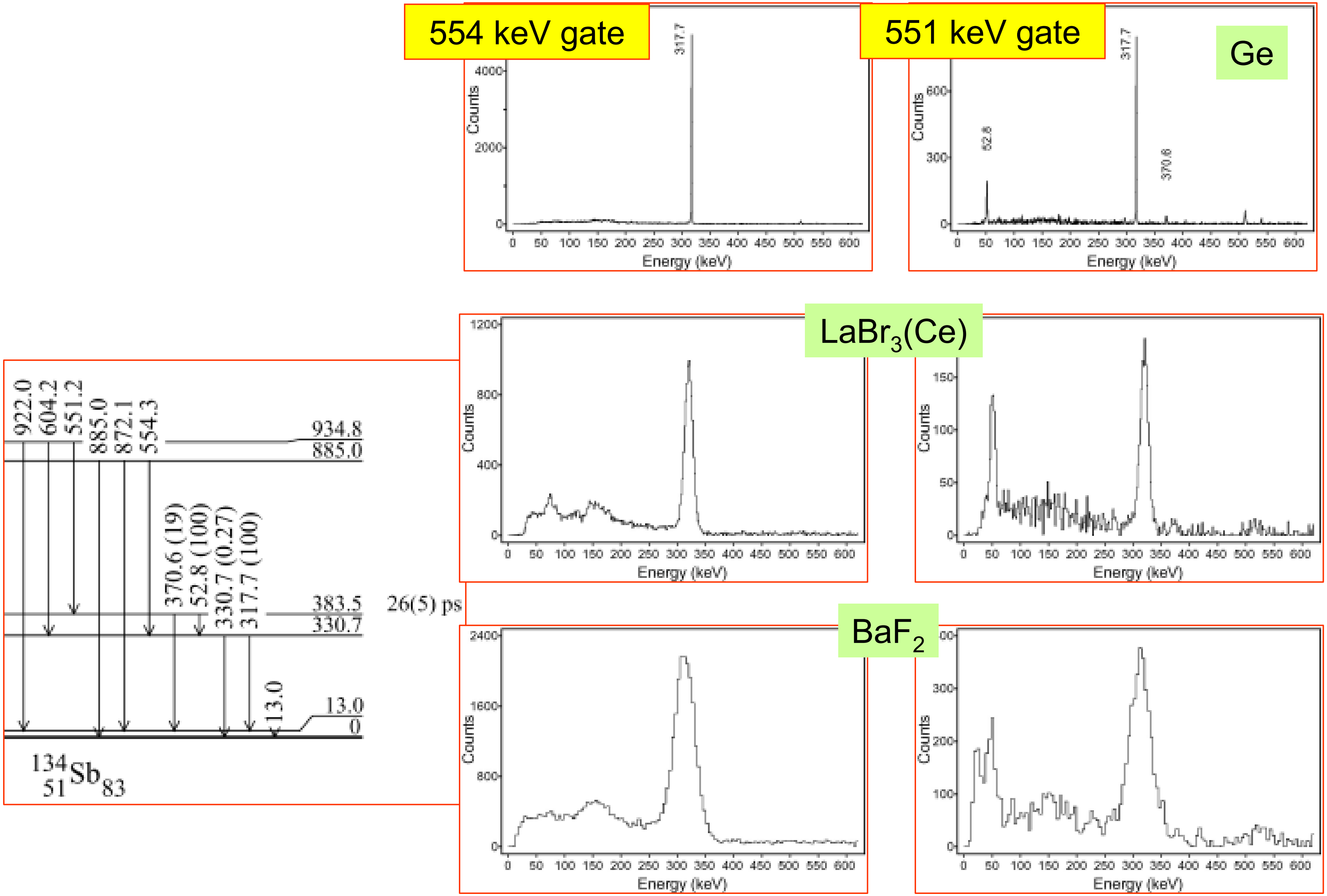

Lifetime measurement of the 383 keV level

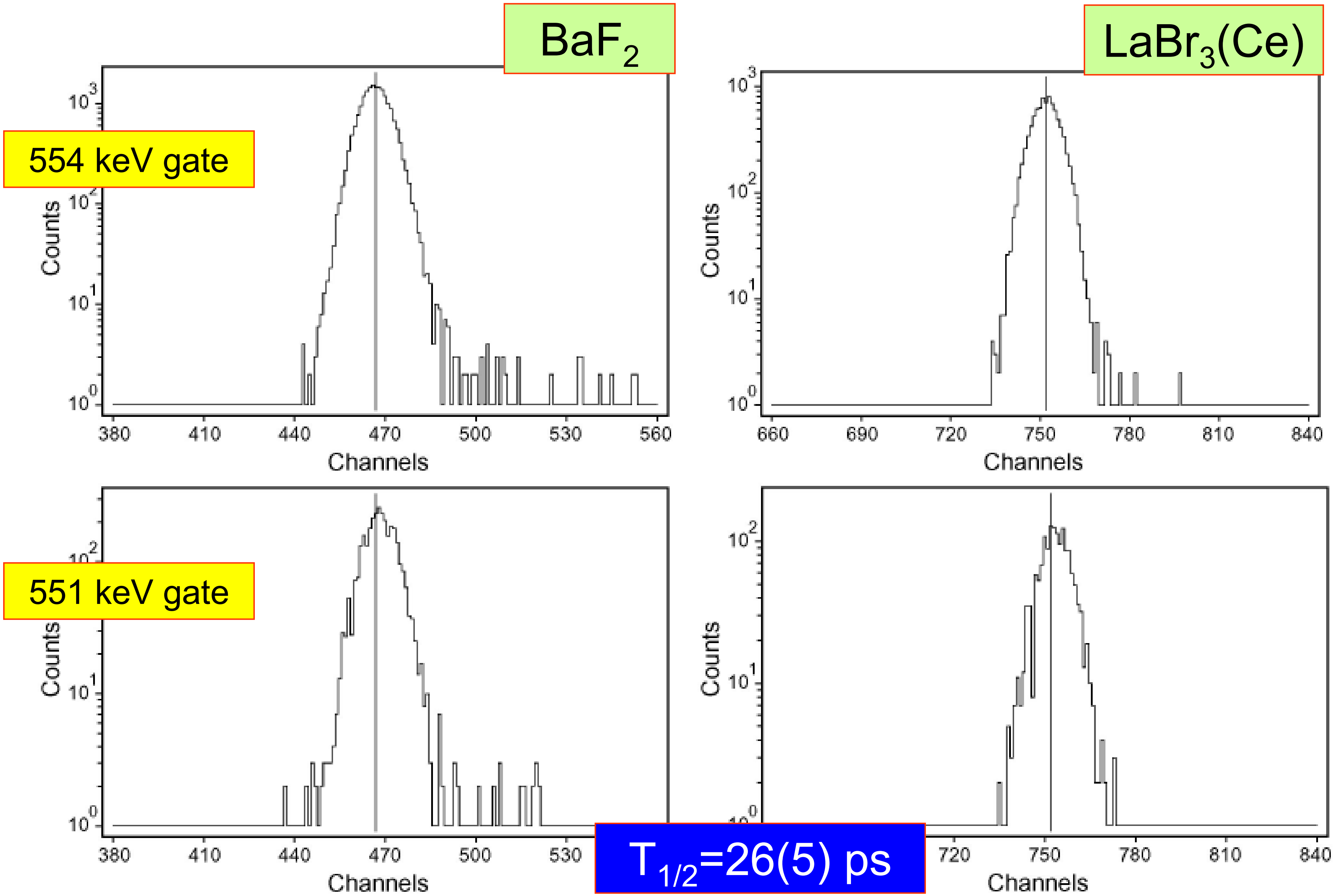

$T_{1/2}$=26(5) ps

Comparison to the shell model calculations

Levels	Exp. (keV)	Brown (keV)	Covello+Gargano (keV)
p $g_{7/2}$ - n $f_{7/2}$			
0-	0	0	0
1-	13	333	52
2-	331	404	385
3-	383	587	429
4-	555	705	621
5-	441	613	494
6-	617	751	727
7-	279	402	407
p $d_{5/2}$ – n $f_{7/2}$			
1-	885	1025	868
2-	935	863	935

Comparison to the shell model calculations

Levels	Exp.	Brown	Covello+Gargano
3- to 2-	B(M1) = 2.0(0.4) u_N^2	1.60	1.39
3- to 1-	B(E2) = 118 (26) e^2fm^4	84	115
2- to 0-	B(E2) = 429(238) e^2fm^4	90	123

Note: B(M1) is one of the fastest in all known nuclei at the excitation energy below 3 MeV !

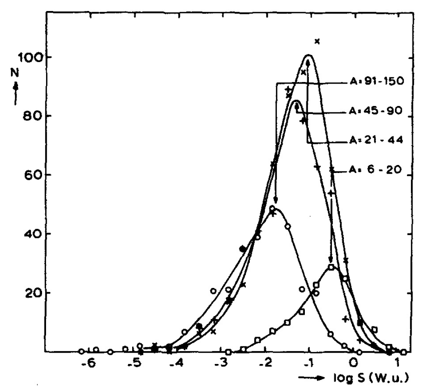

Fig. 6. Comparison of $M1$ strength distributions for different A-regions. Data for A = 6–44 and A = 45–90 are from Refs. 1 and 2, respectively.

Core and valence particles in ^{135}Sb ?

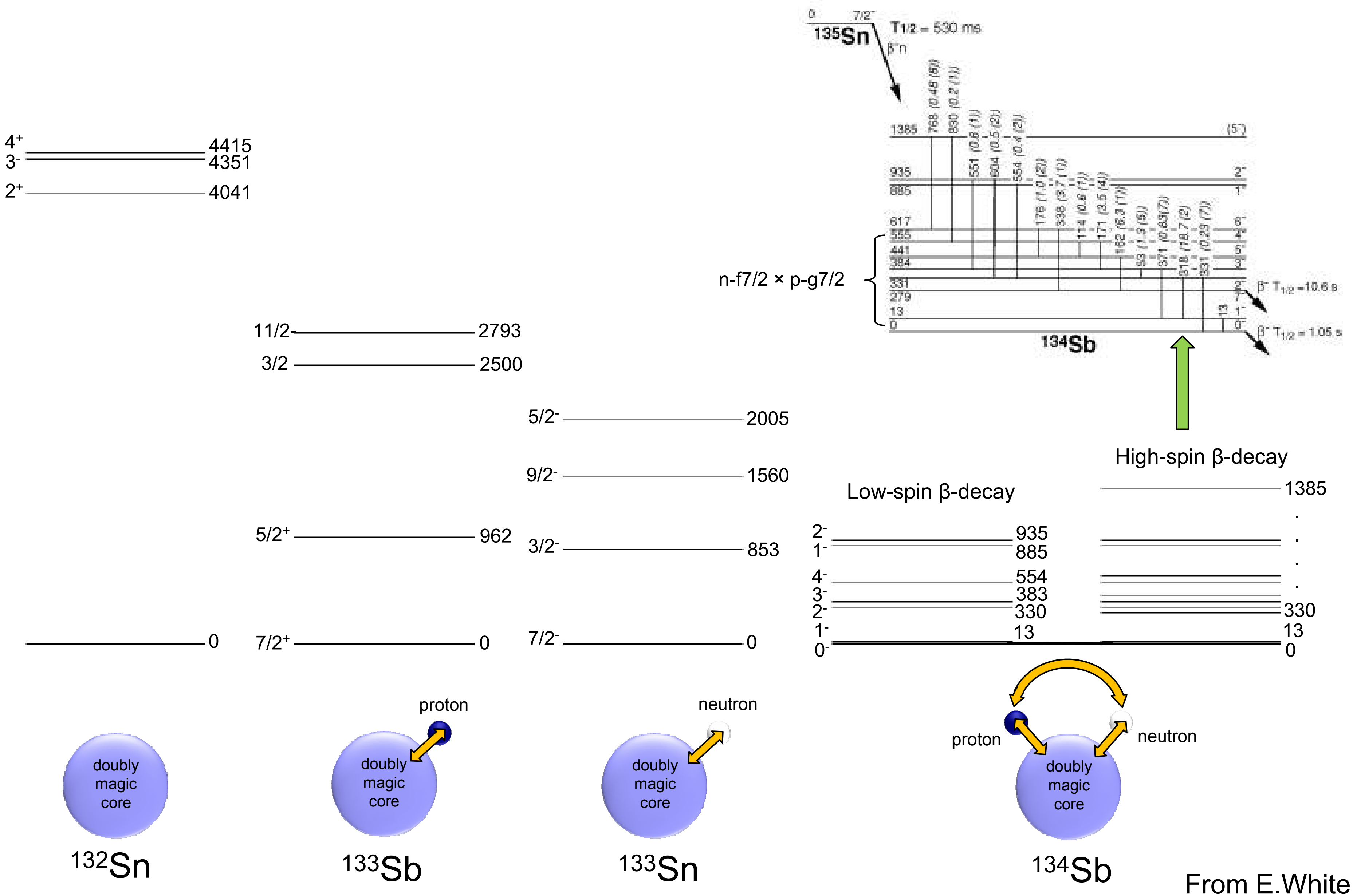

From E.White

The case of ^{135}Sb: one proton two neutrons outside ^{132}Sn

First information on the excited states in ^{135}Sb came from the work by P. Bhattacharyya et al. Eur.Phys.J. A3 (1998) 109

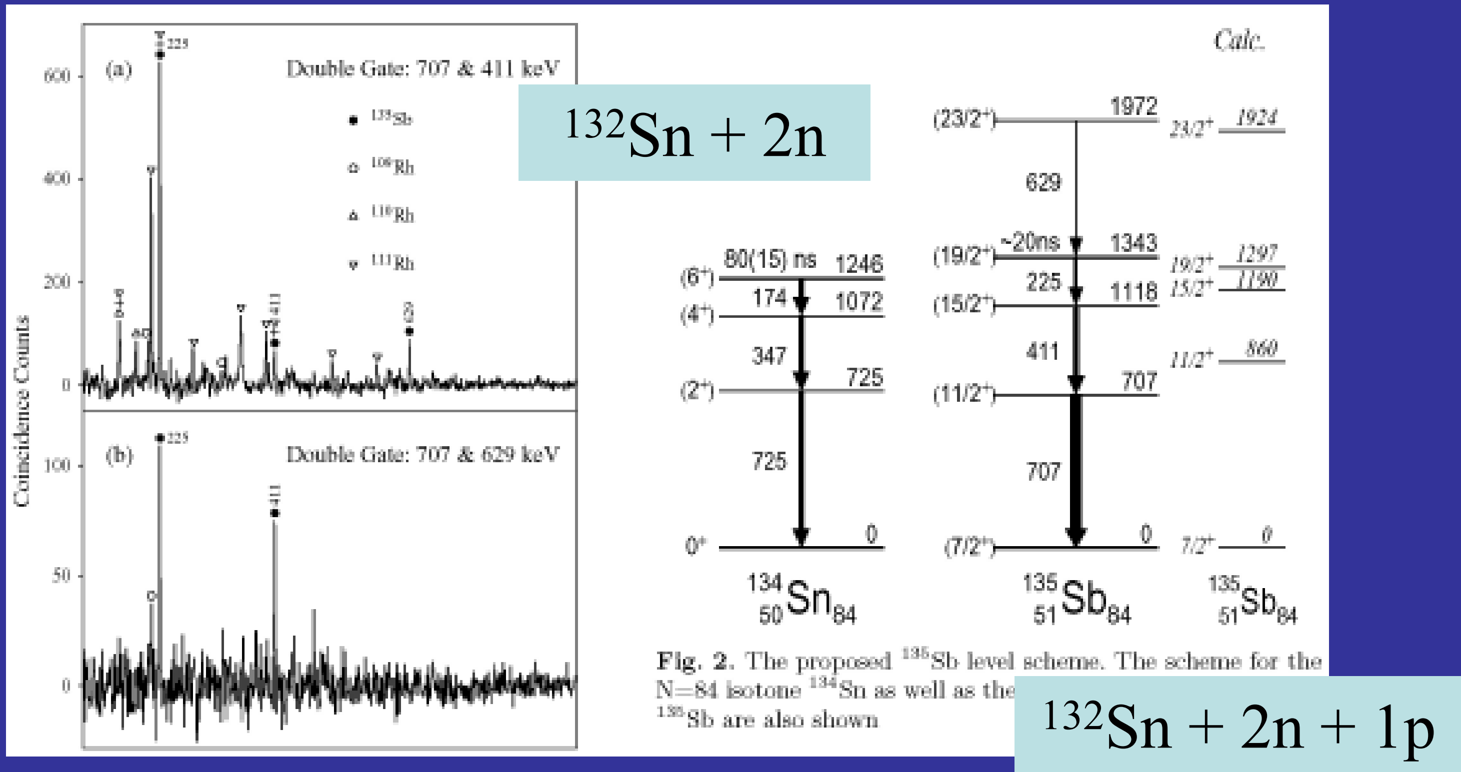

Fig. 2. The proposed ^{135}Sb level scheme. The scheme for the N=84 isotone ^{134}Sn as well as the ... ^{135}Sb are also shown

By analysis of fission product γ-ray data measured at Eurogam II using a ^{248}Cm source, yrast levels up to about 2 MeV in the N=84 three-particle nucleus ^{135}Sb have been identified. These levels are interpreted as $\pi g_{7/2} \nu f^2_{7/2}$ and $\pi g_{7/2} \nu f_{7/2} h_{9/2}$ states with the help of shell model calculations using empirical nucleon-nucleon interactions.

Experiments at the OSIRIS and ISOLDE/CERN facilities confirmed the exceptionally low energy of the first excited state in ^{135}Sb, at only 282 keV

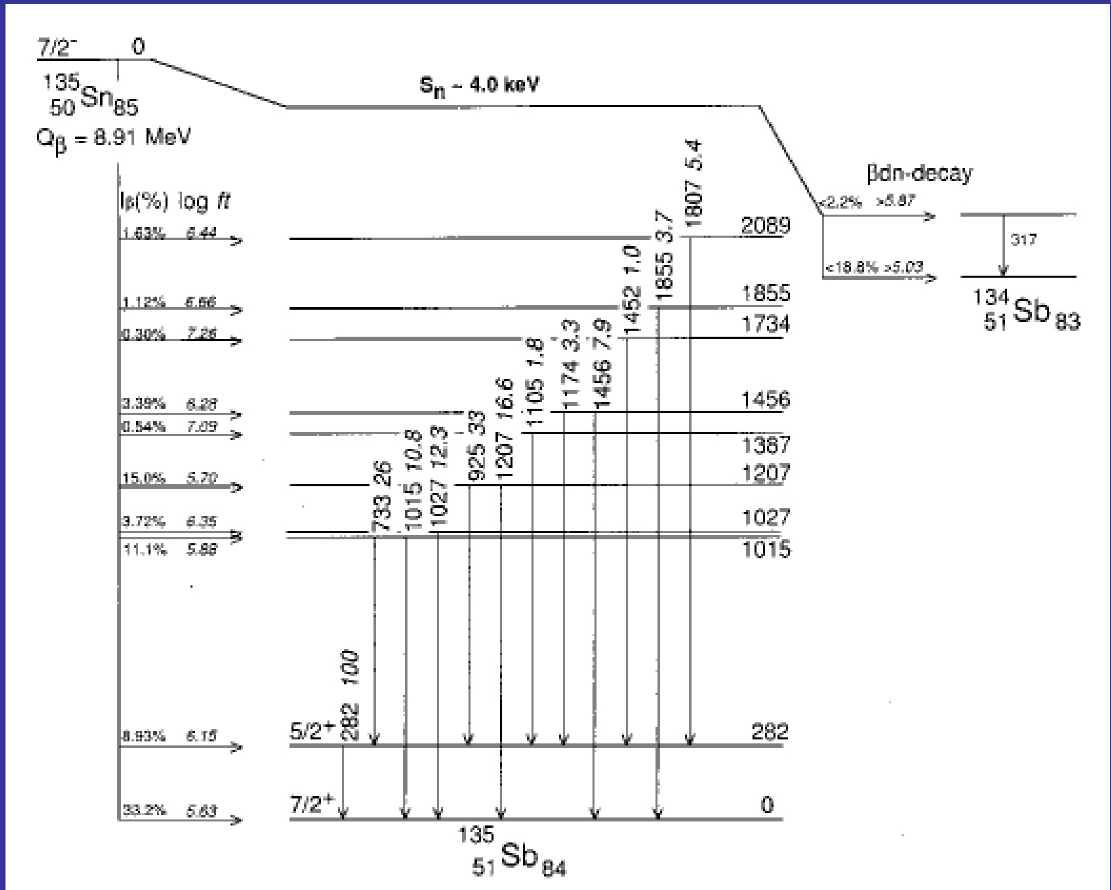

A. Korgul et al., Phys.Rev. C64 (2001) 021302(R)

J. Shergur et al., Phys.Rev. C65 (2002) 034313 shell model study by Alex Brown reveals problem with the excitation energy of the 282 keV level

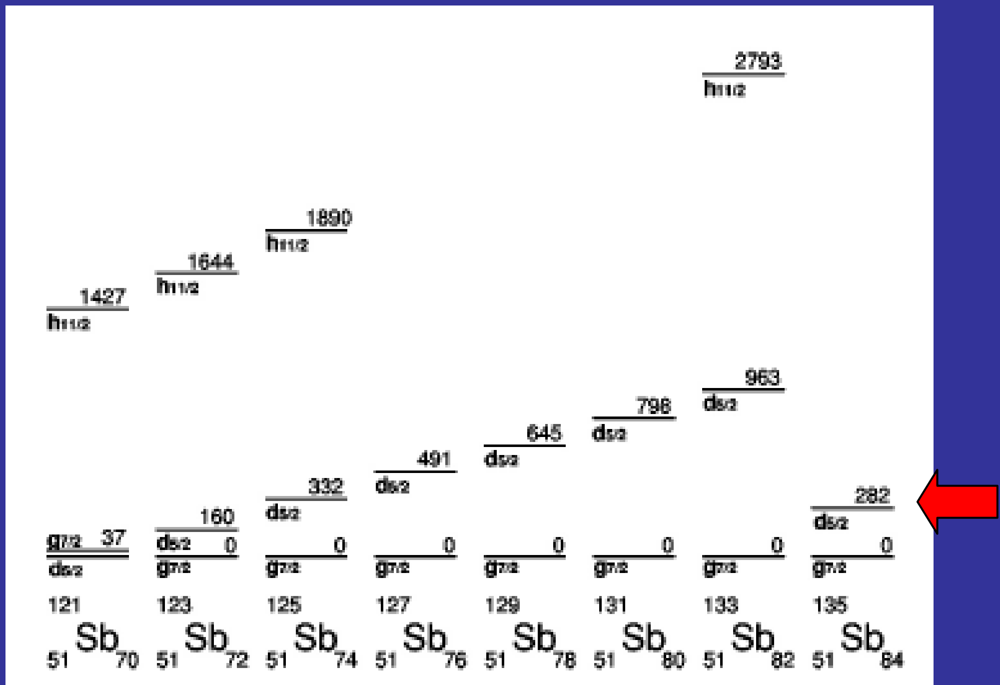

Level systematics of the d5/2 and g7/2 states in odd Sb

The low position of the first excited state in ^{135}Sb provides support for the idea that nuclei with an N/Z ratio that exceeds 1.6 have a more diffuse nuclear surface that changes the relative binding energies of low-spin orbitals when compared to higher-spin orbits.

SM calculations by Alex Brown with shifted $\pi d_{5/2}$ by -300 keV

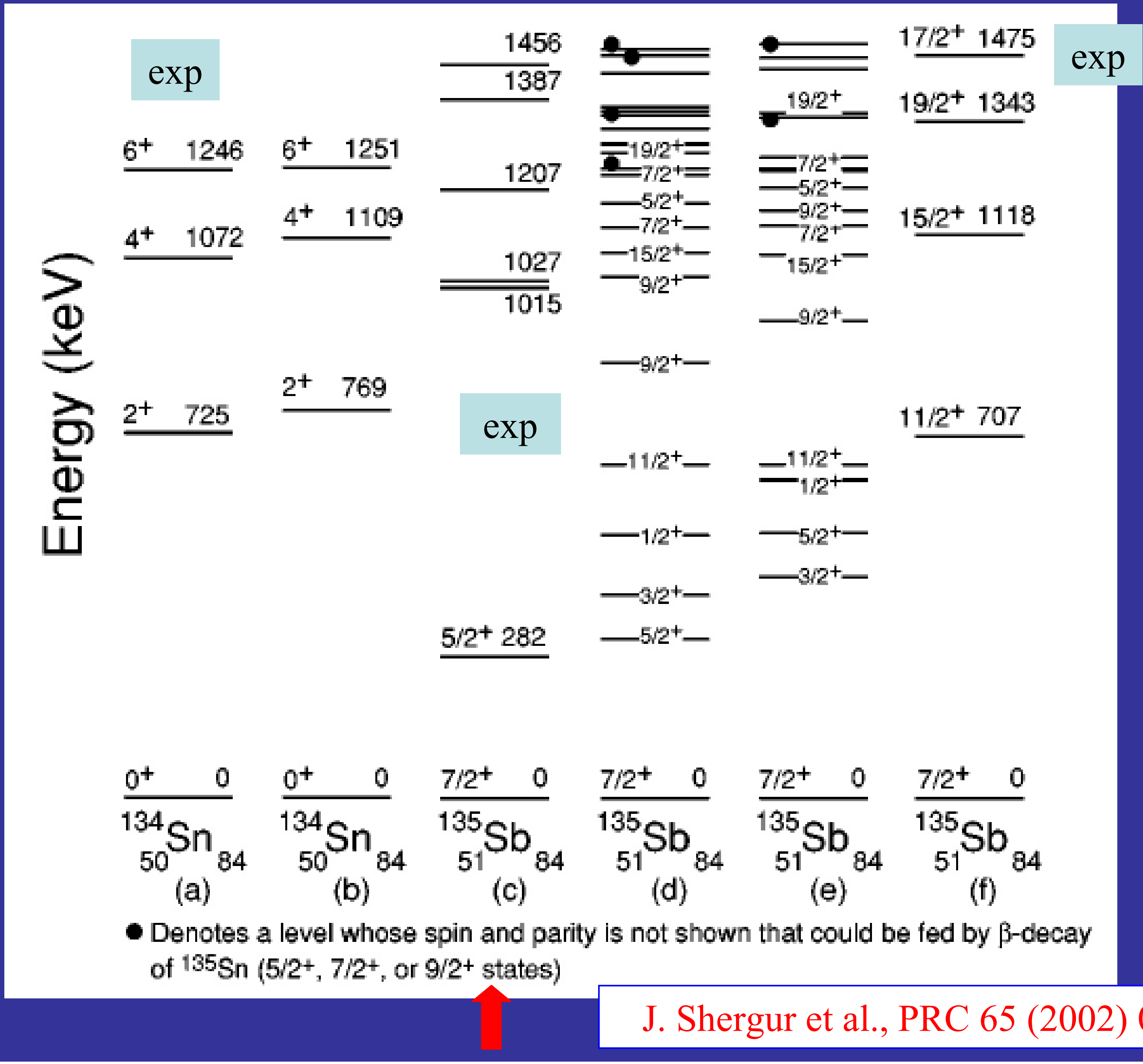

J. Shergur et al., PRC 65 (2002) 034313

A selective shifting of an orbit is an interesting but a very controversial idea!

What can we learn from the B(M1) and B(E2) rates for the 282 keV transition?

Our naive expectation was that if

- the $5/2^+$ 282-keV and the $7/2^+$ ground states are mainly proton $d_{5/2}$ and $g_{7/2}$, then both B(M1) and B(E2) will be slow leading to a long level lifetime

- if the 282-keV state is mainly collective, these rates would be much faster, and the lifetime would be short.

Measurement has been performed at the OSIRIS separator at Studsvik in 2004

$T_{1/2}$ = 6.1 (0.4) ns

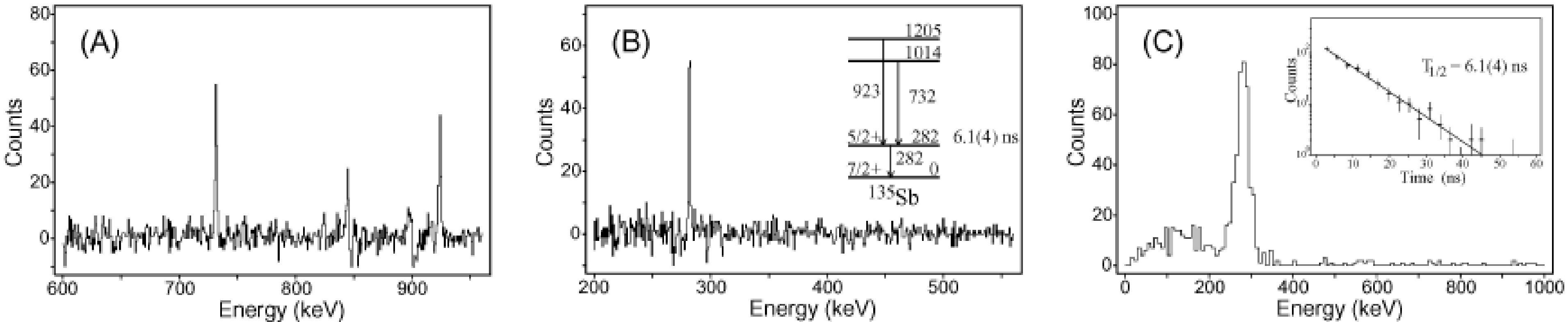

A. Korgul et al., EPJ in press, May 2007

A summary of the experimental situation at the end of Paestum Conference in 2004

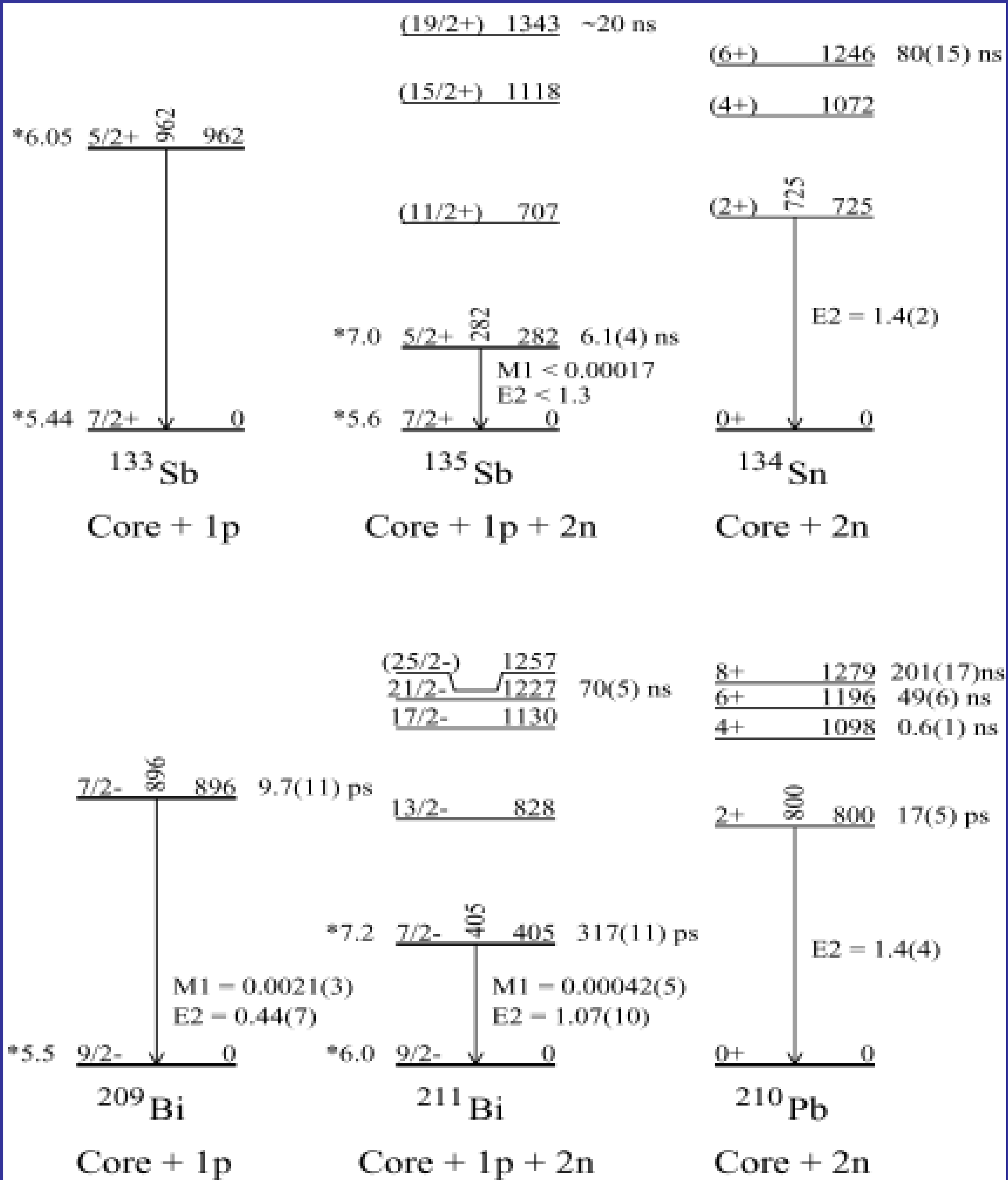

Comparison of the equivalent nuclear systems at ^{132}Sn and ^{208}Pb.

The B(M1) and B(E2) values are in Weisskopf Units.

The low excitation energy of the 282 keV state remains a puzzle.

What next ?

- Situation is not clear in ^{135}Sb.
- More experimental information was needed in order to define better the M1 operator parameters north-west from ^{132}Sn.
- Other transition rates were needed in ^{135}Sb in order to provide more constrains on the calculations.
- Of particular interest was the location of the $1/2^+$ state in ^{135}Sb expected at low excitation energy and whose origin was mainly due to the coupling of $d_{5/2}$ proton to the 2^+ of the core.

Results for ^{135}Sb from the beta-n decay of 0^+ ^{136}Sn

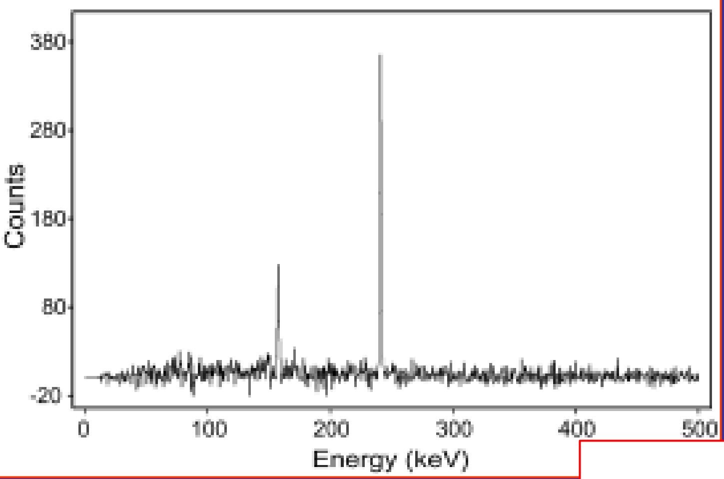

gamma-gamma coincidence spectrum gated by the 282 keV transition in ^{135}Sb. It shows two strong lines at 158 and 241 keV. The first one is known.

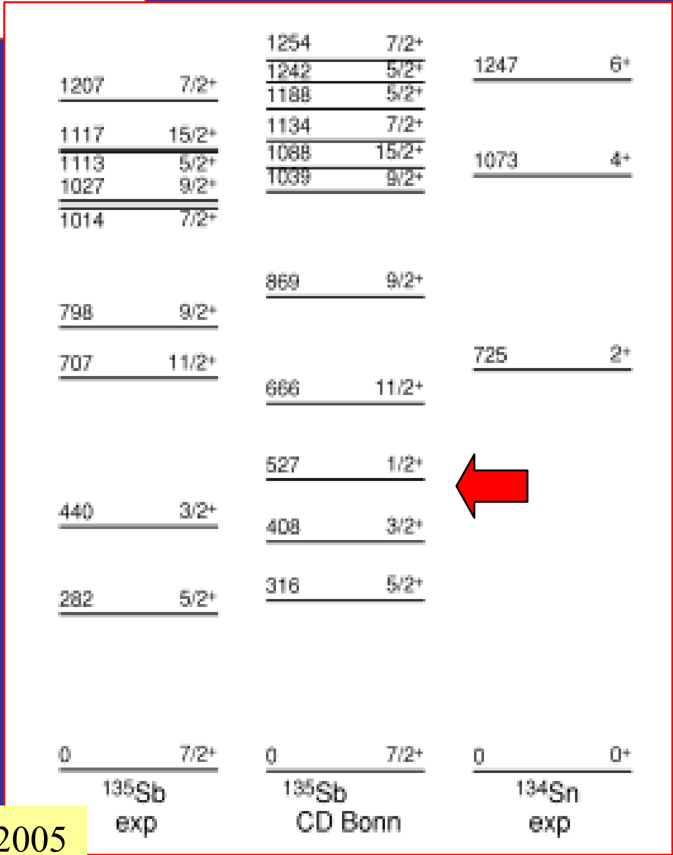

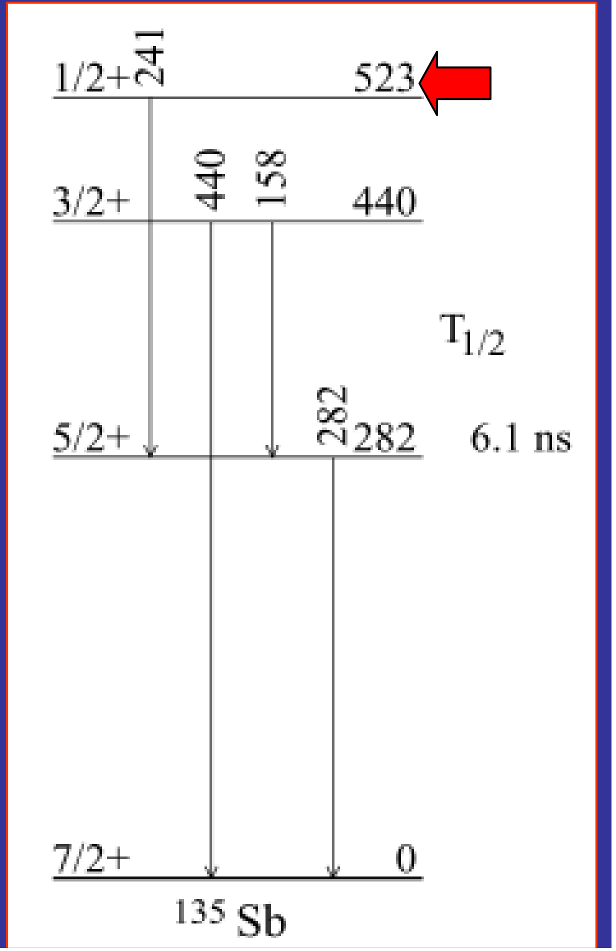

Shergur et al., Phys.Rev C72, 024305, 2005

- If the new state is 1/2+ and it feeds the 5/2+ state at 282 keV, then the transition is E2.
- The model calculations imply that the 1/2+ state is mainly the 5/2+ state coupled to the core 2+.
- The 241 keV transition should then be 'collective' with the B(E2) related to the B(E2) value of the core.
- The 440 keV state is mainly the ground state 7/2+ coupled to the 2+ of the core. Thus the 440 keV transition is basically the core deexcitation, while the 158 keV transition in addition has the d5/2 to g7/2 component – it must be slow.

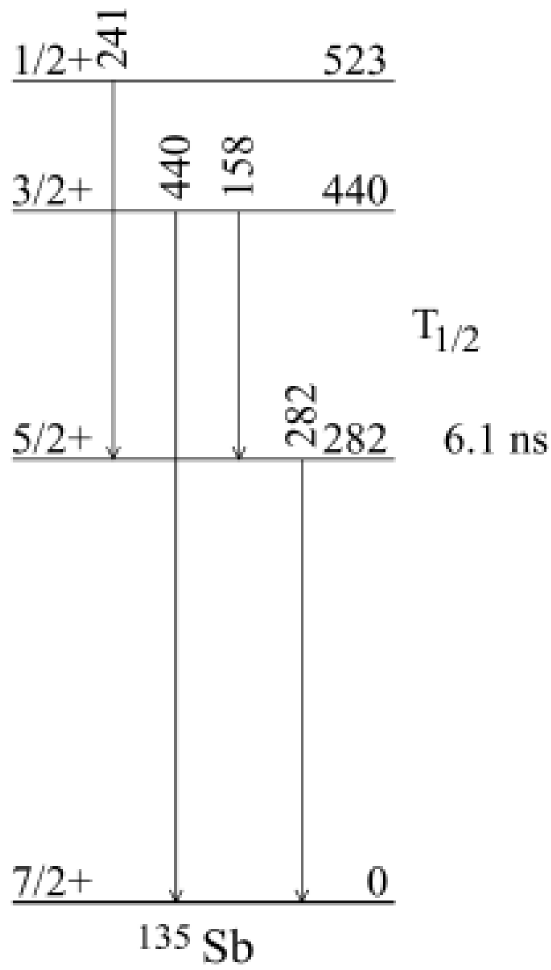

Preliminary !

Lifetime of the 1/2+ state

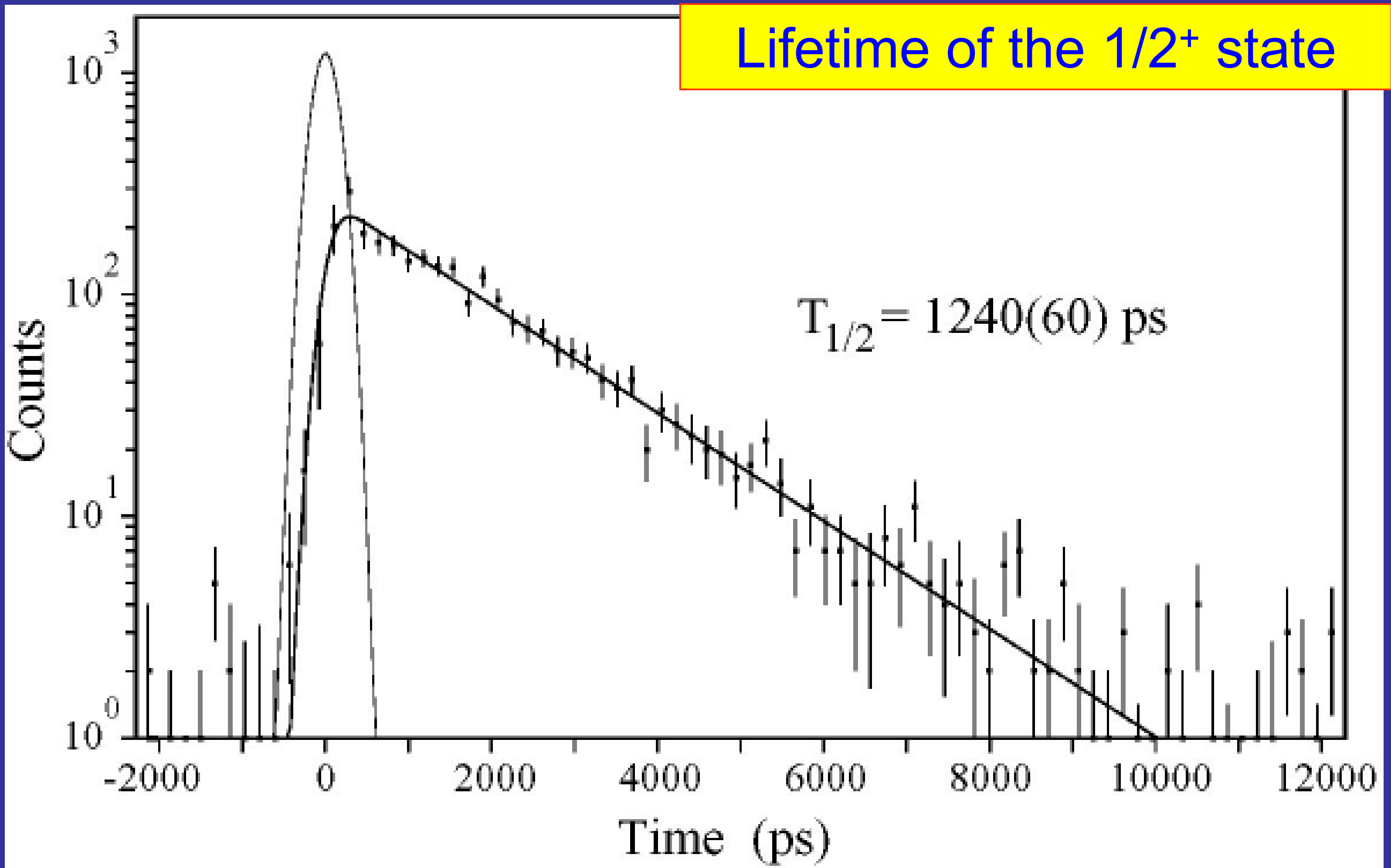

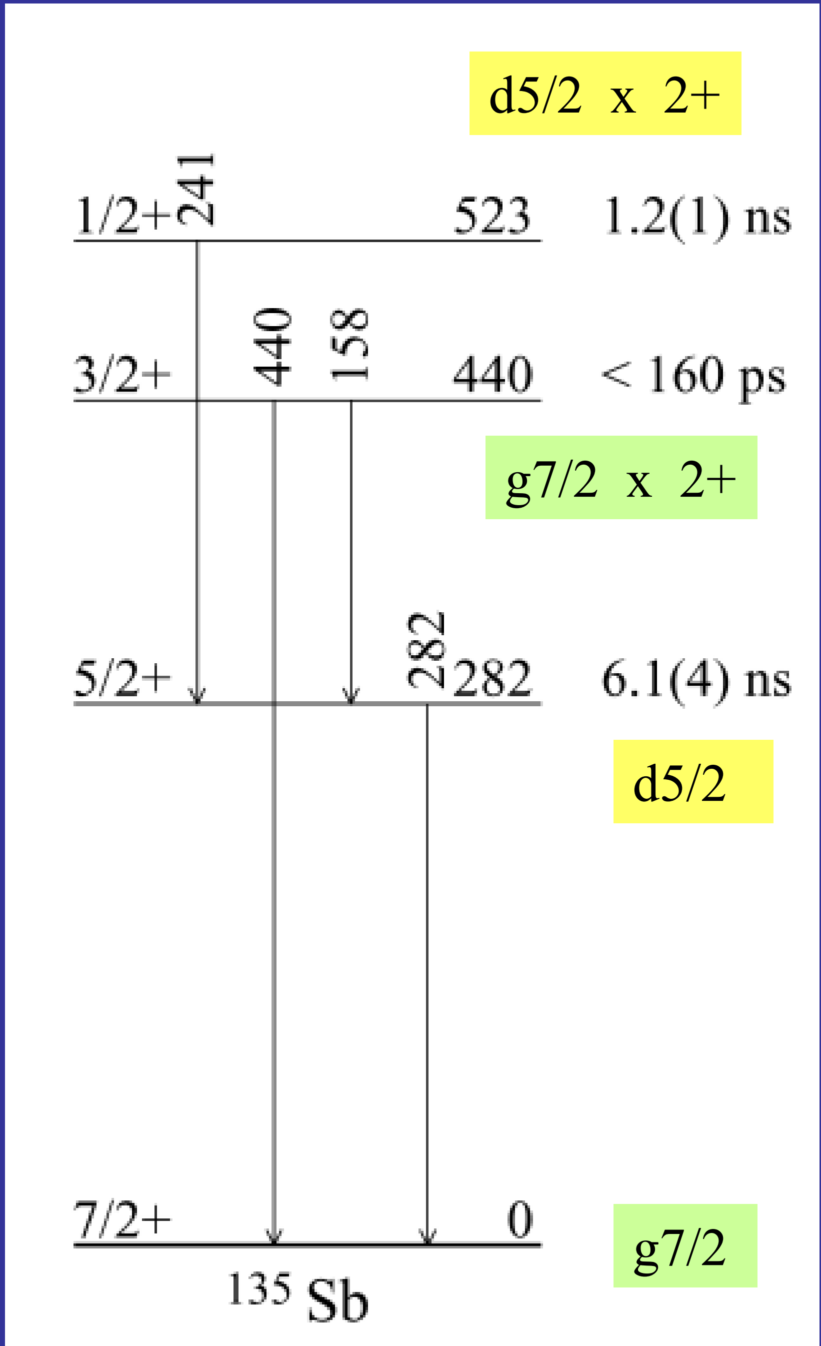

Core excitation:

^{134}Sn B(E2; 2-0) = 1.42 (24) W.u.

(^{136}Te B(E2; 2-0) = 5.0 (7) W.u.)

^{135}Sb

241: B(E2; 1/2 - 5/2) = 13.0 (11) W.u.

440: B(E2; 3/2 – 7/2) > 4.3 W.u.

158: B(M1; 3/2 – 5/2) > 0.004 W.u.

282: B(E2; 5/2 – 7/2) < 1.3 W.u.

282: B(M1; 5/2 – 7/2) < 0.00017 W.u.

Comparison to the shell model calculations

Levels	Exp. (keV)	Brown (keV)	Covello+Gargano (keV)
7/2+	0	0	0
5/2+	282	316	391
3/2+	440	408	509
1/2+	523	527	678
11/2+	707	666	750
9/2+	798	869	813
15/2+	1118	1088	1124

Calculations by A. Brown include the 300 keV lowering of the proton $d_{5/2}$ orbit.

Comparison to the shell model calculations

Levels	Exp.	Brown	Covello+Gargano
5/2 to 7/2	B(M1) < 0.0003 u_N^2	0.0021	0.0040
	B(E2) < 54 e^2fm^4	29	32
3/2 to 5/2	B(M1) > 0.007 u_N^2	0.178 (*)	
3/2 to 7/2	B(E2) > 177 e^2fm^4	408	
1/2 to 5/2	B(E2) = 527(26) e^2fm^4	678	566

(*) The B(M1) value is higher by about factor of 10 than the experimental one.

Note: both calculations predict a very collective B(E2) for the $1/2^+$ to $5/2^+$ transition, but as a consequence they cannot be in agreement with the very low B(E2; 2-0) rate in ^{136}Te !


PSB VISTAR
Supervisor : Benedikt164187
User
Pls
Inj.
Acc.
Ejected
Dest.
ISOHRS
NOKIA

Determination of quadrupole deformation in deformed nuclei

- Quadrupole - ellipsoid shape
- Octupole - pear shaped
- Hexadecapole - extension along axes
- Dipole - ?

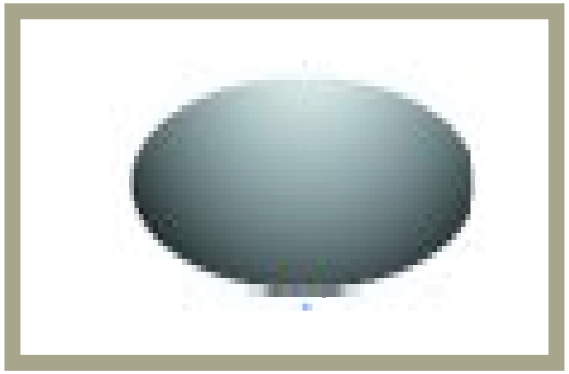
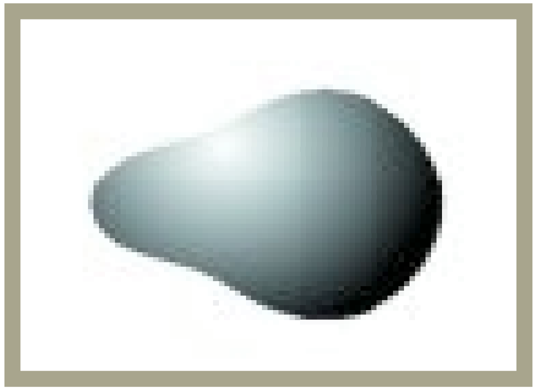
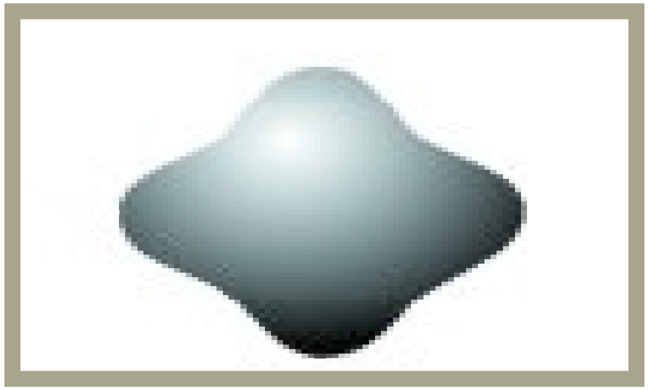

K. Post COS-JAM 2008

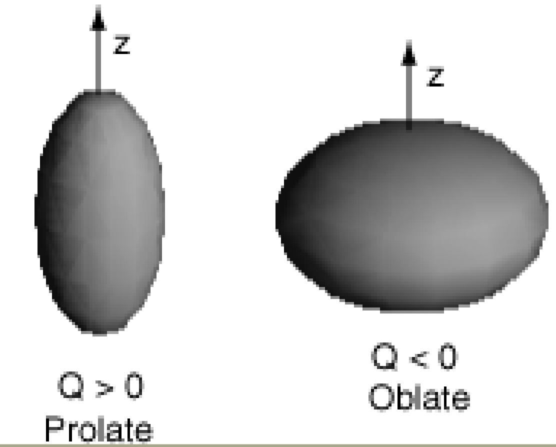

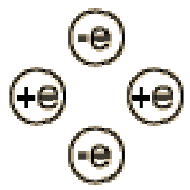

An elementary quadrupole would be seen as having zero charge and zero dipole moment at a great distance. Its interaction with an electric field can be quantified in terms of its quadrupole moment.

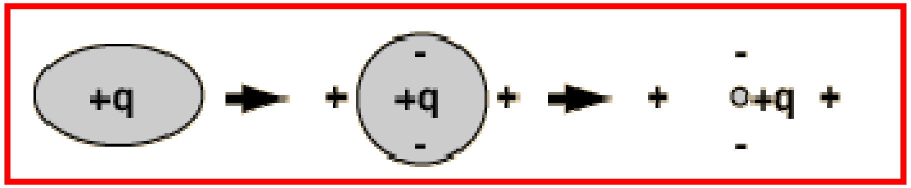

An ellipsoidal charge distribution can be represented by a spherical charge plus a quadrupole, and the spherical charge can be represented by a point charge for assessing its field and potential outside the volume of the charge. It follows that a spherically symmetric charge has no quadrupole moment.

$$
\begin{aligned}
E = \int U(x, y, z)\rho\, d\tau &= U(0) \int \rho\, d\tau \\
&+ \left(\frac{\partial U}{\partial x}\right)_0 \int x\rho\, d\tau + \left(\frac{\partial U}{\partial y}\right)_0 \int y\rho\, d\tau + \left(\frac{\partial U}{\partial z}\right)_0 \int z\rho\, d\tau \\
&+ \frac{1}{2}\left(\frac{\partial^2 U}{\partial x^2}\right)_0 \int x^2\rho\, d\tau + \frac{1}{2}\left(\frac{\partial^2 U}{\partial y^2}\right)_0 \int y^2\rho\, d\tau + \frac{1}{2}\left(\frac{\partial^2 U}{\partial z^2}\right)_0 \int z^2\rho\, d\tau \\
&+ \left(\frac{\partial^2 U}{\partial x\, \partial y}\right)_0 \int xy\rho\, d\tau + \left(\frac{\partial^2 U}{\partial x\, \partial z}\right)_0 \int xz\rho\, d\tau + \left(\frac{\partial^2 U}{\partial y\, \partial z}\right)_0 \int yz\rho\, d\tau \\
&+ \text{higher-order terms.} \qquad (1\text{–}12)
\end{aligned}
$$

Harald A. Enge *Introductio to Nuclear Physics*

Derivation of Quadrupole Moment

$$\Delta E_2 = \frac{1}{2}\left(\frac{\partial^2 U}{\partial z^2}\right)_0 \int z^2 \rho\, d\tau + \frac{1}{2}\left(\frac{\partial^2 U}{\partial x^2} + \frac{\partial^2 U}{\partial y^2}\right)_0 \int \frac{x^2 + y^2}{2} \rho\, d\tau.$$

Now, from Laplace's equation, we have

$$\frac{\partial^2 U}{\partial x^2} + \frac{\partial^2 U}{\partial y^2} = -\frac{\partial^2 U}{\partial z^2}.$$

By substituting this and $r^2 = x^2 + y^2 + z^2$, we obtain

$$\Delta E_2 = \frac{1}{4}\left(\frac{\partial^2 U}{\partial z^2}\right)_0 \int (3z^2 - r^2)\rho\, d\tau = \frac{eQ}{4}\left(\frac{\partial^2 U}{\partial z^2}\right)_0,$$

$$Q = (1/e) \int (3z^2 - r^2)\rho\, d\tau.$$

$$Q_J = \tfrac{2}{5} Z(a^2 - b^2) \approx \tfrac{6}{5} Z R^2 (\Delta R/R).$$

Any deformation can be expanded into a series basic shapes. How to determine them?

- Coulomb excitation by other nuclei
- Hyperfine interaction (via laser spectroscopy)
- Different deformations have specific low lying excited states (called collective states) and collective de-excitation mode

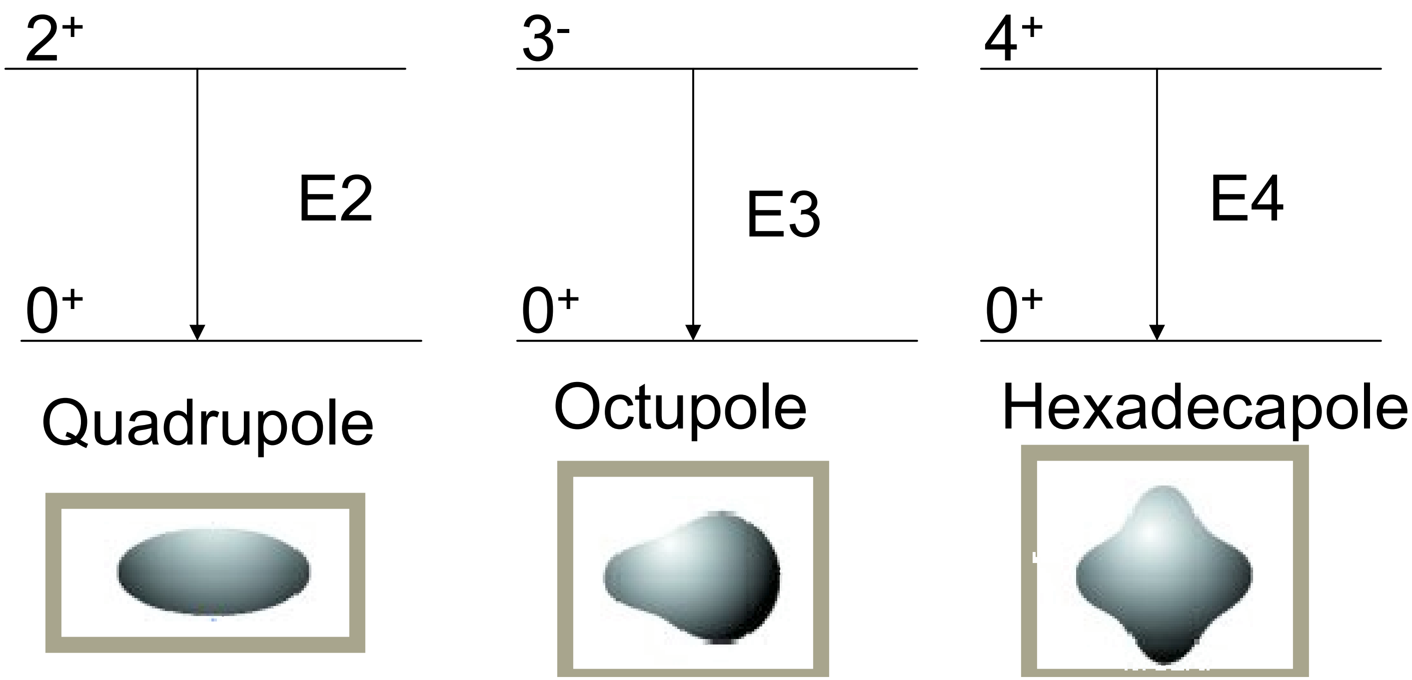

Relationship between deformation, B(E2) and level mean life for the first excited 2+ state in an even-even nucleus

$$B(E2) = 8.20 \times 10^{-12} E_\gamma^{-5} \tau_\gamma^{-1} e^2 fm^4$$

$$B_{W.u.}(E2) = 5.940 \times 10^{-2} A^{4/3} e^2 fm^4$$

$$Q_j = \frac{\sqrt{\frac{16\pi}{5} B(E2; 2 \rightarrow 0)}}{.447}$$

104Mo

TABLE I: Experimental half-lives for the 2_1^+ 192.3-keV state and the B(E2; $0_1^+ \rightarrow 2_1^+$) values for ^{104}Mo.

B(E2; $0_1^+ \rightarrow 2_1^+$) e^2b^2	$T_{1/2}$ ps	Method	Reference
	450(90)	DC-PF [a]	[3]
	911(30)	DC-PF [a]	[4]
	880(100)	DC-PF [a]	[5]
	968(78)	Diff-Plung [b]	[6]
	721(41)	$\beta\gamma\gamma$ [c,d]	[7]
1.34(8)			B(E2) Compilation [1]

[a] delayed coincidence result measured in prompt fission.
[b] Differential Plunger measurement using a ^{252}Cf source with the EUROBALL and SAPHIR multi-detector arrays.
[c] time-delayed triple coincidence $\beta\gamma\gamma$ result.
[d] measured using the JOSEF gas-filled recoil separator.

[1] S. Raman et al., NDT 78 (2001) 1

[6] A.G. Smith et al., J. Phys., G28 (2002) 2307

[7] M. Liang et al., Z. Phys. A340 (1991) 233

104Mo

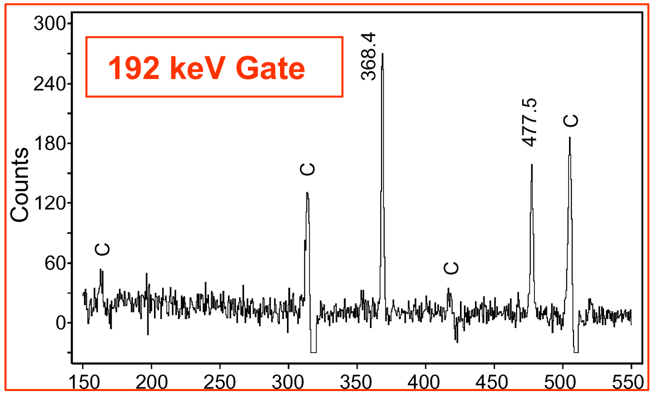

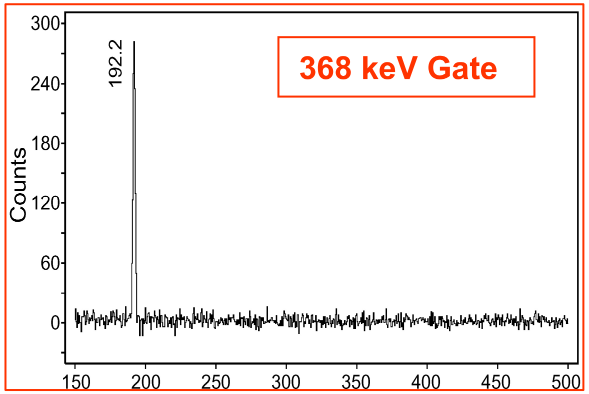

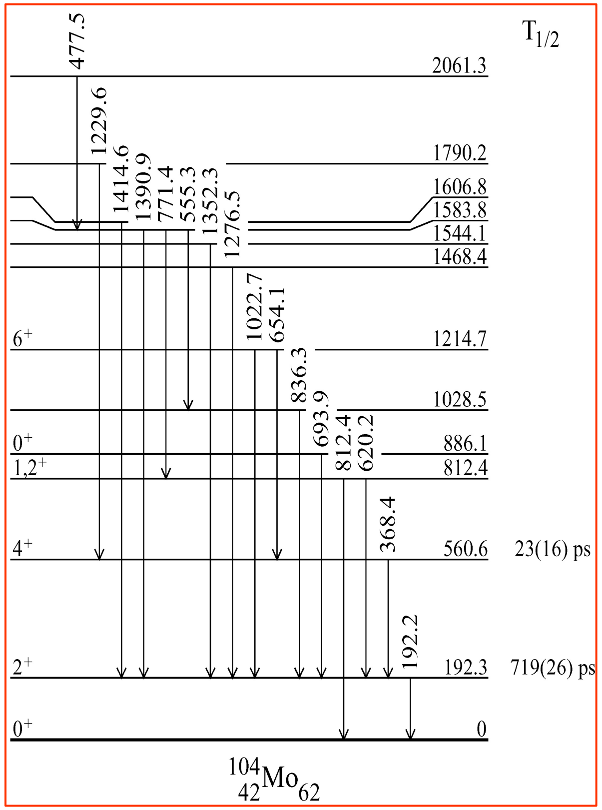

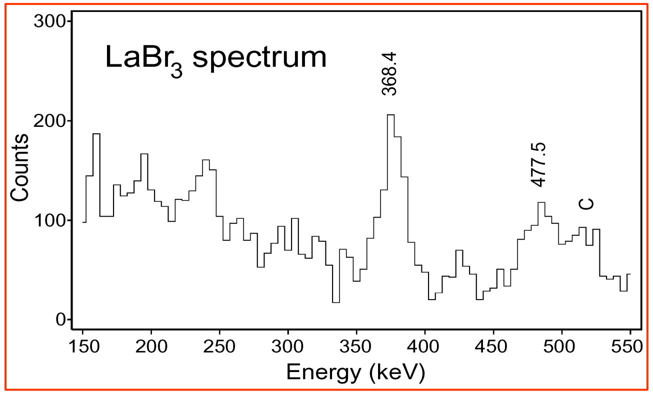

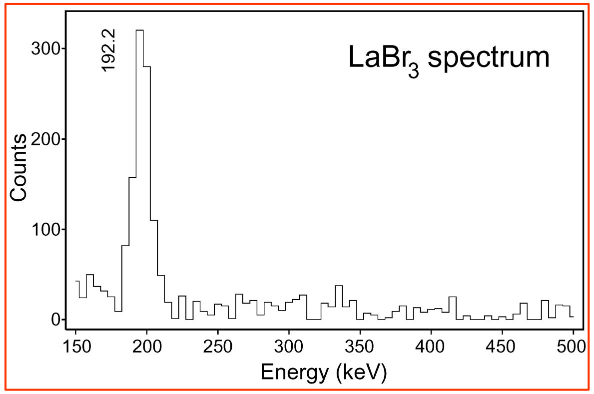

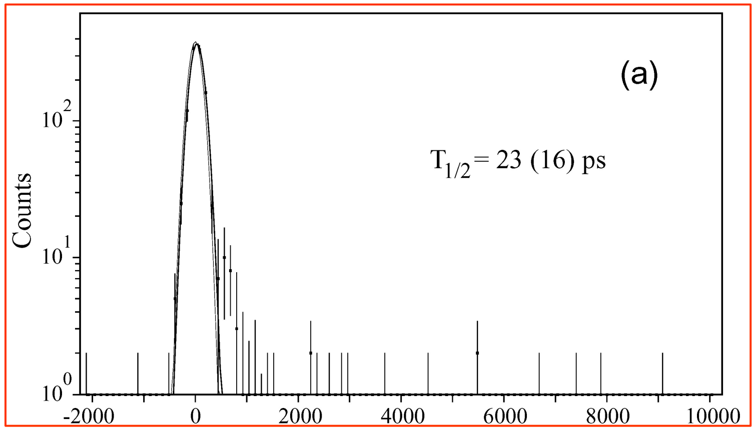

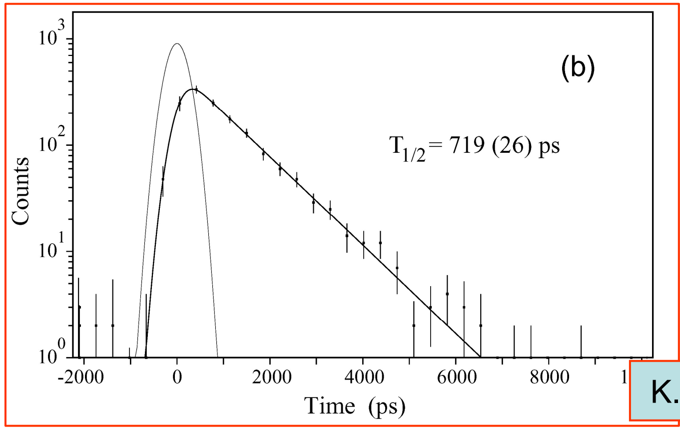

K. Post et al., to be published

104Mo

TABLE I: Experimental half-lives for the 2_1^+ 192.3-keV state and the B(E2; $0_1^+ \rightarrow 2_1^+$) values for ^{104}Mo.

B(E2; $0_1^+ \rightarrow 2_1^+$) e^2b^2	$T_{1/2}$ ps	Method	Reference
	450(90)	DC-PF [a]	[3]
	911(30)	DC-PF [a]	[4]
	880(100)	DC-PF [a]	[5]
	968(78)	Diff-Plung [b]	[6]
	721(41)	$\beta\gamma\gamma$ [c,d]	[7]
1.34(8)			B(E2) Compilation [1]
	719(26)	$\beta\gamma\gamma$ [c,e]	Present Work
1.34(4)	720(22)[d]	$\beta\gamma\gamma$ [c]	Adopted

[a] delayed coincidence result measured in prompt fission.
[b] Differential Plunger measurement using a ^{252}Cf source with the EUROBALL and SAPHIR multi-detector arrays.
[c] time-delayed triple coincidence $\beta\gamma\gamma$ result.
[d] measured using the JOSEF gas-filled recoil separator.
[e] measured using the IGISOL mass separator.
[f] averaged value from the $\beta\gamma\gamma$ results only;

[1] S. Raman et al., NDT 78 (2001) 1
[6] A.G. Smith et al., J. Phys., G28 (2002) 2307
[7] M. Liang et al., Z. Phys. A340 (1991) 233

104Mo

Table 1. The transition quadrupole moments and state lifetimes deduced from our plunger analysis of the yrast bands in ^{100}Zr and ^{104}Mo. Where possible, the results are compared with previous measurements. The quoted uncertainties are purely statistical in origin.

Nucleus	Möller[a] Q (eb)	$I_i \rightarrow I_f$	E_γ (keV)	Previous Q (eb)	This work Q (eb)	This work τ (ps)
$^{100}_{40}Zr_{60}$	3.36	2 → 0	212.7	3.01 (19)[b]	3.19 (14)	928 (75)
		4 → 2	351.9		3.16 (14)	53.4 (5)
		6 → 4	497.4		3.50 (40)	7.0 (16)
		8 → 6	625.6	3.19 (10)[c]	3.23 (16)	2.49 (25)
		10 → 8	738.6	3.19 (10)[c]		
		12 → 10	846.6	3.19 (10)[c]		
$^{104}_{42}Mo_{62}$	3.54	2 → 0	192.2	3.29 (13)[b]	3.35 (14)	1396 (112)
		4 → 2	368.6		3.35 (05)	37.7 (11)
		6 → 4	519.4	3.40 (65)[d]	3.18 (05)	6.83 (21)
		8 → 6	641.8	2.84 (14)[c]	2.68 (07)	3.19 (16)
		10 → 8	733.4	2.84 (14)[c]	2.71 (09)	1.56 (10)

Q = 3.88

[b] S. Raman et al., NDT 36 (1987) 1

A.G. Smith et al., J. Phys., G28 (2002) 2307

104Mo

Table 1. The transition quadrupole moments and state lifetimes deduced from our plunger analysis of the yrast bands in ^{100}Zr and ^{104}Mo. Where possible, the results are compared with previous measurements. The quoted uncertainties are purely statistical in origin.

	Möller[a]			Previous	This work	
Nucleus	Q (eb)	$I_i \rightarrow I_f$	E_γ (keV)	Q (eb)	Q (eb)	τ (ps)
$^{100}_{40}$Zr$_{60}$	3.36	$2 \rightarrow 0$	212.7	3.01 (19)[b]	3.19 (14)	928 (75)
		$4 \rightarrow 2$	351.9		3.16 (14)	53.4 (5)
		$6 \rightarrow 4$	497.4		3.50 (40)	7.0 (16)
R=2.65		$8 \rightarrow 6$	625.6	3.19 (10)[c]	3.23 (16)	2.49 (25)
		$10 \rightarrow 8$	738.6	3.19 (10)[c]		
		$12 \rightarrow 10$	846.6	3.19 (10)[c]		
$^{104}_{42}$Mo$_{62}$	3.54	$2 \rightarrow 0$	192.2	3.29 (13)[b]	**Q = 3.88**	1396 (112)
		$4 \rightarrow 2$	368.6		3.35 (05)	37.7 (11)
		$6 \rightarrow 4$	519.4	3.40 (65)[d]	3.18 (05)	6.83 (21)
R=2.92		$8 \rightarrow 6$	641.8	2.84 (14)[c]	2.68 (07)	3.19 (16)
		$10 \rightarrow 8$	733.4	2.84 (14)[c]	2.71 (09)	1.56 (10)

[b] S. Raman et al., NDT 36 (1987) 1

A.G. Smith et al., J. Phys., G28 (2002) 2307